



HAL
open science

Geological Record of Water and Wind Processes on Mars as Observed by the Mars Express High Resolution Stereo Camera

R. Jaumann, D. Tirsch, S. Adeli, R. Bahia, G. Michael, Laetitia Le Deit, Anna Grau Galofre, J. Head, E. Bohacek, C. Gross, et al.

► To cite this version:

R. Jaumann, D. Tirsch, S. Adeli, R. Bahia, G. Michael, et al.. Geological Record of Water and Wind Processes on Mars as Observed by the Mars Express High Resolution Stereo Camera. *Space Science Reviews*, 2024, 220 (4), pp.45. 10.1007/s11214-024-01076-z . hal-04608462

HAL Id: hal-04608462

<https://hal.science/hal-04608462>

Submitted on 11 Jun 2024

HAL is a multi-disciplinary open access archive for the deposit and dissemination of scientific research documents, whether they are published or not. The documents may come from teaching and research institutions in France or abroad, or from public or private research centers.

L'archive ouverte pluridisciplinaire **HAL**, est destinée au dépôt et à la diffusion de documents scientifiques de niveau recherche, publiés ou non, émanant des établissements d'enseignement et de recherche français ou étrangers, des laboratoires publics ou privés.



Distributed under a Creative Commons Attribution 4.0 International License



Geological Record of Water and Wind Processes on Mars as Observed by the Mars Express High Resolution Stereo Camera

R. Jaumann¹ · D. Tirsch² · S. Adeli² · R. Bahia³ · G. Michael^{1,4} · L. Le Deit⁵ · A. Grau Galofre⁵ · J. Head⁶ · E. Bohacek³ · C. Gross¹ · S.G.H. Walter¹ · H. Hiesinger⁷

Received: 12 July 2023 / Accepted: 8 May 2024
© The Author(s) 2024

Abstract

This review paper summarizes the observations and results of the Mars Express Mission and its application in the analysis of geological processes and landforms on Mars during the last 20 years. The Mars Express observations provided an extended data base allowing a comparative evaluation of different geological surface landforms and their time-based delimitation. High-resolution imagery and digital elevations models on a local to regional scale and spectral measurements are the basis for geological analyses of water-related surface processes on Mars. This includes the nature and discharges of valley networks, formation timescale of deltas, volumina of sedimentary deposits as well as estimating the age of geological units by crater size–frequency distribution measurements. Both the quantifying of geological processes and the determination of absolute model ages allows to constraint the evolution of Martian water-related activity in space and time. Comparative age estimation of fluvial, glacial, and lacustrine deposits, as well as their timing and episodicity, has revealed the nature and evolution of the Martian surface hydrological cycle. Fluvial and lacustrine activity phases are spread over a time span from Noachian until Amazonian periods, but detailed studies show that they have been interrupted by multiple and long-lasting phases of cessation and quiescent. In addition, evidence of glacial activity shows discrete phases of enhanced intensity correlating with increased spin-axis obliquity amplitude. The episodicity of geological processes, erosion, deposition, and glaciation on Mars demonstrate a close correlation between individual surface processes and endogenic activity as well as spin-axis/orbital variations and changing climate condition.

Keywords Mars Express · Surface processes · Water · Wind · Climate

1 Introduction

Mars Express began its observations in early January 2004. The targeted duration of the mission was 1 Martian year (687 terrestrial days). However, the mission is still healthy and operating and has been extended until the end of 2026. After almost 20 years in orbit Mars Express remains one of ESA's most scientifically productive Solar System missions (Martin et al. 2024). Characterization of the surface geology on a local-to-regional scale by Mars Express, ESA's Trace Gas Orbiter (TGO) and NASA's Mars Reconnaissance Orbiter

Extended author information available on the last page of the article

allowed constraints to be placed on geological processes in space and time. Stereo and color imaging produced by the Mars Express High Resolution Stereo Camera (HRSC) (Jaumann et al. 2007) with a resolution of 10 m/pixel provided an unprecedented wealth of information about the geology, geomorphology, and chronology of the Martian surface at a regional scale. Despite the planet's current aridity, past surface water and its geological relevance has also been the major focus of the investigations made by Mars Express. HRSC has sent back thousands of 3D and colour views of the Martian surface at resolution of 10–15 m/pixel, covering almost 90% of the Martian surface. The images show in detail the giant volcanoes and steep-walled canyons, dry river valleys, ancient impact craters and changing polar ice caps. High-resolution digital elevations models on a local to regional scale (~50 m/pixel horizontal and <10 m vertical resolution) are among the unique strengths of the HRSC instrument. HRSC's stereo capability also provides basic data for quantitative analyses to constrain the emplacement of volcanic material, fluvial processes, glacial and periglacial surface modification, and aeolian surface/atmosphere interactions (e.g., Neukum et al. 2004; Head et al. 2005; Jaumann et al. 2010; Tirsch et al. 2011; Erkeling et al. 2012; Bamberg et al. 2014; von Paris et al. 2014). Specifically, based on crater size-frequency distribution analyses (e.g., Michael 2013) the chronology of the geological activity could be constrained (see Werner 2009; Jaumann et al. 2015). The paper focuses on the advantage of HRSC to identify the three-dimensional structure of geological features, map geomorphological units and estimate their age.

In addition the OMEGA (Observatoire pour la Minéralogie, l'Eau, les Glaces et l'Activité) (Bibring et al. 2004) imaging spectrometer onboard Mars Express provides comprehensive assessments of surface mineralogy. OMEGA detected hydrated minerals on Mars for the first time. OMEGA data (Bibring et al. 2004) together with HRSC higher resolution and topography data suggested that water played a geologic role on the surface over periods of time. The surface was greatly modified by liquid water-driven processes, which left their signature in extensive surface erosion and depositional landforms. In addition, if water was stable on the surface over extended periods of time, alteration of surface rocks should occur. OMEGA detected phyllosilicates and hydrated sulphates over large, but isolated, areas on the surface (Bibring et al. 2006; Carter et al. 2013). Although both minerals are the result of chemical alteration of rocks, their formation processes are very different. This pointed to periods of different environmental conditions in the history of the planet, and perhaps different source environments (surface and subsurface). The combination of OMEGA spectral maps with HRSC topographic results of higher resolution allow phyllosilicates to be detected at many locations as dark deposits and eroded outcrops at the base of layered sediments. The most water-related geomorphology results come from the high-resolution HRSC topographic results in combination with OMEGA observations, covering steep-walled canyons, dry river valleys, ancient impact craters and changing polar ice caps. The analyses of this combined data base enabled the quantification of geological processes, such as discharges of fluvial valley networks, formation timescales of deltas, sizes, and volumes of sedimentary deposits, as well as estimates of the ages of geological units by crater size–frequency distribution measurements. Both quantifying geological processes and age determinations allow the evolution of Martian water and wind related geologic activities to be constrained. Besides constraining the ages of surface features, HRSC also provides basic data for quantitative analyses to constrain fluvial erosional processes, glacial and periglacial surface modification, and aeolian surface/atmosphere interactions (e.g. Jaumann et al. 2015).

A second major contribution of HRSC is comparative age dating of fluvial, glacial, and lacustrine deposits providing information about the Martian hydrological cycle (e.g. Jaumann et al. 2015).

2 Properties of H₂O in Relation to Geological Processes

Water is composed of the two most abundant and chemically reactive elements in the universe – hydrogen and oxygen. Water exists as a liquid at pressures above 6.1 mbar and temperatures between 273 K to 373 K. On planetary surfaces, temperatures are determined by the solar irradiance, which is a function of the solar luminosity (L) and the distance from the Sun (D) as L/D^2 . In addition, internal heat sources can provide subsurface conditions that allow a liquid phase of H₂O in planetary bodies. Water is a highly vital, flexible, changeable, and moveable substance that alters and evolves other materials. The H₂O-molecule is a major component of planets, moons, asteroids, and comets and acts in atmospheres, on surfaces and in the subsurface as a weathering agent and a transportation and sedimentation medium. Depending on temperature and pressure, H₂O appears as gas, fluid or solid. The H₂O-molecule interacts in each physical state with its environment causing varying types of alteration. Water and ice driven erosion is one of the most effective processes for changing solid surfaces.

The hydrogen atom is small compared to oxygen, resulting in an uneven charge distribution of the H₂O-molecule. Due to this polar characteristic H₂O is able to dissolve and chemically alter almost all natural substances with time. Like most substances, H₂O contracts with decreasing temperature. However, below 277 K, due to the beginning of crystallization, it starts to expand and below 273 K it erratically increases its volume by 9%. Therefore, H₂O can mechanically destroy almost all natural substances with time. The specific capabilities of H₂O to dissolve and break material, makes it a constructor of specific surface and subsurface environments by burying, excavating, and undermining. Freezing reduces the density of H₂O with the result that ice floats on water. Thus, bodies of water freeze from top to bottom enabling water to be liquid and active even under extreme conditions. Finally, the low viscosity of water provides high mobility, even for ice, which results in the ability to transport materials and exchange materials between environments. As habitable environments are closely correlated with erosion and sedimentation processes caused by H₂O, it is obvious that geological investigations can detect and identify such environments via the tell-tale traces of water and ice.

The versatility of H₂O is largest where all its three physical states can exist simultaneously. Earth is obviously such a place, but in the geologic past Mars and the subsurface of some icy moons might also have experienced comparable conditions for water in these three states. In terms of aqueous environments we must distinguish between surface and subsurface conditions. On planets within the habitable zone that are protected by an atmosphere, H₂O-driven geologic processes build water and ice bodies within marine, lacustrine, fluvial, and glacial environments. The geologic traces of such processes are shorelines, layered sediments, deltas, river valleys and glacial features such as flow fronts, moraines, eskers, drumlins, and dewatering systems. These water and ice related geologic traces can be found widespread on Mars (e.g. Carr 1996; Masson et al. 2001; Jaumann et al. 2002; Neukum et al. 2004; Head et al. 2005; Jaumann et al. 2005, 2015). Subsurface cavities ranging from sub- μm scale to huge volumes allow water and ice to be present in the underground, protected from harsh surface conditions. Evidence of groundwater and ground ice can be traced on the surface by features such as depressions, retreating erosion, permafrost, thermocarst, and polygons that can also be found on Mars (e.g. Carr 1996; Clifford and Parker 2001; Masson et al. 2001; Jaumann et al. 2002, 2015). In addition, interactions of volcanism or impact bombardment with groundwater and ground ice will trigger hydrothermal processes that can form warm, habitable environments.

3 Fluvial/Lacustrine Related Environments and Activity

Valley networks and rivers: NASA's Mariner 9 1970s discovered that Mars is heavily incised by troughs that resemble terrestrial fluvial valleys (Masursky 1973). Developments in data resolution has revealed that numerous ancient valley networks dissect the southern highlands of Mars, providing evidence of a past water cycle on the planet (Milton 1973; Carr and Clow 1981; Carr 1996; Hynek and Phillips 2001; Baker 2001; Howard et al. 2005; Hoke and Hynek 2009; Carr and Head 2010; Hynek et al. 2010; Fassett and Head 2008a, 2011; van Berk et al. 2012; Jaumann et al. 2002, 2007, 2014, 2015; Kite 2019).

Most networks formed during the Late Noachian to Early Hesperian period, around 3.7 billion years ago, with surface runoff by precipitation-fed (rain and/or snowmelt) fluvial erosion being the major formation mechanism (e.g., Craddock and Howard 2002; Head and Marchant 2014), with subglacial incision and sapping erosion playing a more minor role (e.g., Grau Galofre et al. 2020a). This period is believed to have been the peak of valley formation (Hynek et al. 2010; Carr and Head 2010; Carr 2012). The formation of valley networks rapidly decreased near the Noachian-Hesperian boundary (Fassett and Head 2008a,b); at later Martian periods (Hynek et al. 2010; Carr 2012), localized incision is observed in some areas (e.g., Dickson et al. 2009; Mangold et al. 2012a; Bishop et al. 2013; Salese et al. 2016; Adeli et al. 2016; Wilson et al. 2016), particularly the flanks of volcanoes (Gulick and Baker 1989; Gulick et al. 1997; Gulick 2001; Basilevsky et al. 2006; Fassett and Head 2007; Hynek et al. 2010; Bahia 2022).

The availability of near global coverage of HRSC images (Neukum et al. 2004; Jaumann et al. 2007), which provides regional scale high-resolution images and allows for the development of higher resolution than previously available regional scale digital elevation models (DEMs) (Scholten et al. 2005; Gwinner et al. 2009, 2010, 2016), has revealed new and vital information about the number, locations, origin, and duration of Martian fluvial activity component.

The Number and Locations of Martian Valley Networks: The most up-to-date global valley map of Mars was mapped using a combination of data from several instruments (Hynek et al. 2010), including THEMIS (Thermal Emission Imaging System) daytime and nighttime IR (infrared) data with a resolution of 100 m/pixel, MOC (Mars Orbital Camera) wide-angle images with a resolution of 231 m/pixel, and MOLA (Mars Orbital Laser Altimeter) topographic data with a resolution of approximately 500 m/pixel. However, mapping efforts using HRSC images has revealed a much greater quantity of valley networks, indicating HRSC can allow for a more comprehensive archive of Martian valley networks (Fig. 1).

For example, valley mapping based on HRSC of a latitudinal strip between 20°E–20°W by Bahia et al. (2022) revealed ~ 1.5 times greater valley drainage density than the previous valley map (Hynek et al. 2010). Mapping of localized areas, e.g., Huygens crater (13.88°S, 55.58°E), the Aeolis region (3.25°S, 219.37°E), and the West Echus plateau (2.61°N, 283.23°E), resulted in drainage densities 3 times greater than those observed in MOLA data (Ansan et al. 2008). While drainage density can be influenced by various factors, such as relief, maturity, and lithology, it is most sensitive to climatic conditions, particularly precipitation intensity and frequency, which affect the kinetic energy of streamflow needed to carve channels and create drainage networks, with high drainage density values generally associated with semiarid regions on Earth that experience intermittent high-intensity rains (e.g. Woodyer and Brookfield 1966). The increase in drainage densities, revealed by HRSC images, indicates that Mars was likely to have been semi-arid during the Late Noachian – Early Hesperian, which is supported by paleolake geometries (Stucky de Quay et al. 2020) and branching angles of valley networks (Seybold et al. 2018). Furthermore, valley mapping using HRSC data has revealed valley networks in locations that they

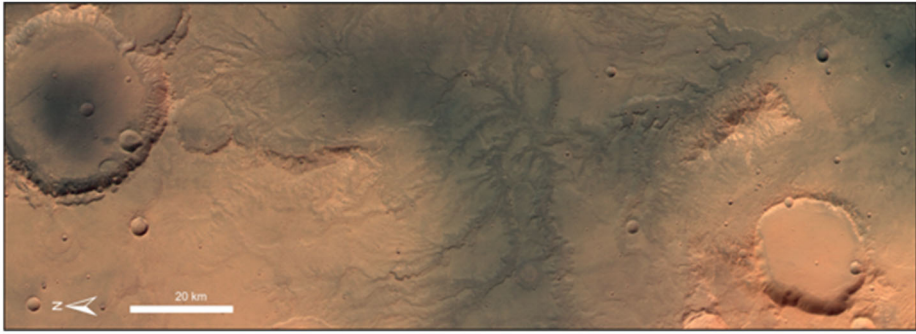


Fig. 1 HRSC orbit i831 showing extensive dendritic valley networks in the Terra Sabea region. The image is centered at 66° East and 17° South. (DLR/ESA/FU-Berlin)

were not previously identified (e.g., west of Hellas Basin (40.29°S, 46.28°E), Libya Montes (1.44°N, 88.22°E)) (Bahia et al. 2022; Jaumann et al. 2010), which holds important implications for inferring the formation mechanisms of valley network from climatic modelling (e.g., Wordsworth et al. 2013, 2015; Bouley et al. 2016; Boatwright and Head 2021, 2022a,b).

The Origins of Martian Valley Networks: HRSC DEMs and images have enabled the high-resolution reconstruction of Martian drainage basins, and in turn, allowed for greater scrutiny of the origins of fluvial activity (e.g., Basilevsky et al. 2006; Fassett and Head 2006; Ansan et al. 2008; Jaumann et al. 2005, 2010; Bishop et al. 2013; Buhler et al. 2014; Grau Galofre et al. 2020a; Boatwright and Head 2022b; Bahia 2022; Bahia et al. 2023). Late Noachian – Early Hesperian valleys are generally attributed to precipitation-fed fluvial activity (e.g., Craddock and Howard 2002). However, Grau Galofre et al. (2020a,b), using the MOLA-HRSC blended DEM and HRSC images, revealed that the profiles and morphologies of Late Noachian – Early Hesperian valley networks indicated the predominant formation mechanisms are fluvial and subglacial erosion, opening the possibility of melting of large-scale ice sheets not only in the southern latitudes (e.g., Head and Pratt 2001; Fastook et al. 2012) but also in the mid-latitudes of ancient Mars with sapping erosion playing a comparatively minor role (e.g. Jaumann et al. 2015). This is supported by Fairén et al. (2012), Hobley et al. (2014), and Buffo et al. (2022), who hypothesize that valleys leading into Gale Crater (5.37°S, 137.81°E) may have formed due to glacial ice-melt. Support for supra-glacial ice-melt as a source for these valley networks was also strengthened by Antarctic terrestrial analogs (e.g., Head and Marchant 2014)

The age analysis of large and sparsely dissected valley networks, such as Nanedi Valles (5.08°N, 49.59°W), Nirgal Vallis (29.10°S, 41.65°W), valleys in fretted terrain, and tributaries of outflow channels and Valles Marineris chasmata (13.75°S, 58.74°W), was conducted using HRSC data sets. Harrison and Grimm (2005) and Jaumann et al. (2015) found that Late Noachian – Early Hesperian valley networks are predominantly of fluvial origin, transitioning to predominantly sapping in origin thereafter. Additionally, Xanthe Terra (1.61°N, 48.04°W) displays older valleys that appear to form precipitation-fed fluvial activity and younger valleys that are sourced from more confined water sources (e.g., groundwater sapping) (Kereszturi 2010, 2014). However, further examination of Naktong Vallis (4.89°N, 33.39°E) revealed a strong link between sapping erosion and overland fluvial activity, suggesting that these processes may have occurred simultaneously in this area (Bouley et al. 2009).

The resolution of HRSC datasets is particularly necessary for the analysis of smaller valley networks, such as those that form during the Late Hesperian – Amazonian periods, revealing that fluvial activity persisted in areas after the Late Hesperian. After the Early Hesperian, Mars' global climate is hypothesized to be generally extremely arid (e.g., Harrison and Grimm 2005; Bibring et al. 2006), however there appears to be a secondary peak in valley formation during the Early Amazonian (~2.9 Ga) particularly on the flanks of young volcanoes (Fassett and Head 2007; Hynes et al. 2010). Analysis of HRSC datasets, both morphologically and hydrologically, has shed light on the origins of flank valleys. Most of the small valleys among the flank valleys are attributed to volcanic activity, such as the collapse of lava tubes, followed by fluvial activity (Bahia 2022). On the other hand, larger valleys are mainly caused by ice-melt or snowpack melt due to geothermal heating of high-altitude snow and ice, and not to any major global climate change (Fassett and Head 2007; Bahia 2022). Additionally, very recent (≤ 25 –40 Myr) valley formation on the eastern flank of Olympus Mons (18.34°N, 133.31°W) has been attributed to flowing liquid water induced by dike emplacement leading to cryosphere cracking and groundwater release (Basilevsky et al. 2006).

In other regions of Mars e.g., the Deuteronilus Mensae region (45.11°N, 23.92°E), localized valley formation during the Late Hesperian – Amazonian is largely attributed to ice-melt due to impacts or volcanic activity, or snowpack melting during periods of high-obliquity (Morgan et al. 2009; Dickson et al. 2009; Fassett et al. 2010; Harrison et al. 2010; Parsons et al. 2013; Hopley et al. 2014). Additionally, Peel and Fassett (2013) have observed valleys in 96 Late Hesperian – Amazonian craters, and their formation is commonly attributed to precipitation (likely snowfall) associated with the impact that formed the crater (Peel and Fassett 2013; Goddard et al. 2014).

The Duration of River Incision and Valley Network Formation: HRSC DEMs are more effective in accurately reconstructing Martian drainage basins compared to MOLA DEMs due to their higher lateral resolution when applying paleohydraulic calculations that rely on topographic data such as Hack's Law and Flint's Law (Hack 1957; Flint 1974). Using these drainage basins one can gain insight into the duration of fluvial activity required to carve a valley. Hoke et al. (2011) determined that large Martian valley networks have formation timescales indicative of cumulative fluvial activity ranging from 10^5 to 10^7 years, with runoff similar to intense streams such as wadis, when flooded in arid regions on Earth. This fluvial activity was likely spread over much greater time periods. For example, examination of valleys incised in the Libya Montes region (1.44°N, 88.22°E) (Fig. 2) reveal that fluvial activity was likely to have extended from ~4.1 Ga to 3.3 Ga (Erkeling et al. 2011) or even until 1.4 Ga (Jaumann et al. 2010).

Furthermore, analysis of valley network longitudinal profiles (i.e., elevation vs. valley length) based on HRSC DTM has revealed that the fluvial activity that fueled Late Noachian – Early Hesperian valley formation was likely ephemeral/episodic (e.g., Penido et al. 2013; Buhler et al. 2014; Grau Galofre et al. 2020b).

Localized studies provide evidence that supports the occurrence of episodic fluvial erosion events. For instance, the western Libya Montes valley system and Mangala Valles (11.33°S, 151.38°W) have both shown signs of several such events (Jaumann et al. 2005, 2010). Additionally, research into the intermittency factor of fluvial activity in the Paraná Valles region (23.18°S, 9.79°W) has indicated that valleys were formed by flood events that had intermittent periods of inactivity lasting years to decades (Buhler et al. 2014). Finally, Fastook and Head (2014) explored the distribution of glacial snow and ice in the valley network headwaters predicted by icy highlands climate models (e.g., Wordsworth et al. 2015) and found that the total volume of water estimated to have filled the lakes associated with

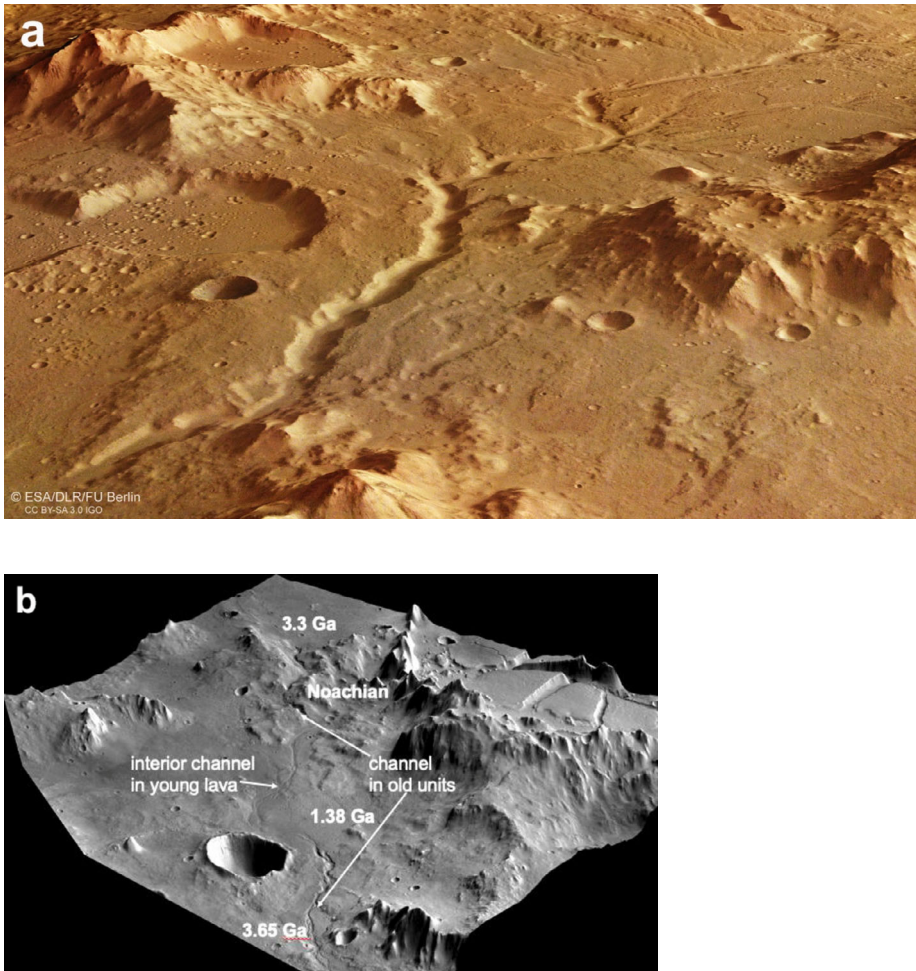


Fig. 2 a) Oblique view in southern direction showing an extensive valley network in Lybia Montes (HRSC orbit g647). The valley width in the foreground measures 1.5 km. The more longitudinal shaped valley in the center of the image was carved by flowing water and later modified by groundwater-induced processes. The course of the stream is characterized by abrupt changes in direction that indicate the influence of local topography. (HRSC color image superimposed on a HRSC DTM, image bottom to horizon is about 50 km). b) Three-dimensional view of a valley in the Lybia Montes region originating from a lava plane in the south (top), incising an old Noachian massif and entering younger lava plains (middle). At the bottom of the image the channel reenters an older former valley system possibly by a cataract and further discharge to the north. The old channel south and north is older than the channel in the young lava flow indicating different episodes of activity. (HRSC nadir image superimposed on a HRSC DTM, image width is about 60 km). (DLR/ESA/FU-Berlin)

valley networks could have been supplied by either the raising of surface temperatures to 273 K for a single Mars summer, or a 2000 year period of moderately higher temperatures (warming of +18 K above icy highlands MAT of ~ 226 K).

Discharge: River discharge refers to the volume of water that flows through a river channel per unit time. It is typically measured as m^3s^{-1} . The discharge of a river can reveal information about the hydrological cycle and the overall water balance of a planet. For example,

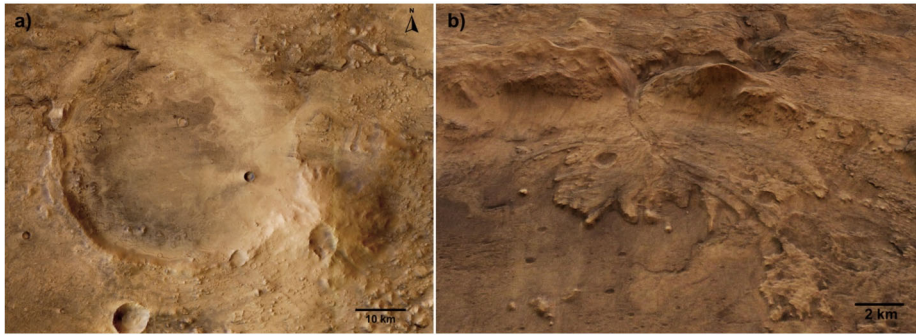


Fig. 3 a) Overview of Jezero crater, derived from the HRSC MC13-east quadrangle mosaic. b) Oblique view of the Jezero delta, view to the west. (DLR/ESA/FU-Berlin)

a high discharge rate indicates that the region received a significant amount of precipitation or had many sources of groundwater or surface water. Discharge values can be calculated from the dimensions (e.g., cross-sectional area and local slope) of Martian channels (e.g., Wilson et al. 2004). To measure these dimensions high-resolution imagery and DEMs are required. Jaumann et al. (2005, 2010) shows that HRSC datasets are sufficient to calculate the discharge values of the interior channel of a 400 km long valley network system located in Libya Montes. They found the discharge of the interior channel was $\sim 4800 \text{ m}^3 \text{ s}^{-1}$, which corresponds to a daily runoff production rate of around 1 cm, which is comparable to terrestrial rivers of the same size (Jaumann et al. 2005). In the absence of HRSC DEMs, the width of a channel (W) can be used to gain estimates of the bankfull river discharge (Q , the maximum amount of water that a stream or river channel can hold before it overflows its banks and spills onto the surrounding floodplain) (e.g., Irwin et al. 2005). The equation below is for a river that has a bankfull discharge recurrence interval of 2 years:

$$Q_{bf} = 0.76(1.9W^{1.22})$$

Due to preservation issues, interior channels are rare on Mars (e.g., Irwin et al. 2005), however, using HRSC images, Penido et al. (2013) determined that the channels that are present on Mars have a width of around 0.14 of the valley width, meaning that one can make inferences about the discharge that would have been required to form the valley.

Paleolakes: The same circumstances that led to the creation of valleys on Mars also created favorable conditions for the formation of lakes (e.g., Carr and Head 2010). As catalogued by Fassett and Head (2008b) Mars is home to both open-basin paleolakes (those with an inlet and outlet) and closed-basin paleolakes (those with an inlet and no outlet), the majority of which are Late Noachian – Early Hesperian Lakes. HRSC DEMs were utilized to conduct detailed analyses of the morphology of open basin paleolakes and their corresponding deposits (Goudge et al. 2012a) (Fig. 3).

All the 226 open-basin lakes examined have experienced some level of resurfacing after their formation, due to volcanism (Goudge et al. 2012b), impact crater formation, glacial and periglacial activity and/or aeolian activity. Using HRSC DEMs, Goudge et al. (2015) performed morphometric measurements of 205 closed basin paleolakes, resulting in an inferred maximum volume of water represented by these basins is approximately equivalent to a global equivalent layer (GEL) of water that is 1.2 meters, only a small fraction of the modern water ice reservoir present on Mars (Carr and Head 2015).

The existence of open-basin lakes suggests that certain basins have accumulated enough water to overcome their constraining topography (e.g., Cabrol et al. 1999; Baratti et al. 2015), resulting in disastrous flooding and the carving of outlet canyons (Goudge et al. 2019). Analysis of the outlet canyons with the assistance of HRSC datasets has revealed that despite constituting only $\sim 3\%$ of the entire length of incised Martian valleys are responsible for $\sim 24\%$ of the total eroded volume (Goudge et al. 2021). This observation suggests that the canyons were a dominant erosive agent, probably leading to significant modifications in the local topography where they developed (Goudge et al. 2021; Diamant et al. 2022). Some of these outlet canyons display evidence for multiple flow events, indicating that the lakes may have been episodically present (e.g., Balme et al. 2011).

Similarly, paleolakes also display evidence of multiple lake-forming periods. Reconstruction of the hydrological history of an unnamed complex crater in the Xanthe Terra region (1.61°N , 311.96°E) (Di Achille et al. 2006), primarily using HRSC data sets, has revealed that a lake was present during the Late Noachian – Early Hesperian period, with a maximum depth of approximately 700 m, as determined from measurements of a delta-like feature, a central terrace, and two small longitudinal scarps. It is possible that the lake underwent multiple formation periods, and the impact of cratering could have affected the system through heating effects that may have accelerated or rejuvenated the recharge of the local aquifer.

Quantitative measurements of water volumes within Late Noachian – Early Hesperian paleolakes have been calculated using HRSC DEMs. Buhler et al. (2011) examined inlet and outlet valleys, as well as fan morphologies of paleolakes in Erythraea Fossa (27.27°S , 329.06°E) (adjacent to Holden crater (26.04°S , 325.98°E)) and determined that the three paleolakes were likely precipitation-fed and contained $\sim 56 \text{ km}^3$ of water. In a manner similar to valleys on Mars, the Late Noachian to Early Hesperian lakes are hypothesized to have been supplied by multiple fluid flow events. Based on an analysis of the geometry and morphology of Gale Crater (Palucis et al. 2016), and the depositional fans within it, it is inferred that the at least three principal lake levels were present within Gale Crater that persisted for a duration of at least 1000 years each.

Furthermore, these lacustrine systems formed after the current topographical configuration of Mount Sharp. The Hesperian period ($< 3.7 \text{ Ga}$) is also hypothesized to have had similarly large paleolakes. Using HRSC DEMs, Dehouck et al. (2010), examined layered deposits $> 300 \text{ m}$ thick at the base of a fan within the impact basin Ismenius Cavus (33.89°N , 16.86°E) (an impact basin), revealing that it likely had a 600 m deep lake during this period.

HRSC images used in synergy with HiRISE images have enabled the identification of potential lake strandlines (ridges that are visible markers of past water levels) in Shalbatana Vallis (7.33°N , 317.91°E), indicating that a $> 400 \text{ m}$ deep lake (Di Achille et al. 2007) was present there during the Hesperian period ($\sim 3.4 \text{ Ga}$) (Di Achille et al. 2009). It is uncertain whether the hydrological activity relied solely on a favorable climate, or if other regional factors, such as volcanism, impact cratering, and tectonism, may have also played a role in initiating or accelerating the local groundwater activity. This suggests that the system may have developed relatively independently of climate conditions.

Late Noachian – Early Hesperian groundwater-fed paleolakes are present in Terra Sirenum (39.49°S , 205.85°E) (Wray et al. 2011). However, it is apparent that other Hesperian paleolakes were possibly climatically sourced, e.g., paleolakes in Ares Vallis (10.29°N , 334.39°E) are hypothesized to be evidence of transient warm and wetter climates (Warner et al. 2010a,b). Salese et al. (2016) utilized hydrological computations of the inflow and overflow rates of the Liberta crater lake (35.23°N , 304.55°E), determining that the entire fluvial network was created within a short to medium (< 1000 years) timescale. However, the size and shape of the observed fluvial-lacustrine features imply prolonged periods of

activity, akin to similar features found on Earth. The source of water for the 300 km long fluvial system is interpreted to have been derived from melting shallow ice caused by thermal anomalies generated by impact crater formation.

Similarly, the plain encircling Rahway Vallis (unofficially called “Rahway basin”, (8.49°N, 173.57°E)) had a lake that was rapidly filled by fluvial flooding, followed by lake drainage. Possible drainage events may have been instigated by the failure of an ice or debris dam, either during or following the development of the extensive and proximate fluvial flood channel known as Marte Vallis (14.09°N, 182.9°E) (Ramsdale et al. 2015).

The Eridania paleolake system (Adeli et al. 2015; Pajola et al. 2016; Dang et al. 2020), situated along the 180° meridian of Mars, represents one of the most sizable lacustrine environments that existed in the planet’s past. Based on its morphological characteristics, it is believed that this system was comprised of interconnected basins that contained water to a depth of around 2400 m, with a minimum volume of 562,000 km³.

The youngest Amazonian-aged valley network system on Mars (Fassett and Head 2008a), located in association with the ~225 km diameter Lyot crater in the northern lowlands (Harrison et al. 2010), has been interpreted to be due to the effects of hot Lyot impact ejecta melting of surface snow and ice emplaced during periods of high obliquity (Weiss et al. 2017), and not due to the release of groundwater by the impact (e.g., Russell and Head 2002).

The presence of relatively recent hydrological activity (likely during the Amazonian period (Adeli et al. 2016)) that was likely supported by groundwater replenishment and/or ice/snow melt further corroborates the notion that hydrological activity may have persisted after the Noachian-Hesperian boundary. This is commonly understood to mark the beginning of the current cold and arid Martian climate (Bibring et al. 2006), although Mars is thought to have had a cold climate incapable of sustaining liquid water at the surface after the Late Hesperian.

Sedimentary Deposits of uncertain Origin: While part of the Martian sedimentary record is clearly associated with ancient fluvial or lacustrine environments, a significant portion of it is not clearly associated with a depositional context. These sedimentary deposits of uncertain origin consist of light-toned and layered materials, reaching hundreds of meters to several kilometers in thickness, and mostly occur between $\pm 30^\circ$ (Tanaka 2000; Malin and Edgett 2000). First identified using Viking Orbiter data, acquisition of HRSC images and digital terrain models permitted improved characterization of these large-scale deposits in terms of their spatial distribution, morphology, and layer attitudes (Fig. 4).

These sedimentary deposits are observed in various settings, including in the topographic depressions of the Valles Marineris canyons (or chasmata) (e.g., Mangold et al. 2008; Le Deit et al. 2008; Flahaut et al. 2010; Wendt et al. 2011) the chaotic terrains (e.g., Massé et al. 2008; Sowe 2009; Sowe et al. 2012), impact craters (e.g., Le Deit et al. 2013; Pondrelli et al. 2011a, 2019) and extensive plains such as those in Arabia Terra (e.g., Pondrelli et al. 2015; Schmidt et al. 2021).

In the Valles Marineris, the sedimentary deposits form mounds of material several kilometers thick. Layers are mostly continuous, parallel, and often have a sub-horizontal to shallow dip in the direction of topographic slopes (e.g., Fueten et al. 2008). The combined analysis of HRSC data and the hyperspectral OMEGA data revealed that most of these sedimentary deposits contain mono- and poly-hydrated sulfates, with poly-hydrated sulfates being located topographically higher than monohydrated sulfates (e.g. Gendrin et al. 2005; Mangold et al. 2008; Carter et al. 2024).

Ferric oxides have also been observed locally (e.g., Le Deit et al. 2008; Wendt et al. 2011). Over the years, several depositional environments have been suggested for the sedi-

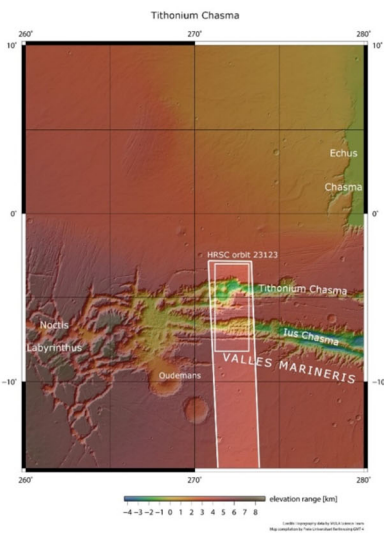
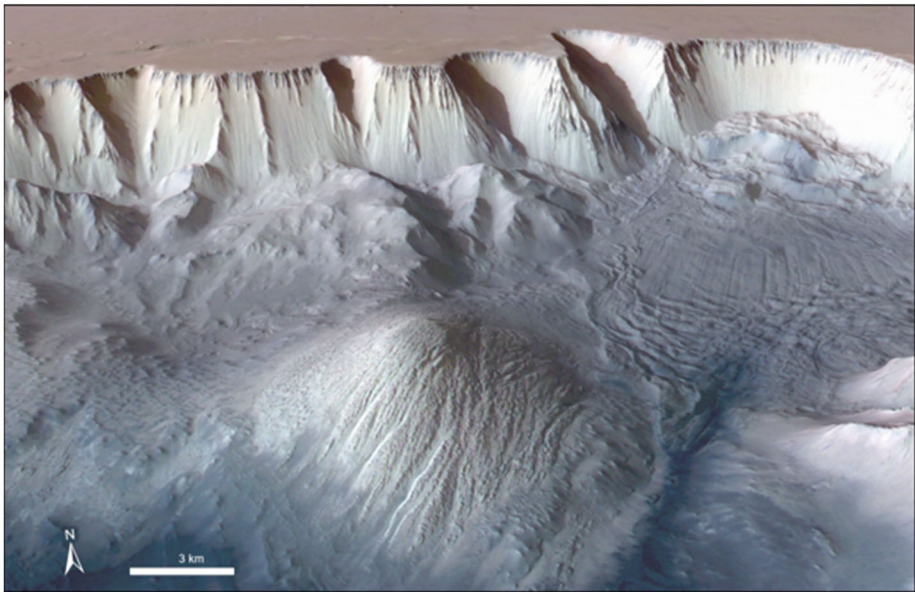


Fig. 4 top: HRSC orbit n123. Perspective view on a hydrated sulphate-bearing mound in Tithonium Chasma, Valles Marineris (DLR/ESA/FU-Berlin); bottom: context image (NASA/JPL-Caltech/MOLA; FU Berlin)

mentary deposits in the Valles Marineris and other geological settings such as aeolian (Peterson 1981), lacustrine (Nedell et al. 1987; Lucchitta et al. 1992; Quantin et al. 2005), ancient polar deposits made of ice and aeolian dust (Schultz and Lutz 1988), groundwater upwelling leading to spring deposit precipitation (Rossi et al. 2008; Pondrelli et al. 2011a, 2019), the upwelling of hydrothermal fluids in a hypersaline lake (Al-Samir et al. 2017), and interplay between airfall and aeolian processes and groundwater fluctuations (Andrews-Hanna et al. 2007; Mangold et al. 2008).

Overall, the presence of sulfate salts in sedimentary deposits argues for either direct evaporation in a lacustrine environment or cementation of clastic sediments at depth by diagenesis. In addition, these large-scale sedimentary deposits occur in various geological settings, which are likely to have involved mixed origins. Observations of the sedimentary record made *in situ* by the Mars Exploration Rover *Opportunity* in the extensive plains of Meridiani Planum and the Mars Science Laboratory *Curiosity* rover in Gale crater do confirm that several depositional environments are recorded in the hundreds of meters of vertical stratigraphy (e.g., Arvidson et al. 2011; Grotzinger et al. 2015). In terms of the formation age, most of these sedimentary deposits were formed over a long-time span, ranging between the early to late Noachian and possibly as late as the Amazonian (e.g., Loizeau et al. 2012; Tanaka et al. 2014).

Alteration Products: The OMEGA instrument allowed the identification of large kilometer-scale exposures of secondary minerals, mostly clays and sulfates in the Valles Marineris, Mawrth Vallis, Nili Fossae and Sinus Meridiani regions (e.g., Bibring et al. 2006; Poulet et al. 2007, 2008; Loizeau et al. 2007; Gendrin et al. 2005; Mangold et al. 2007; Carter et al. 2023) (Fig. 5).

This OMEGA global-scale inventory of secondary minerals has been refined and improved by the CRISM instrument, revealing significantly more diverse and widespread aqueous alteration on Noachian and Hesperian terrains than previously seen (e.g., Mustard et al. 2008; Murchie et al. 2009; Carter et al. 2013, 2023, 2024).

Over the last twenty years, spectral observations have been combined with HRSC images and digital elevation models to help constrain the geological context of aqueous mineral deposits. This includes their spatial distribution, morphology, stratigraphy, thickness, and timing of deposition. A significant result of the OMEGA/HRSC joint analyses is the discovery of the most extensive (300 km x 400 km) and thick (≥ 300 m) clay-rich exposure detected on Mars in the region of Mawrth Vallis, formed during the early to late Noachian (e.g., Loizeau et al. 2007, 2010, 2012) (Fig. 6).

Several outcrops may contain as much as 50% clay minerals (Poulet et al. 2014). The upper part (<30 m) of the mineralogical stratigraphy consists of Al-clays, such as kaolinite overlying Fe-Mg smectites, which are typically observed associated with weathering profiles on Earth (e.g., Loizeau et al. 2010; Bishop et al. 2008; McKeown et al. 2009). Many extended regions on Mars exhibit weathering profiles, suggesting that pedogenetic alteration of the Noachian basement may have occurred at a global scale during early Mars history, and thus under clement climatic conditions (e.g., Carter et al. 2015; Le Deit et al. 2012; Adeli et al. 2015; Loizeau et al. 2018).

Outflow channels: The giant outflow channels on Mars suggest an origin due to enormous floods of water (e.g. Baker 2001). Measurements of Ares Vallis made with HRSC data contributed to the understanding of the geological history of this outflow channel and helped to constrain the timing of its evolution and to characterize potential climatic variations induced by catastrophic floods (e.g. Jaumann et al. 2015). Ares Vallis extends over 8000 km from about 0.3°N, 342°E to 20.8° N, 324°E, and consists of a system of channels originating from Iani, Hydaspis and Aram Chaos, and debouches into Chryse Planitia. The main valley is divided into two regions characterized by a narrower up-stream reach, about 25 km wide and 1500 m deep, and a broader downstream reach, about 100 km wide and 1000 m deep. Two valley arms, originating from eastern Iani and Hydaspis Chaos, debouch into the main valley. A third valley arm originates from Aram Chaos: it appears as a relatively short, narrow gorge, 10 km wide and 2000 m deep (e.g. Jaumann et al. 2015).

The morphology is characterized by catastrophic flood-induced erosional and depositional features, smaller sinuous channels, and ice-related glacial and periglacial morphologies. Erosional features consist of terraces, streamlined uplands, anabranching channels,

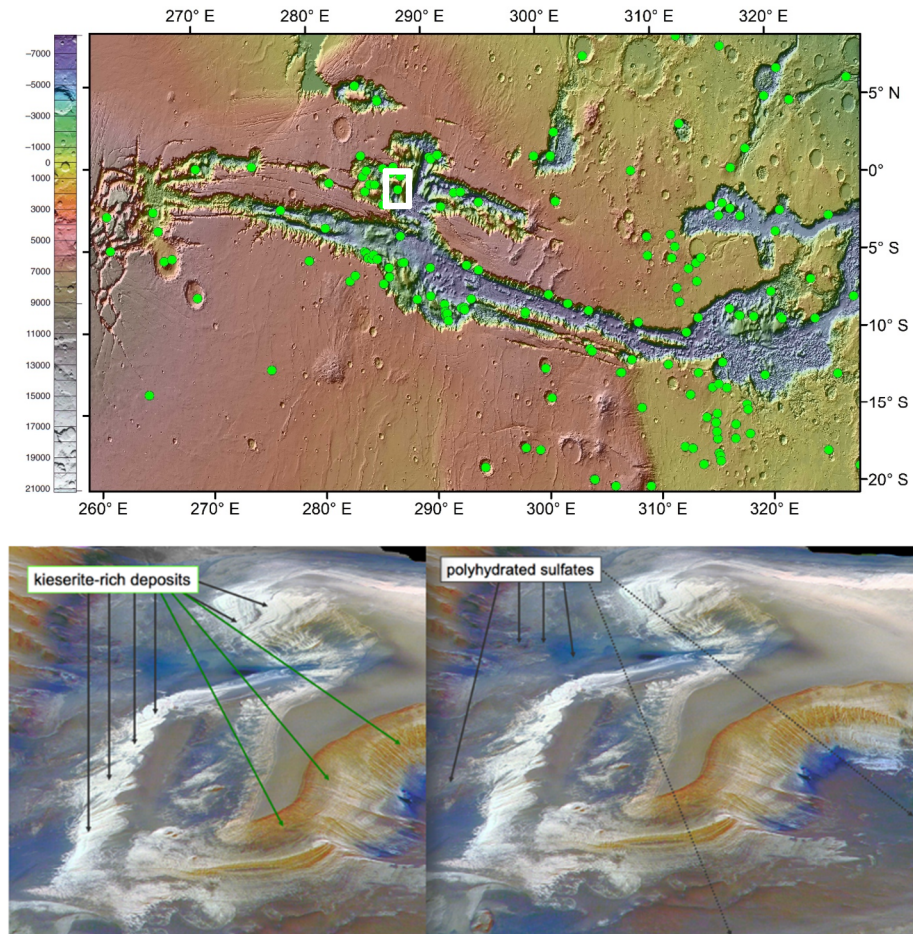


Fig. 5 Top: MOLA map showing the greater Valles Marineris region. All MEX/OMEGA and MRO/CRISM detections of hydrated minerals are represented as green dots (data from Carter et al. 2013). Bottom: HRSC Candor Chasma false color and spectral analyses of different deposits by OMEGA of Candor Chasma (inlet above) (Bibring et al. 2005). ((DLR/ESA/FU-Berlin; NASA/JPL)

giant cataracts, and grooved terrains. Sedimentary features mainly consist of giant bars and pendant bars. Erosional terraces are hundreds of meters high relative to the deepest channel floor, and suggest existence of at least six different, temporally distinct, flooding episodes, based on morphological evidence and impact craters densities (Pacifiçi 2008; Pacifiçi et al. 2009; Warner et al. 2009). The catastrophic flow(s) responsible of the outflow channel formation was at least 500 m deep in the narrow reach of Ares Vallis (Pacifiçi 2008; Pacifiçi et al. 2009).

High-resolution impact crater statistics acquired from each surface using both CTX and HRSC imagery reveal an Early Hesperian (3.6 Ga) post-flood impact crater population resurfacing age for the topographically highest surface relative to the Early Amazonian post-resurfacing age (2.5 Ga) for the lowest flood terrain (e.g. Jaumann et al. 2015). The HRSC observations suggest an origin mechanism for Ares Vallis and neighboring outflow systems that involved long-lived episodic recharge of water from different sources. These results

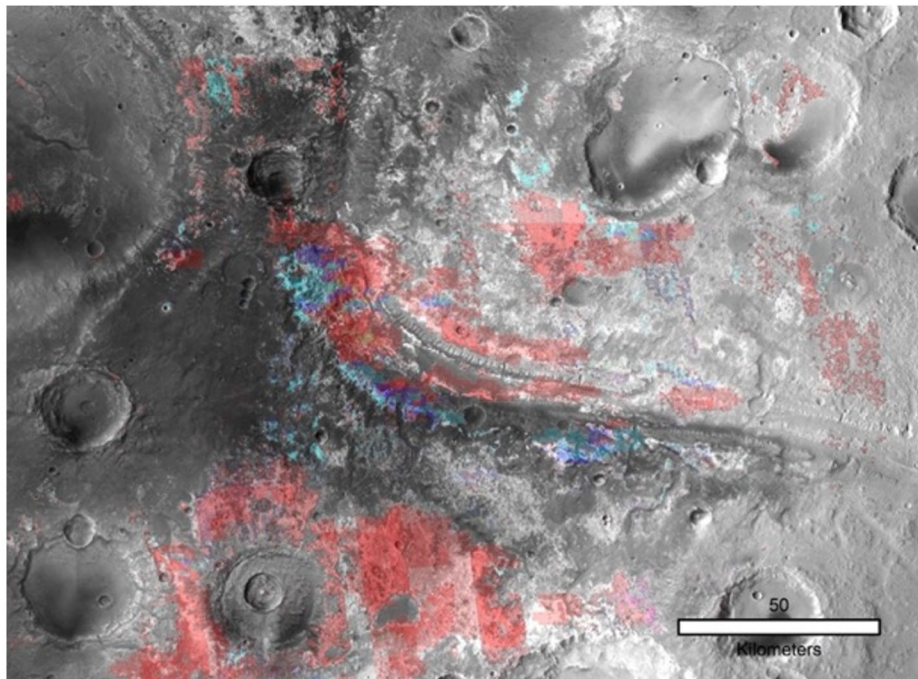


Fig. 6 Combined OMEGA/CRISM/HRSC mosaic of the Mawrth Vallis region. Fe/Mg-rich materials in red, Al-rich in blue, Sulfate-rich materials in green derived from data from the ExoMars candidate landing site study (Poulet et al. 2020). North is up. (DLR/ESA/FU-Berlin; NASA/JPL)

support more regional outburst models for outflow channel formation (e.g. Jaumann et al. 2015), and render local generation/release of liquid water in a single instance of time less likely. They are also consistent with periodic top-down melting of surface snow and ice and volcano-ice interactions to produce episodic meltwater floods (e.g., Cassanelli et al. 2015; Cassanelli and Head 2019). In addition, ice-related morphologic features of Ares Vallis consist mainly of kame-like features and thermocarst depressions. These features are interpreted as ice-contact deposits by emplacement of sediments in subglacial, englacial or supraglacial ice-walled streams or lakes (Costard and Baker 2001; Pacifici 2008; Pacifici et al. 2009) indicating cool climate condition at least part of formation, an interpretation supported by observations of glacial-like lobes in association with the source of Mangala Valles (Head et al. 2004; Basilevsky et al. 2009).

Oceans: Long before the MEX mission, it was suspected that there might have been an ocean in the northern lowlands of Mars (e.g., Parker et al. 1989; Baker et al. 1991; Parker et al. 1993; Clifford and Parker 1999; Head et al. 1999; Carr and Head 2003). These lowlands, north of the global crustal dichotomy boundary, constitute three-quarters of the planet's surface area and form the largest watershed on Mars (Smith et al. 1999). Evidence cited in support of the presence of former oceans include its remarkable flatness, the diverse range of distinctive morphological features such as deltas and possible shorelines, the mineralogical composition of specific geologic units as well as the fact that several large outflow channels and countless valley networks drain into the lowlands. These have been interpreted to mean that a significant body of water existed in this area in the past (e.g., Baker et al. 1992; Squyres et al. 1992; Thomas et al. 1992; Fuller et al. 2002; Di Achille

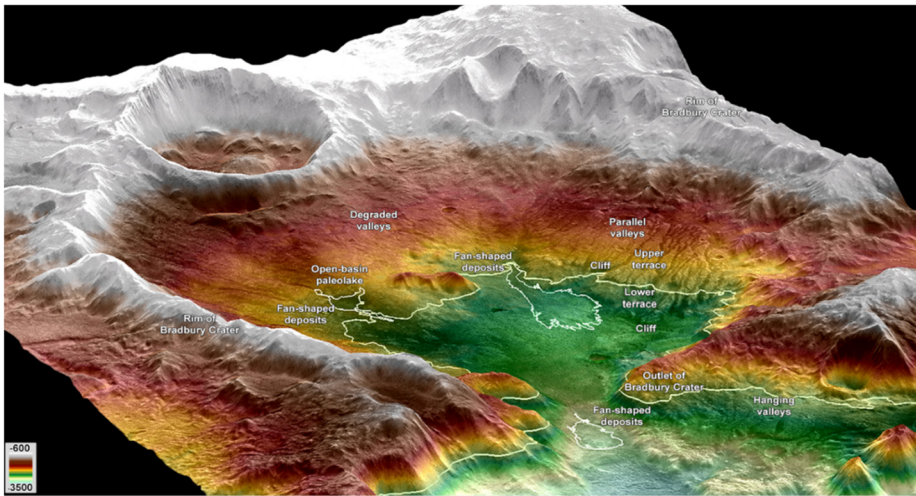


Fig. 7 Perspective view of Bradbury crater at the southern rim of Isidis Planitia. The crater-lake shows a variety of landforms resulting from fluvial, lacustrine, and possibly fluvio-glacial processes. These include degraded valleys, parallel valleys, two cliffs and a terrace, an outlet cut into the northern rim of Bradbury Crater. A delta with Al-rich phyllosilicates, another delta with areas of light-colored, polygonally fractured Fe/Mg phyllosilicates and an alluvial fan are further evidence of the lacustrine activity in this crater. Color-coded HRSC DTM from orbit 2126_0000 on CTX mosaic (from Erkeling et al. 2016)

and Hynes 2010; Wezel and Baioni 2010; De Blasio 2014; Luo et al. 2017) during both the Late Noachian (valley network era) and the Early Hesperian (outflow channel era). However, for the past 20 years, this concept has also been questioned multiple times (e.g., Malin and Edgett 1999; Ghatan and Zimbelman 2006; Head et al. 2018; Sholes et al. 2019; Dickson and Davis 2020; De Toffoli et al. 2021) and it still represents one of the most significant unknowns in the field of Mars exploration.

Various materials like volcanic deposits, the latitude dependent mantle, glacial and periglacial deposits as well as windblown sand and dust suppress indicative features and obscure spectral observations of the surface that could potentially provide evidence for a former ocean in the northern lowland. As a result, it is difficult to find direct evidence of an ocean within the northern lowlands, and many studies instead focus on landforms along the planetary dichotomy, which is suggested to be the location of at least two ancient shorelines, called the Arabia level/shoreline (Late Noachian) and the Deuteronilus level/shoreline (Early Hesperian) (e.g., Parker et al. 1989, 1993; Clifford and Parker 1999; Head et al. 1999; Carr and Head 2003, 2019).

The utilization of HRSC imagery and topographic data aided in enhancing the understanding of the oceans hypotheses and identifying arguments for and against the ocean theory based on geomorphological and topographical features. Investigations of the southern rim of the Isidis basin suggest that potential coastal cliffs around -3600 and -3700 m represent the Arabia shoreline (Fig. 7) shaped by two distinct stillstands and wave-cut action of a former sea at Isidis Planitia during the Early Hesperian period (Erkeling et al. 2012, 2014). In addition, the authors of these studies interpret the Deuteronilus shoreline to be at -3800 m, which is believed to be the result of the edge of a sublimation residue from a frozen Late-Hesperian/Early-Amazonian sea that may have filled the Isidis basin, similar to the Vastitas Borealis Formation (VBF) in the northern lowlands (Tanaka and Scott

1987; Tanaka et al. 2005; Carr and Head 2003, 2019). Fan-shaped deltaic deposits at Bradbury crater directly adjacent to the supposed Arabia shoreline (Fig. 7) (Erkeling et al. 2012; Bishop et al. 2013; Tirsch et al. 2016, 2018; Bramble et al. 2019) have been interpreted as evidence of past discharge into the proposed Isidis sea (Erkeling et al. 2012).

An ocean in the adjoining Utopia Planitia has also been proposed from an analysis of diagnostic landforms such as mud volcanoes, etched flows, polygons as well as rampart and pancake craters within the plains which suggest a large reservoir of water or mud in central Utopia (Ivanov et al. 2014). Surface observations in Utopia Planitia by the Zhurong Rover have revealed evidence interpreted to support the presence of shallow marine tidal currents in a large body of water in the Utopia basin (e.g., Xiao et al. 2023)

HRSC single strip DEMs and the HRSC-MOLA blended DEM (Ferguson et al. 2018) have been used to re-examine the hypothesized shorelines proposed in earlier studies with higher resolution topographic data, resulting in a markedly different picture (Sholes et al. 2019, 2021; Sholes and Rivera-Hernández 2022). These studies argue that the putative coastal landforms lack diagnostic shoreline characteristics, which should, for instance, feature a common elevation level and have a flat top with a step-like flank but are instead curvilinear, tilt in different directions and are laterally not continuous (Sholes et al. 2019).

Moreover, remapping of the global shoreline locations and levels by Sholes et al. (2021) revealed larger differences in elevation as well as lateral offsets of several hundred kilometers. The discrepancies observed between the various levels seem to be attributable to a variety of factors, such as errors resulting from the digitization process, the use of generalizations and extrapolation when determining placement, the combination of data from multiple maps, and the redrawing of sections based on revised interpretations. These findings cast doubt on the efficacy of supposed shorelines as proof of past Martian oceans and suggest the requirement for further meticulous analysis and updated cartography.

HRSC imagery has also been used to discern erosional and depositional features in the northern lowlands that testify to the action of water currents through distinct geomorphology, such as large-scale furrows as well as smaller traction textures (De Blasio 2014). The blended HRSC-MOLA-DEM was used to hypothesize mega-tsunami deposits along the Chryse Planitia margin interpreted to be caused by an impact into a Martian ocean (Rodríguez et al. 2022).

Other studies identify breaks in the longitudinal profile of outflow channel slopes as potential knickpoints that likely formed by base-level changes of an ocean (Duran et al. 2019). These results imply that certain knickpoint elevation zones might have been shaped either during two stable ocean level periods or through multiple phases of fluvial activity combined with varying northern ocean levels (Duran et al. 2019). For instance, the topography of the Kasei Valles outflow channel shows signs of episodic flooding events (ranging from 3.7 to ~2.0 Ga) interacting with changing ocean/base levels (between 3500 m and 2500 m) in the form of theatre-headed knickpoints that share the same elevation with knickpoints elsewhere on Mars, supporting the hypothesis of a global base-level and thus a global ocean (Duran and Coulthard 2020).

Deltas along the dichotomy boundary are among the most unambiguous geomorphologic landforms indicative of standing bodies of water, and thus have been thoroughly investigated to determine whether they actually attest to an ocean in the northern lowlands. Rivera-Hernández and Palucis (2019) analyzed 50 fan-shaped landforms approximately 500 km east and west of Gale crater and recognized significant elevation differences (up to ~2400 m) of the delta fronts, which cannot be explained by modelled deformations by Tharsis or polar wander. Thus, the authors conclude that these deltaic deposits are not an indication of a semi-global northern ocean but are rather formed in several larger paleolakes (between ~330 and ~13.000 km² in size) aligned along the dichotomy boundary.

A similar conclusion was drawn from a study that investigated 161 deltas distributed globally to test the hypothesis that these sedimentary formations could delineate an ancient ocean (De Toffoli et al. 2021). The authors analyzed the morphology, elevation, geographic location, and formation time of these fan-shaped deposits and found only six candidates that can potentially be associated with the shoreline of a former Martian ocean. The other deposits show wide discrepancies in age and location and tend to indicate that they were formed in individual smaller standing bodies of water. Thus, relying solely on deltas is insufficient evidence to establish a universally coherent ancient oceanic shoreline. However, deltas can be useful in restricting water levels locally both in terms of space and time (De Toffoli et al. 2021).

4 Glacial/Periglacial Environments and Activity

The Amazonian era on Mars is characterized by ice deposits within the polar caps as well as glacier-related features, latitude-dependent mantles, and remnant debris-covered glaciers in the high to mid-latitudes and at low to tropical latitudes.

Increases in the spin-axis obliquity of Mars cause polar water ice to be mobilized and to be redeposited in the now-colder lower latitude regions (Richardson and Wilson 2002; Haberle et al. 2003; Mischna et al. 2003; Forget et al. 2006) to form regional mantles (e.g., latitude dependent mantles, LDM; Head et al. 2003) and ice sheets, and associated glacial flow features (e.g., lobate debris aprons, LDA; lineated valley fill, LVF; and concentric crater fill, CCF; Neukum et al. 2004; Head et al. 2005; Hauber et al. 2005). When obliquity decreases, the process reverses and equatorial and midlatitude surface ice ablates and returns poleward to be redeposited, leaving some remnant ice deposits protected by a sublimation lag (LDM, LDA, LVF, CCF) or crater ejecta (pedestal craters; Kadish et al. 2010). When mid-to low-latitude glacial ice was not debris-covered, its presence is often revealed by glacial lobe-shaped depressions and related tell-tale features (Head et al. 2008; Hauber et al. 2008).

Head et al. (2003) hypothesized an ice age between 2.1 and 0.4 Ma ago, when the obliquity might have exceeded 30° and Mars was in an “ice age”. During higher obliquity phase, water ice was removed from the polar regions and transported to mid-latitudes. Global circulation models suggest that periods of high obliquity ($>30^\circ$) may have caused the mobilization of polar volatiles and water vapor in the atmosphere toward the equator and therefore redeposition of ice and snow in lower latitudes (Forget et al. 2006; Madeleine et al. 2009; Mischna et al. 2003). The rapid accumulation of north polar layered deposits resulting from the retreat of ice from the mid-latitudes (Smith et al. 2016) marks the end of this hypothesized ice age. Obliquity variations have been calculated for the past 20 Ma ago (Laskar et al. 2004), but it is likely that the surface of Mars repeatedly experienced such climate changes leading to cycles of deposition and sublimation/evaporation of ice and glacial deposits (e.g. Head et al. 2005; Fassett et al. 2014; Smith et al. 2016). During low obliquity phases, ice and snow are transported back to the poles (Greve et al. 2010; Head et al. 2005; Levrard et al. 2007; Madeleine et al. 2012; Smith et al. 2016).

Mars Express with its HRSC stereo images and high-resolution DEM, greatly contributed to the finding of the major water ice deposits and glaciers on Mars, as well as providing geological context for a deeper understanding of formation and time span of these features.

Past Record: Current Martian ice distribution is largely controlled by insolation and surface thermal characteristics, but in the early periods of Mars’ history a thicker atmosphere would have favored ice deposition both in high elevation and in high latitude regions, as

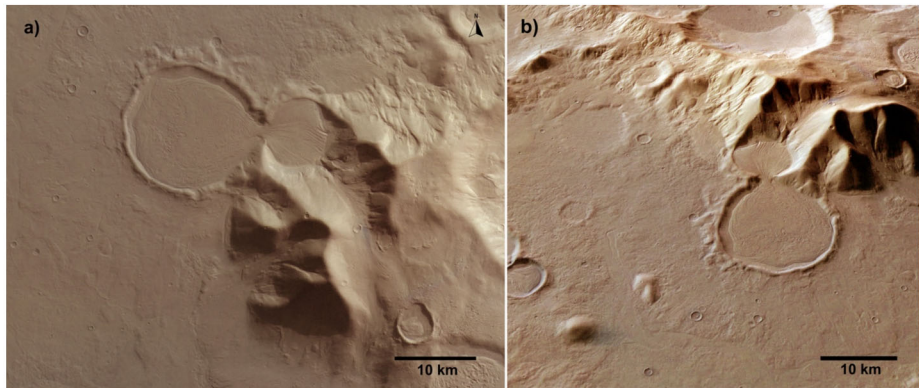


Fig. 8 (a) ‘Hourglass craters’ and surroundings as seen by HRSC orbit 0451. Debris covered ice deposits flowed from crater the small crater, converged in the bottleneck between the craters and flowed into the bigger, producing the hourglass morphology. (b) Perspective view to the east the mountainous area is 3000 m high. (DLR/ESA/FU-Berlin)

observed on Earth (e.g., Wordsworth et al. 2015; Wordsworth 2016; Palumbo et al. 2018; Kite 2019). Global Climate Models (GCM) of early Mars predict ice deposition in high elevation areas of the highlands, notably in the southern circumpolar region and the equatorial Tharsis bulge. Geological evidence for past ice on Tharsis includes arcuate ridges in Arsia and Pavonis Mons, interpreted to be cold-based moraines deposited by flank glaciers or ice sheets, in agreement with results from Amazonian ice sheet models (Head and Marchant 2003; Parsons et al. 2021; Fastook et al. 2008).

Glacial modification likely also played a role in the sculpture of the outflow channels (Lucchitta 2001, Chapman et al. 2010a and 2010b), and in shaping the basal escarpment and aureole surrounding Olympus Mons, as part of a glaciovolcanic complex (Hodges and Moore 1979; Cassanelli and Head 2019), although submarine or landslide hypotheses have also been raised (De Blasio 2018; Lopes et al. 1980; Tanaka 1985). At the dichotomy boundary, notably around Deuteronilus and Proteronilus Mensae, several landforms are interpreted to be of glacial origin based on analogue landscapes (Fig. 8). This includes U-shaped valleys, cirque-like valley heads, arete-like flank valley walls, and overall canyon scale (Davila et al. 2013).

An informally termed hourglass-shaped crater (Fig. 8) is located in Promethei Terra at the eastern rim of the Hellas impact basin (39° S, 102.8° E).

The impact crater is filled by what was described as a debris-covered piedmont-type glacier based on analysis of HRSC data (Head et al. 2005). The most widespread large-scale past glacial record appears to be in the Noachian-Hesperian southern circumpolar Dorsa Argentea Formation (DAF) (Tanaka and Kolb 2001) and related highland glacial ice accumulations (Wordsworth et al. 2013, 2015, Fastook and Head 2014). The DAF includes sinuous ridges interpreted to be eskers, which formed as sediment accumulated within former subglacial drainage channels (Kargel and Strom 1992; Head and Pratt 2001; Butcher et al. 2016; Scanlon et al. 2018). The record also includes large, elongated basins, interpreted to be subglacial and proglacial meltwater cavities (Head and Pratt 2001), and possibly subglacial volcanoes in the Sisyphi Montes (Ghatan and Head 2002), but does not include characteristic landforms such as drumlins, moraines, or glacial grooves, which are not expected to extensively form under the lower Martian gravity (Grau Galofre et al. 2022).

Current Record: Mars hosts two large polar ice deposits in the north and south polar regions, consisting largely of water ice with a small dust fraction (5–10% respectively, Smith et al. 2020; Orosei et al. 2024). These deposits exchange volatiles and dust with the atmosphere and regolith on timescales from seasonal to hundreds of millions of years, and thus their internal structure holds a long-term record of climate (Byrne 2009; Milkovich et al. 2008, Becerra et al. 2017, 2019). Both the north and south polar deposits consist of a basal unit, a permanent polar layered deposit (PLD), a residual cap, and a seasonal cap (Byrne 2009; Orosei et al. 2024); however, the ages of the two deposits diverge, with the south polar deposit being much older (~100 Myr) than the northern one (~10 Myr) (Byrne 2009). Orosei et al. 2024, contains a detailed account of the polar deposits of Mars.

There are various lines of evidence for excess ice in the mid-latitudes of Mars (+/- 30 degrees) (e.g. Bramson et al. 2017; Dundas et al. 2018; Levy et al. 2014; Stuurman et al. 2016; Viola and McEwen 2018; Dundas et al. 2023), both at present and in the past. In addition, water ice at the midlatitude regions has been detected at both shallow (~1–2 m) and greater depth (a few tens of meters). Fresh impact craters uncover the presence of shallow buried ice in the mid-latitudes (Byrne 2009; Dundas et al. 2018, 2023), and subsurface radar reflections reveal the presence of debris-covered glaciers (Holt et al. 2008; Plaut et al. 2009). However, it is still unclear whether the small-scale debris-covered glaciers on the surface have a similar origin, age, and formation mechanism to the deeper excess ice (Dundas et al. 2018). The formation and distribution of debris-covered glaciers (Fig. 8) are controlled by the climate and therefore provide a unique record of the past and recent climate of Mars (e.g., Forget et al. 2006).

The debris-covered glaciers include lobate debris aprons (LDA) (e.g., Mangold 2003; Hauber et al. 2008), lineated valley fill (LVF) (e.g. Head et al. 2006), concentric crater fill (CCF) (e.g., Levy et al. 2010a), viscous flow features (e.g., Milliken et al. 2003), and glacier-like forms (e.g., Hubbard et al. 2014). Their formation time frame varies among different studies, but they are generally believed to have formed during the Middle to Late Amazonian (e.g., Berman et al. 2015, Head et al. 2005, 2010, Mangold 2003; Parsons and Holt 2016). Tropical Mountain Glaciers (TMG), Latitude dependent mantle (LDM) covers a large part of the mid- and high latitudes in both hemispheres (e.g., Kostama et al. 2006; Mustard et al. 2001; Kreslavsky and Head 2002; Head et al. 2003).

Periglacial Landforms: Geomorphological interpretations of periglacial landforms first aided in the identification of ground ice on Mars from Viking images, with later efforts focusing on the link between distribution and morphology of patterned ground and buried ice, followed by the in-situ detection of a shallow ice table by the Phoenix lander (e.g., Squyres and Carr 1986; Mangold 2005; Morgan et al. 2021).

HRSC data has allowed for a medium resolution characterization of the geomorphology and regional distribution of Martian patterned ground, including stripes, polygons, scalloped depressions, stone circles, mounds, pitted terrain, brain terrain, and lobate gelifluction forms (e.g., Balme et al. 2013), which form due to the near surface thermal expansion and phase changes (melt/sublimation) within ice rich substrates upon daily, seasonal, or obliquity driven surface temperature and pressure conditions. Examples of patterned ground observations focus notably on the northern hemisphere, (e.g., Balme et al. 2013; Korteniemi and Kreslavsky 2013), with some focus on equatorial regions, (e.g., Fairén et al. 2012; Balme and Gallagher 2009), and globally (Levy et al. 2009). Comparisons with terrestrial patterned ground analogues in Svalbard using the DLR airborne HRSC-AX camera, with HRSC-like capabilities (Hauber et al. 2011) have been key to the interpretation of Martian patterned ground types and their implications for the emplacement environment (sublimation/melt) and substrate nature and have highlighted important Earth-Mars differences in scale and morphometry here, as well as in Antarctica (e.g., Levy et al. 2010b).

Multiple processes, including links with ground ice and snowpacks, have been identified as possibly responsible for Martian gully formation. Several studies have concluded that gullies could form or be considerably modified without the need for liquid water, through dry mass wasting, ‘frosted granular flows’ (FGFs), or CO₂ sublimation. However, water has also been invoked as a possible mechanism driving gully incision and may involve a combination of several processes, from ice or snowmelt, possibly sourced from latitude dependent mantle, groundwater, or debris flows (e.g., Balme et al. 2006 and Kneissl et al. 2010 for Mars Express derived observations, Harrison et al. 2015 for the most recent global map). Most recently, Dickson et al. (2023) have shown that CO₂ mobilized from the south polar region can raise atmospheric pressure sufficiently to permit ice melting and water flow at gully locations, suggesting a hybrid CO₂-liquid water flow origin. See also Thomas et al. 2024.

Climate implication: HRSC, through topographic and image data, has highlighted the glacial landforms that have been key to understanding both the early and recent climate history of Mars (Fig. 9). The presence, direction, and distribution of eskers on the Dorsa Argentea Formation enabled the placing of constraints on the pressure conditions of Mars’ atmosphere at the Noachian-Hesperian transition, as well as its water inventory and surface temperature (e.g. Fastook et al. 2012; Butcher et al. 2017). HRSC observations of LDM and VFF distribution demonstrated the presence of ice on sites where it is not currently stable, implying that past obliquity and atmosphere conditions were once more conducive to the accumulation, crystallization, and flow of ice, and thus that Mars has undergone ice ages (e.g., Head et al. 2003; Head 2011).

Once more, the distribution of ice deposits by latitudinal bands with little control by elevation, as is inferred from SWIM team mapping efforts incorporating HRSC data (Fig. 9), implies little adiabatic cooling (thus low atmospheric pressure) since the time of VFF formation. In contrast, findings of tropical glaciers and ice masses on the Tharsis Montes flanks demonstrated fundamental Earth-Mars ice mass balance differences driven by lower surface pressures and low surface temperatures (Fastook et al. 2008). Current presence of ground and buried glacial ice is recorded by periglacial landforms, including polygons and other patterned ground. On Mars, as on Earth, surface and ground ice is fundamental to the understanding of past climate: its distribution records atmospheric and orbital characteristics, its flow the surface and subsurface thermal history, its extent is limited by the water inventory at the time (e.g. Carr and Head 2015), and its presence could provide water sources in recent periods of Mars history.

5 Ages of Erosional/Depositional Activity

The analysis of accumulated crater populations is a key technique in understanding the sequence and timing of action of geological processes on the surface of Mars. Being one of the scientific justifications for the HRSC instrument, the application of the method has considerably expanded over the 20 years of the Mars Express mission. Here we summarise the findings of more than 75 studies of the timing of fluvial, glacial and aeolian processes which made use of HRSC data, often in combination with other datasets.

Among the works analysed, authors used three different Mars chronology systems, commonly referred to as the Neukum, Hartmann and Ivanov chronologies (Hartmann and Neukum 2001; Neukum et al. 2001; Ivanov 2001). Although the systems differ in the detail of their numerical description, they are fundamentally close in concept, even sharing

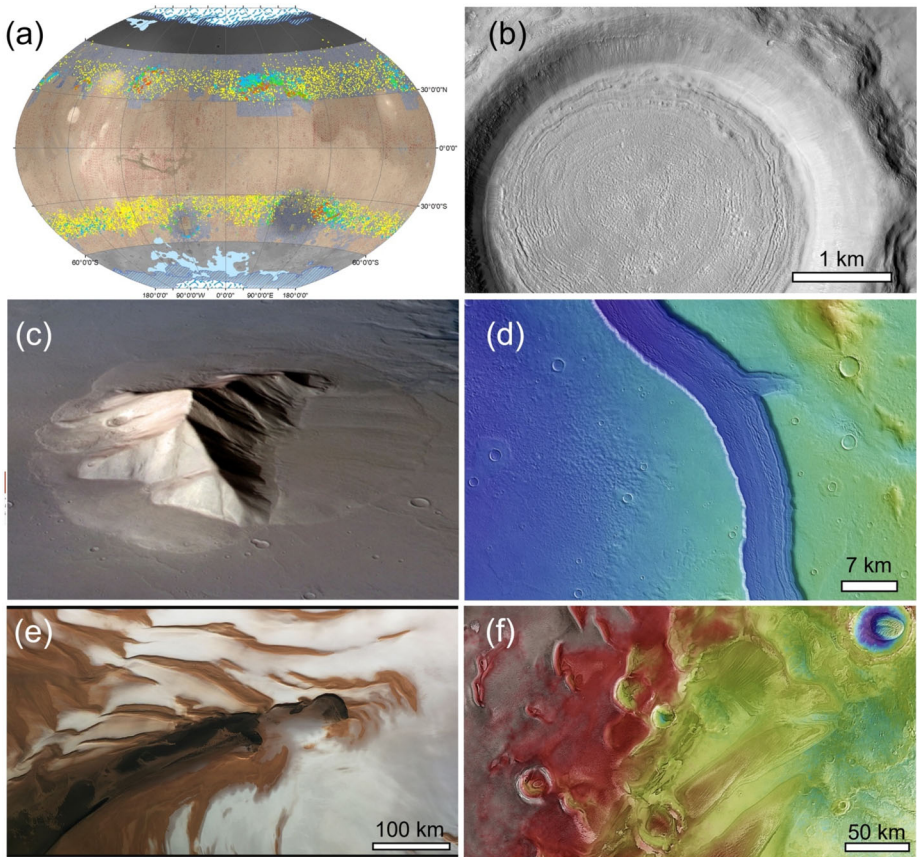


Fig. 9 Glacial deposits as seen by HRSC. (a) Global map of Mars showing the distribution of ice and glaciogenic deposits on Mars, excluding periglacial terrain and LDM (MOLA/HRSC with hillshade). Late Amazonian north and south polar residual caps (PRC) are drawn in patterned white and blue, whereas Amazonian polar layered deposits (PLD) are shown in dashed blue lines. Hesperian polar units, including the Daf, are shown in light blue in the polar regions. Mid latitude ice is shown in yellow (CCF), blue (LDA), orange (LVF), and younger GLFs are shown in green. Ice rich zones, as determined by the Subsurface Water Ice Mapping (SWIM) program are shown in blue, whereas ice depletion is shown in brown. The four panels show examples of glaciogenic terrains: A CCF (b), an LDA (c), a color-shaded terrain image of Reull Valles LVF (d), a scarp on the NPLD (e) and color-shaded terrain in Ulyxis Rupes showing the SPLD (f) (all north to the top). (b)-(f) (ESA/DLR/FU Berlin)

parts of their functional descriptions. While it is possible to convert between model ages derived in the different systems, to do it exactly requires knowledge of the crater populations and size ranges used to make the estimates, which are not always described. We therefore present the model ages as given, regardless of the system. The split timescale as shown on Fig. 10, logarithmic back to 3 Ga and switching to linear thereafter, rather well reflects the time-resolving ability of the crater-counting method: it is robust in distinguishing, say, a third of an order of magnitude below 3 Ga, and likewise in resolving 100 Ma beyond. All three chronology systems should agree to those precisions; for finer differentiation between surfaces, measurements within a single chronology system should be used.

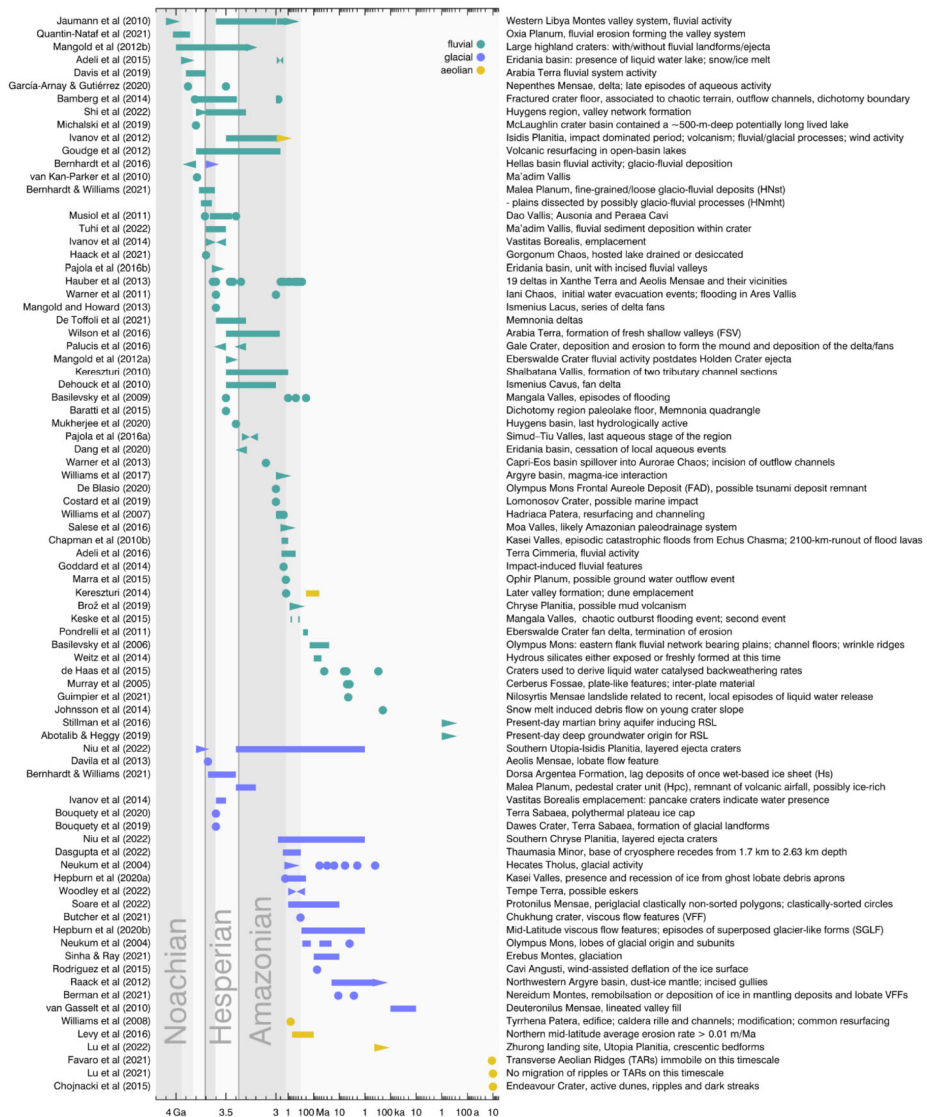


Fig. 10 Overview of chronological studies relating to fluvial, glacial and aeolian surface features from crater size–frequency measurements using HRSC data, coloured by geological process (circles: point measurements, bars: intervals, tapered bars: upper/lower limits). See also Jaumann et al. (2015) citations prior to 2015

A summary of the dating measurements of fluvial landforms (in about 70 works), glacial landforms (about 30) and aeolian features (about 8) using HRSC data is shown in Fig. 10. The measurements are shown in groupings for each published work, organised first by type: fluvial (also including other liquid water processes), glacial, or aeolian; then by maximum model age measured in the work. Each entry is accompanied by a brief description of the site and process as well as the citation. Where a publication describes the transition from one type of process to another, these are shown in a single grouping. The Bernhardt and Williams

(2021) measurements, exceptionally, are shown over four rows. While the symbols illustrate the spread of measured ages for each category of process, it should be noted that the scale of studied areas can vary greatly between works. The intensity of activity may thus be only loosely related to frequency of measurement.

The transition across the timescale for fluvial features, from valley systems, through basin lakes, sediment and delta deposition, channelling, and surface drainage, up to snow melt and RSL features, reflects not only the timing of occurrence of those particular formation processes in particular locations, but also the bias of our backward-looking view onto the history of the planet. The sequence is simultaneously one of survivability, the evidence of events which can be observed today being only that which has not been obliterated by later activity, which therefore, in general, has to be progressively diminishing in topographic expression. No doubt, many of the events along the timescale were preceded by others of similar type from which traces no longer remain. A symbol of this sort may perhaps be usefully interpreted as a record of the last survivors of traces from different processes, rather than a transparent view of the history of all their activity.

This sequence of survivability relates to a general expectation in crater dating that smaller scale features will be found to be younger. Occasionally proffered as a limitation of the dating technique, that argument is unsatisfying. More directly considered, it results from the fact that as you examine smaller areas, the features you observe relate to a shallower depth of surface material, which is indeed likely to have changed more recently. It is always imprecise to think of a region of surface as having 'an age': it is a witness to a complete history of processes which leave traces of different magnitudes. The traces themselves, as structural configurations of surface material, may have ages, and various at different scales can be present at the same location.

Because ice has a lower efficiency than water in moving material, it may be expected to produce features with less topographic expression for comparable time of action, making its traces less survivable, which could be a factor in the later onset of glacial forms. Obviously, for aeolian processes, this efficiency effect is extreme, so that remaining features relate only to recent time periods.

The HRSC studies indicate the availability of liquid water at the surface of Mars through most of its history until recent periods. Modelling of flow transport processes revealed that the formation of deltas on Mars geologically requires only brief timespans (Hauber et al. 2009; Kleinhans et al. 2010) and, based on discharge estimates, the formation of erosional valleys also needs short geological timespans (Jaumann et al. 2005, 2010). A major contribution of Mars Express is the discovery of repeated H₂O-related geological processes on Mars (e.g., Neukum et al. 2010). Crater counting model ages (Michael 2013) representing resurfacing events account of the times when fluvial/glacial processes were active, revealed by comparative age dating of, fluvial, glacial, and lacustrine deposits (Neukum et al. 2010), (Fig. 10). Evidence for water related geological activity could be identified from times before 4 Ga until today, showing episodic events with pulses in the intensity of fluvial/glacial processes at ~ 3.8 – 3.3 Ga, 2.0 – 1.8 Ga, 1.6 – 1.2 Ga, ~ 800 – 300 Ma, ~ 200 Ma, and ~ 100 Ma, and possibly a weaker phase around ~ 2.5 – 2.2 Ga ago (Neukum et al. 2010). Some identified geological activities partially coincide with the known age groupings of the Martian meteorites at ~ 1.3 Ga, ~ 600 – 300 Ma, and ~ 170 Ma (e.g. Neukum et al. 2010; Jaumann et al. 2015).

6 Aeolian Activity and Landforms

The action of wind has left its traces all over the Martian surface. Today, it is the only agent (besides impact erosion) that still shapes the planet's surface to a notable degree. In its geologic history, Mars provided an abundance of sources and processes (glacial, fluvial, volcanic) that produced fine grained material, that can be transported by wind. In its early history, when the atmosphere was thicker, winds on Mars were even more capable of lifting surface sand and dust particles but also nowadays wind action is still observable. The bedforms and landforms shaped by aeolian processes on Mars are subdivided by the two major types of wind action: deposition and erosion. We focus here on geomorphological features that have been observed and analyzed visually by Mars Express HRSC data. Some features of aeolian deposition and erosion including transverse aeolian ridges (TARs), depositional wind streaks, the north polar erg (Olympia Undae), laminated polar terrain as well as smaller erosional features like ventifacts, grooves, periodic bedrock ridges (PBRs) will not be discussed here.

Depending on the grain size and wind speed and the resulting mode of transport mechanism (suspension, saltation, and creep (e.g., Bagnold 1974)), aeolian deposition results in a dune by saltation or a sand or dust sheet by suspension or creep. The dune type itself is dependent on the degree of sand availability and the wind regime.

Aeolian Deposits

In contrast to Earth, most of the prominent Martian dunes are dark-toned. Lower resolution images (150–300 m/pixel) from Mariner- and Viking-times showed “dark splotches” in impact craters (Christensen 1983; Thomas 1984) associated with emergent wind streaks. But also, widespread dark sand sheets are likewise prominent on the Martian surface and were discovered by telescopic observations long before the age of orbital remote sensing. Already early spectral investigations revealed the mafic composition of the dark aeolian material, dominated by pyroxene and olivine, disclosing its unweathered nature (Carter et al. 2024)

Dune Types and their Distribution: Dune types on Mars comprise all common shapes that occur also on Earth but in different abundances. Their small-scale (< 20 m/pixel) morphology was already identified with visual imagery acquired prior to the MEX mission. The first global inventory and characterization of dunes on Mars was provided by the Mars Global Digital Dune Database (MGD3) – a survey based on THEMIS VIS and MOC NA data and later extended to polar regions and higher resolution CTX data (e.g., Hayward et al. 2007; Hayward 2011; Hayward et al. 2014; Fenton 2020). The statistics revealed that barchan dunes and barchanoid ridges are the most common dune types on Mars (e.g., Breed et al. 1979), followed by transverse dunes, linear dunes, star dunes and domes (e.g. McKee 1979). A non-negligible portion accrues to unclassified dunes, which are either intermediate dune types of unusual morphology or not classifiable due to insufficient image resolution.

A detailed global investigation of dark dunes in Martian craters based on HRSC data has been accomplished (Tirsch 2009; Tirsch et al. 2011). They studied 70 intra-crater deposits across Mars, characterized dune deposition types, mineralogical composition, grain size, formative wind directions and its relation to local wind patterns, determined the potential mobility of the dunes, checked for dependencies of these parameters among each other and with geographical location as well as deduced possible sources of the dark aeolian sediments. Their findings on the dune type distribution agree perfectly with the MGD3 results. In more than half of the 70 studied craters, the aeolian bedforms were associated with sand sheets, which is likewise consistent with the statistics of the MGD3. It is interesting to note the least common type on Mars, i.e., linear, or longitudinal dunes, is the most common type on Earth, whereas barchans dominate the Martian dune types indicating limited

sand supply on Mars. Larger dark dune fields on Mars often exhibit a complex dune pattern, with different dune types coexisting or overlapping like in ergs or draas on Earth (Wilson 1972). Silvestro et al. (2008) and Silvestro et al. (2010) analyzed complex dunes fields in the Thaumasia region with HRSC data and found them to comprise barchans, barchanoid ridges, transverse dunes, reversing dunes, star dunes and domes indicating that complex multi-directional wind regimes influenced the development of the dune fields. Secondary dune patterns and slip faces furthermore point to subsequent episodes of aeolian deposition and modification.

Measurements in HRSC DEMs revealed complex dune field heights of up to 400 m and volumes of up to 84 km³ for the ergs in Thaumasia (Silvestro et al. 2008, 2010; Dasgupta et al. 2022). Dune volume calculations by means of HRSC data have also been presented by Jouannic et al. (2012), who studied the Russel crater dune field and estimated a volume of $\sim 3.9 \times 10^{10}$ m³ for this megadune. This number was crucial for the estimation of the possible water content of this frozen dune that in turn was used to explain the occurrence of more than 300 gullies on its slip faces (Reiss and Jaumann 2003).

Chojnacki et al. (2010), Chojnacki et al. (2014a) and Chojnacki et al. (2014b) accomplished comprehensive studies of dune fields in Valles Marineris and used HRSC topographic profiles to evaluate potential sand transport pathways in relation to chasm wall slopes and slip face orientation. The derived chasm slopes showed angles of response that clearly indicate downslope transport of the sand-sized dune material. For many of the Valles Marineris dunes, relatively short (<10 km) and narrow (<1 km) distinct sand transport pathways could be identified by means of HRSC slope profiles (Chojnacki et al. 2014b), proving chasm walls to be local erosional sources for the falling and floor dunes at Valles Marineris.

Dunes and their Relation to Wind Regimes: To analyse whether Martian dunes could be records of past wind regimes and climates a morphological study of 550 dune fields based on HRSC (among other visual imagery) has been conducted by Gardin et al. (2012). The results demonstrated that dunes slip faces are only partially in agreement with current wind regimes predicted by General Circulation Models (GSM) leading to the conclusion that larger parts of them are fossilized and have accumulated under paleoclimate conditions. These findings are consistent with the HRSC-based investigations (Tirsch et al. 2006; Tirsch 2009) who already suspected that dune fields on Mars are constituted of active and fossilized dunes, as indicated by their misalignment with current wind models of the Mars Climate Database (Forget et al. 2007). Some dune fields in this study are even to be indurated or are covered by duricrusts as indicated by their higher thermal inertia in TES and THEMIS data. These key observations and predictions have been recently confirmed by Tianwen-1 Zhurong rover surface observations in the Utopia Planitia region, where dune orientation, cementation and erosion have been linked (Liu et al. 2023) to the end of the recent ice age (Head et al. 2003).

Origin of dark Aeolian Material: A major finding of this global HRSC-based study of dark intra-crater deposits was that re-exposed dark layers (of possible volcanic ash) seem to serve as local sources for the dark aeolian deposits in impact craters on Mars (Tirsch et al. 2011). This conclusion is strengthened by HRSC perspective views showing such layers at crater walls, intra-crater pit walls (Fig. 11), or smaller craters on the floor of larger craters, intersecting dark-toned layers beneath the crater fill.

Curiously, there is ample evidence of dark aeolian material being transported out of the craters, in the form of wind streaks, but almost no evidence of material being transported into the craters from the outside. HRSC color data suggest that the supposed dark sources in smaller craters are not shadows, but are in fact composed of mafic material, which is typically shown in the blue color in the RGB composites. Confirmation of the mineralogical congruence between the suggested source layers and the dune sands has been provided

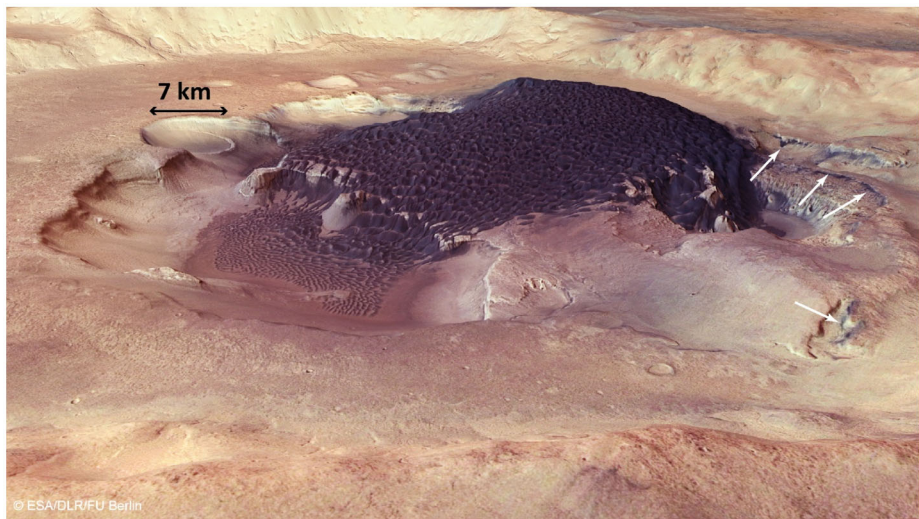


Fig. 11 HRSC perspective view of a dark barchanoid dune field in Rabe crater superposing a large intra-crater pit. Dark layers exposed along the pit walls (white arrows) seem to serve as local sediment sources for the dune material (e.g., Tirsch et al. 2011). The mean diameter of this irregular pit is 55 km. (ESA/DLR/FU Berlin)

by spectral analyses of OMEGA and CRISM data presented in this study. Measurements in topographic profiles derived from HRSC DEMs showed that the elevations of craters that expose dark source layers vary in depth, suggesting that multiple layers of buried dark material may exist in the Martian subsurface (Tirsch et al. 2011).

A similar hypothesis was put forward in another HRSC-based study of dark material on the plateaus of Valles Marineris by Chapman et al. (2011), who suggest that the material might have been locally derived from eroded outcrops of lithified dark-toned layered rocks between <10 m and >100 m thick. Central mounds in impact craters in Arabia Terra were analyzed using HRSC and other datasets to answer the question of whether they could serve as local sediment sources (Pan et al. 2019). However, the results did not provide a clear picture, and the authors suggest that young volcanic processes may have contributed to the formation of the mafic sands.

It should be noted that several other sources for the dark dune material on Mars were proposed based on analyses of various orbital datasets. These involve the disintegration of lithified lava (Greeley and Spudis 1981; Edgett and Lancaster 1993), the breakdown of the Medusae Fossae Formation (Burr et al. 2011), the action of glacier retreat at shield volcanoes (Grégoire et al. 2007), erosion of intra-rift sediment sources including interior layered deposits (Chojnacki et al. 2014b) or the erosion of proximal sand-bearing basaltic sedimentary rocks (Ehlmann et al. 2017; Lapotre et al. 2017). For the dunes in Gale crater, different local sediment sources have been suggested. These involve eroded and transported mafic bedrocks from Gale's crater wall (Ehlmann and Buz 2015) and felsic crater floor materials (Sautter et al. 2015; Lapotre and Rampe 2018).

Deflation is a process by which wind turbulences lifts and removes loose material from the surface. Traction or surface creep, saltation, and suspension are the three mechanisms by which this occurs. Traction or surface creep involves larger grains sliding or rolling across the surface. Saltation involves particles bouncing across the surface for short distances, while suspended particles are fully carried by the wind for long distances.

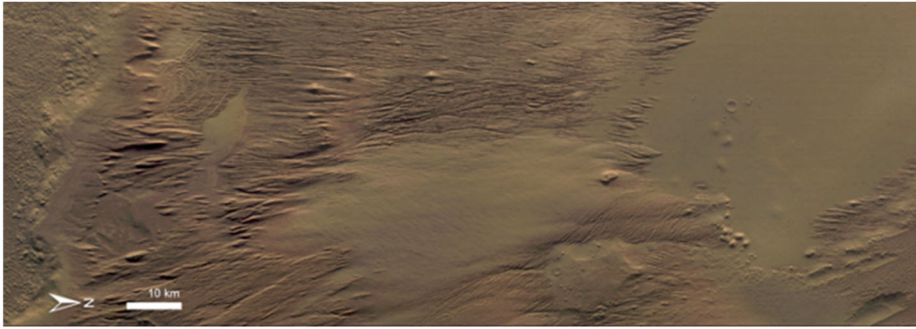


Fig. 12 HRSC orbit 5114 showing extensive yardang fields in the Medusae Fossae formation

Abrasion (also termed corrasion) is the process by which suspended or saltated grains wear material from consolidated landforms. Rock clasts shaped by aeolian abrasion develop facets perpendicular to the formative wind, termed ventifacts.

When fine dust particles are transported from the surface into the atmosphere this is known as dust raising or dust lifting. On Mars this is typically caused by wind, as with deflation described above, and thermal changes. Diurnal and seasonal thermal cycles can cause air near the surface of the planet to expand or contract, creating air currents that can lift dust.

Types and Distribution of Erosional Landforms: Aeolian erosion of large bedrock exposures produces yardangs (e.g. Ward 1979; Ward et al. 1985; Melosh 2011; Mandt and Leone 2015) (Fig. 12), which typically exhibit a streamlined shape resembling inverted boat hulls on Earth and Mars. They form parallel to their formational wind in erodible bedrock exposures due to abrasion from entrained sediments.

They form on highly erodible rocks or consolidated sediment and are on Mars typically observed in the equatorial regions (Ward 1979; Greeley et al. 1993). According to Neukum et al. (2010), yardangs are relatively young features due to their low crater densities. Additionally, Ward (1979) observed that many yardangs do not align parallel to the direction of wind streaks, suggesting that they were formed by different winds from those that created the wind streaks.

HRSC imagery showed that yardangs can exhibit linear ridge and curvilinear morphologies in the Medusae Fossae Formation (Liu et al. 2021). HRSC Digital Elevation Models (DEMs) were used to classify yardang morphology and suggest an evolutionary sequence (Wang et al. 2018).

Wind streaks are linear features that are typically several kilometers long and less than 100 meters wide. Bright wind streaks appear bright and contrast with the darker surface material, while dark wind streaks appear darker than the surrounding surface material. The higher albedo of the bright wind streaks is believed to be due to the removal of darker surface material by deflation, exposing a lighter layer beneath. They are often seen in areas with a lot of loose, fine-grained material, such as sand dunes or rocky terrain. On the other hand, the lower albedo of the dark wind streaks is believed to be due to the accumulation of windblown dust and sand on the surface.

Multitemporal HRSC coverage revealed that both bright and dark wind streaks on Mars are active surface processes can change over time as they are eroded away by the wind or covered over by new deposits of dust and sand. Jehl et al. (2008) demonstrated that multiple HRSC passes over the same region could be used to derive integrated phase functions over a

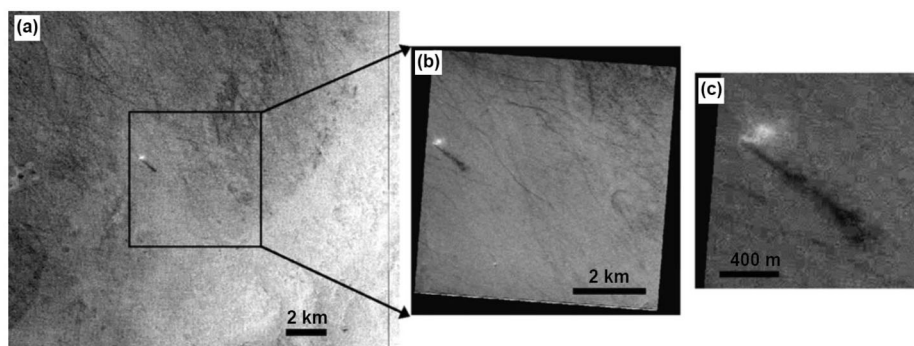


Fig. 13 Dust devil and dust devil tracks in Peneus Patera as seen in the HRSC nadir image of orbit 2133 (map scale 25 m/pixel). The black square outlines the location of the corresponding SRC image. (b) The higher resolution SRC image (with 5 m/pixel) reveals many more dust devil tracks than seen in the nadir image. (c) A magnified view of the dust devil captured in the SRC image in panel (b), highlighting the kink between its lower and upper sections. North is to the top of each image. (modified from Stanzel et al. 2008)

wide range of phase angles, which shed light on the photometric diversity of Martian surface properties. The dark streaks at Gusev crater, the Spirit rover landing site, were deemed to be consistent with large basaltic sand grain sizes organized in more or less packed layers. This was evidenced by their low single scattering albedo, greater backscattering than any other surface across Gusev and Apollinaris, high surface roughness, and present variable surface states. Multi-temporal HRSC and THEMIS-VIS imagery were used to investigate variations in wind streaks and dust devil tracks in Gusev crater, as reported by Greeley et al. (2005) and Greeley et al. (2006). The study revealed that the streaks exhibited a fading trend, resulting in increased brightness, which may be attributed to the deposition of atmospheric dust. Thomas et al. (1981) investigated wind streaks on a northern area of Mars and suggested that they served as a pathway for sand transport within the crater (Rodriguez et al. 2010).

Dust devils (Fig. 13) are low pressure atmospheric vortices that entrain dust and (potentially) sand from Mars' surface. Much like their terrestrial counterparts, these swirling columns of air are caused when the surface is heated by the sun and the resulting temperature difference between the surface and the overlying air causes a vortex to form. On Earth dust devils are rare events confined to arid environments, whereas Martian dust devils occur at an estimated rate of 1 per sol per km² (Jackson et al. 2018) ubiquitously across the surface and moreover are three times larger than Earth dust devils (Lorenz 2020). Consequently, they are a major contributor to dust lifting into the atmosphere and the background dust haze (Balme and Greeley 2006), which profoundly influences global climate as these aerosols alter atmospheric thermal structure and circulation (Kahn et al. 1992; Reiss et al. 2011).

Before Mars Express, much of these details about the sizes and dynamics of dust devils was unknown, as the only way to detect them was to monitor variations in local meteorological parameters, such as wind velocity, pressure, temperature, and dust loading at landing sites (Ringrose et al. 2003). The nadir and stereo views of HRSC enabled the capture of multiple instances of individual dust devils (Stanzel et al. 2006, 2008), which have been observed to have diameters of 50 meters or greater. The ability to consistently determine the forward motion parameters of dust devils in orbital images has been significantly improved by HRSC, which provides time-sequence imaging of the planet's surface (Neukum et al. 2004; Jaumann et al. 2007). By analyzing images from the HRSC's nadir and two stereo

channels, Stanzel et al. (2006) were the first to study the motion of dust devils and reported the forward speeds of 205 events across both hemispheres of Mars. They compared the observed forward velocities with the wind regime predicted by the Martian Climate Database (MCD) (Lewis et al. 1999; Forget et al. 1999; Millour et al. 2008) and found that the vortex directions were generally consistent with the modelled winds. However, they also noted cases of chaotic behavior in the dust devil forward directions, such as in Terra Cimmeria. Reiss et al. (2011) compared images from the HRSC, and the Martian Orbital Camera (MOC) taken of Syria Planum with a time delay of up to 12 hours to identify dust devils captured by both instruments. Based on the HRSC images, they estimated an average travel speed of 12 m/s.

7 Climate Record and Implication for Climate History

One of the key parameters for reading and interpreting the record of the ancient climate of Mars is the presence of landforms and deposits that provide proxies for ambient “warm and wet” conditions (evidence for running water, streams, lakes, and oceans; mean annual temperatures (MAT) $\gg 273\text{K}$) and proxies for ambient “cold and icy” conditions (polar ice caps, ice-covered surfaces, glacial and periglacial landforms; mean annual temperatures (MAT) $\ll 273\text{K}$). A second major proxy for reading the climate record is the nature of the alteration of surface mineralogy (phyllosilicates suggesting warm, water-rich environments; sulphates suggesting the role of volcanic gas exhalations; anhydrous ferric oxides suggest a cold and liquid water-poor climate. A third proxy for reading the climate record is the combination of these two: the geological setting of surface mineralogical alteration.

Mars Express data have provided substantial and compelling evidence for documenting and deciphering the Mars climate record. Although phyllosilicates have been shown to be widespread in Noachian-Early Hesperian environments (Bibring et al. 2006), suggesting a ‘warm and wet’ climate, the geological setting of many of these occurrences are often not in association with other morphological features (valley networks, etc.) indicative of surface water. Some studies have suggested a subsurface alteration source, perhaps related to warm groundwater flow (Ehlmann et al. 2011 Ehlmann and Edwards 2014) and subsequently brought to the surface by impact cratering (e.g., Carter et al. 2013). Others suggest that near-surface weathering under different climate conditions (e.g., Bishop et al. 2018), impact-generated hydrothermal alteration (e.g., Tornabene et al. 2013), torrential hot rains accompanying the Early Noachian large impact basins (e.g., Hellas, Isidis, Argyre; Palumbo and Head 2017), and/or a supercritical steam atmosphere associated with the late stages of the magma ocean era (e.g. Cannon et al. 2017), may have been factors.

The geological evidence for surface liquid water runoff of Mars in the Late Noachian-Early Hesperian is irrefutable; Mars Express data have documented the distribution, topography, morphology, and impact crater size-frequency distribution (CSFD) absolute model ages (AMA) for fluvial valley networks and associated open and closed-basin lakes. These data have also revealed the downslope destination of the combined drainage networks, permitting assessment of their relationship to a hypothesized Noachian northern lowland ocean; recent studies (e.g., Deutsch et al. 2020) fail to find a convincing link. Despite these convincing data, at issue is their relationship to the ambient, or background climate. An excellent case has been made that they represent the presence of a Late Noachian-Early Hesperian ambient ‘warm and wet’ climate, characterized by ambient clement climate with MAT $\gg 273\text{K}$. In stark contrast, climate models for this period of Mars history are unable to reproduce such conditions, due to the “faint young Sun” effect (75% current luminosity), even under a wide

range of model parameters. Instead, the climate models predict a “cold and icy” climate, with MAT of $\sim 225\text{K}$, accompanied by an adiabatic cooling effect that produces snow and ice deposits in the high topography above about +1 km elevation. Although this ambient ‘cold and icy highlands’ scenario places glacial water as ice at the headlands of many valley network systems, it requires a transient heating mechanism (e.g., release of greenhouse gases, etc.) to melt the snow and ice to form the valley networks, open and closed-basin lakes. This debate is currently ongoing and Mars Express data are being used to marshal evidence to test both hypotheses, and to propose new experiments and future missions.

Geomorphic evidence for huge outflow channels, sourced primarily in the circum-Tharsis region, and mineralogic and geomorphic evidence for Interior Layered Deposits (ILD) on the floor of Valles Marineris, are also proxies for ambient climate conditions in the Hesperian. What is the origin, state, and depositional environment of the water that produced the outflow channels? Most hypotheses call on catastrophic release of overpressurized groundwater for the outflow channels, an interpretation that requires a global cold and icy ambient climate and a continuous global cryosphere that is sufficiently thick in equatorial regions. On the other hand, processes for the closely contemporaneous ILD deposits and adjacent similar deposits at Meridiani, require equatorial rainfall, shallow groundwater migration, and groundwater upwelling at mid-latitudes, a climate interpretation inconsistent with the presence of a global cryosphere. Furthermore, in a global cold climate, Tharsis is predicted to be the site of extensive snow and ice deposits, and the confluence of extensive Tharsis volcanism and surface snow and ice have compelled researchers to re-examine the role of volcano-ice interactions as a potential source of large quantities of liquid water. Whatever its origin, what is the fate of the massive volumes of water that flowed through the outflow channels? Detailed analysis of morphology and ages from Mars Express data show that the water debouched into the northern lowlands, and many investigators believe that it filled the lowlands with a vast ocean of liquid water that persisted for significantly long periods of time, such that subsequent impacting bolides into the ocean produced massive tsunamis (De Blasio 2020). Others have postulated that the outflow channels formed episodically, each separated by tens to hundreds of millions of years, and that any liquid water flowing into the northern lowlands would rapidly freeze and sublimate, returning to global cold traps. Mars Express data are essential to addressing these conundra, and in designing and planning new missions to help resolve them.

Mars Express data for Amazonian-aged morphologic features, deposits, and mineralogy have provided widely accepted evidence that the ambient Mars climate was cold, dry, and icy. Surfaces of these ages are characterized by Antarctic Dry Valley-like alteration environments (anhydrous ferric oxides), typical of very cold ambient temperatures, low atmospheric water abundances, and generally anhydrous conditions. Morphologic and topographic data and investigations from Mars Express have amply and convincingly compiled copious amounts of supporting data for the presence of this ambient climate in the form of a wide variety of glacial and periglacial landforms (e.g., lobate debris aprons, lineated valley fill, glacial mantles, contraction-crack polygons, etc.). Located at a full range of latitudes (all the way down to tropical mountain glaciers), these features, and the CSFD absolute model ages enabled by Mars Express data, reveal a record of the importance of obliquity changes driving mobilization of polar ice and its redistribution to varying latitudes throughout the Amazonian, as a modulator of the ambient cold and icy climate. The presence of gullies (alcove, channel, and fan) has been interpreted to indicate melting of snow and ice even under these extremely cold and dry conditions, similar to today’s Antarctic Dry Valley climate, but alternate “dry” scenarios involving CO_2 sublimation appear to be a convincing contributor to currently observed changes in the gully morphology. Current debate centers on whether

one process or the other dominates, or whether they might operate in concert over longer timescales.

Taken together, Mars Express geomorphological data have provided a giant leap in our documentation and understanding of the record of water-related process on Mars, and as proxies for deconvolving the complex and debated climate history of Mars. In addition to a significant increase in our understanding, these Mars Express data have sharpened the new questions that have arisen, giving rise to many concepts and future mission proposals to address outstanding question and resolve remaining conundra.

8 Summary and Conclusions

Mars Express data have provided substantial insights into the geological record of water-related processes on Mars, documenting the morphological characteristics, topographic relationships, and chronology of the associated landforms and deposits. Together, these data have revealed a consistent and compelling picture of the role of liquid water flow during the Late Noachian-Early Hesperian (e.g., valley networks, open and closed-basin lakes, and possible northern lowland oceans) and the role of these features in distinguishing between ambient “warm and wet” and “cold and icy” climates that might have been characteristic of early Mars. For the Early Hesperian period, Mars Express data have helped in characterizing volcanic landforms and their chronology, revealing evidence for volcano-ice interactions and the generation of meltwater, the role of volcanic eruption-induced warming and ice melting, as well as the potential contributions of degassed water to the atmosphere and its effects on climate. Important in this regard is the detailed morphologic, mineralogic and topographic characterization of the ILDs, dominated by sulphate deposits in various hydration states. For the Late Hesperian and Early Amazonian period, Mars Express data have revealed details of the morphology and chronology of the massive outflow channels, enabling improved assessment of the quantity of liquid water involved, the timing of its emplacement, and the testing of hypotheses for the formation and fate of a northern lowlands’ ocean. For the Amazonian period, Mars Express data have enabled discovery and documentation of numerous occurrences of non-polar ice deposits, including tropical mountain glaciers associated with the Tharsis Montes; taken together, these deposits have been dated and reveal the presence of ancient ice preserved beneath sublimation till, providing a history of obliquity-induced climate change, and a roadmap for future robotic and human exploration missions. Gullies (alcoves, channels, and fans) mapped in association with a geologically recent obliquity-induced latitude-dependent ice mantle, have suggested either meltwater or CO₂-assisted erosion as the dominant process, a debate that continues today. All these features provide examples of various environments that are known to harbor life on Earth. These discoveries and hypotheses thus provide numerous compelling questions that can be address with future orbital-lander-rover-sample return robotic missions and coordinated human exploration expeditions.

Geomorphological features of aeolian deposition and erosion including transverse aeolian ridges, depositional wind streaks, the north polar erg, laminated polar terrain as well as smaller erosional features like ventifacts, grooves, periodic bedrock ridges are observed by HRSC. Complex dunes fields are found to comprise barchans, barchanoid ridges, transverse dunes, reversing dunes, star dunes and domes indicate complex multi-directional wind regimes. Dark multiple layers in impact crater point to the source dark dune fields that might have been locally derived from eroded outcrops of these lithified dark-toned layered rocks. Over its operational period HRSC images have captured multiple instances of dust devils

with diameters of 50 meters or greater. Comparison of the observed forward velocities with the wind regime predicted by the Martian Climate Database (MCD) show that the vortex directions were generally consistent with the modelled winds.

Acknowledgements The authors thank the International Space Science Institute (ISSI) in Bern, Switzerland for the support. We acknowledge support from ESA. Data Availability Statement The HRSC terrain models and image data are available at the data archives of ESA and NASA and in the map-based data portal at <https://maps.planet.fu-berlin.de> (Walter et al. 2018).

Funding Open Access funding enabled and organized by Projekt DEAL.

Declarations

Competing Interests The authors have no conflicts of interest to declare. All co-authors have seen and agree with the contents of the manuscript and there is no financial interest to report. We certify that the submission is original work and is not under review at any other publication.

Open Access This article is licensed under a Creative Commons Attribution 4.0 International License, which permits use, sharing, adaptation, distribution and reproduction in any medium or format, as long as you give appropriate credit to the original author(s) and the source, provide a link to the Creative Commons licence, and indicate if changes were made. The images or other third party material in this article are included in the article's Creative Commons licence, unless indicated otherwise in a credit line to the material. If material is not included in the article's Creative Commons licence and your intended use is not permitted by statutory regulation or exceeds the permitted use, you will need to obtain permission directly from the copyright holder. To view a copy of this licence, visit <http://creativecommons.org/licenses/by/4.0/>.

References

- Abotalib AZ, Heggy E (2019) A deep groundwater origin for recurring slope lineae on Mars. *Nat Geosci* 12:235–241. <https://www.nature.com/articles/s41561-019-0327-5>
- Adeli S, Hauber E, Le Deit L, Jaumann R (2015) Geologic evolution of the eastern Eridania basin: implications for aqueous processes in the southern highlands of Mars. *J Geophys Res, Planets* 120:1774–1799. <https://doi.org/10.1002/2015JE004898>
- Adeli S, Hauber E, Kleinhans MG, Le Deit L, Platz T, Fawdon P, Jaumann R (2016) Amazonian-aged fluvial system and associate ice-related features in Terra Cimmeria, Mars. *Icarus* 277:286–299. <https://doi.org/10.1016/j.icarus.2016.05.020>
- Al-Samir M, Nabhan S, Fritz J, Winkler A, Bishop JL, Gross C, Jaumann R (2017) The paleolacustrine evolution of Juventae Chasma and Maja Valles and its implications for the formation of interior layered deposits on Mars. *Icarus* 292:125–143. <https://doi.org/10.1016/j.icarus.2016.12.023>
- Andrews-Hanna JC, Phillips RJ, Zuber MT (2007) Meridiani Planum and the global hydrology of Mars. *Nature* 446:163–166. <https://doi.org/10.1038/nature05594>
- Ansan V, Mangold N, Masson P, Gailhardis E, Neukum G (2008) Topography of valley networks on Mars from Mars Express high resolution stereo camera digital elevation models. *J Geophys Res* 113:E07006. <https://doi.org/10.1029/2007JE002986>
- Arvidson RE et al (2011) Opportunity Mars rover mission: overview and selected results from purgatory ripple to traverses to endeavour crater. *J Geophys Res* 116:E00F15. <https://doi.org/10.1029/2010JE003746>
- Bagnold RA (1974) *The physics of blown sand and desert dunes*, 4th edn. Dover, Mineola. <https://link.springer.com/book/10.1007/978-94-009-5682-7>
- Bahia RS (2022) Morphological and hydrological analysis of volcanic flank valleys evidence for a volcanic origin. *Planet Space Sci* 223:105592. <https://doi.org/10.1016/j.pss.2022.105592>
- Bahia RS, Covey-Crump S, Jones MA, Mitchell N (2022) Discordance analysis on a high-resolution valley network map of Mars: assessing the effects of scale on the conformity of valley orientation and surface slope direction. *Icarus* 383:115041. <https://doi.org/10.1016/j.icarus.2022.115041>
- Bahia RS, Grau Galofre A, Mitchell N, Covey-Crump S, Jones M (2023) The fluvial and glacial history of the Argyre Region – as revealed by new valley mapping techniques. *Icarus*, Under Review
- Baker V (2001) Water and the Martian landscape. *Nature* 412:228–236. <https://doi.org/10.1038/35084172>

- Baker VR, Strom RG, Gulick VC, Kargel JS, Komatsu G (1991) Ancient oceans, ice sheets and the hydrological cycle on Mars. *Nature* 352:589–594. <https://doi.org/10.1038/352589a0>
- Baker VR, Carr MH, Gulick VC, Williams CR, Marley MS (1992) Channels and valley networks. In: Kieffer HH, Jakosky BM, Snyder CW, Matthews MS (eds) *Mars*. University of Arizona Press, Tucson, pp 493–522
- Balme MR, Gallagher C (2009) An equatorial periglacial landscape on Mars. *Earth Planet Sci Lett* 285(1–2):1–15. <https://doi.org/10.1016/j.epsl.2009.05.031>
- Balme M, Greeley R (2006) Dust devils on Earth and Mars. *Rev Geophys* 44(3). <https://doi.org/10.1029/2005RG000188>
- Balme MR, Mangold N, Baratoux D, Costard F, Gosselin M, Masson P, Pinet P, Neukum G (2006) Orientation and distribution of recent gullies in the southern hemisphere of Mars: observations from High Resolution Stereo Camera/Mars Express (HRSC/MEX) and Mars Orbiter Camera/Mars Global Surveyor (MOC/MGS) data. *J Geophys Res* 111:E05001. <https://doi.org/10.1029/2005JE002607>
- Balme RM, Gallagher CJ, Gupta S, Murray JB (2011) Fill and spill in Lethe Vallis: a recent flood-routing system in Elysium Planitia, Mars. *Geol Soc (Lond) Spec Publ* 356(1):203–227. <https://doi.org/10.1144/SP356.11>
- Balme MR, Gallagher CJ, Hauber E (2013) Morphological evidence for geologically young thaw of ice on Mars: a review of recent studies using high-resolution imaging data. *Prog Phys Geogr* 37(3):289–324. <https://doi.org/10.1177/0309133313477123>
- Bamberg M, Jaumann R, Asche H, Kneissl T, Michael GG (2014) Floor-fractured craters on Mars: observations and origin. *Planet Space Sci* 98:146–162. <https://doi.org/10.1016/j.pss.2013.09.017>
- Baratti E, Pajola M, Rossato S, Mangili C, Coradini M, Montanari A, McBride K (2015) Hydraulic modeling of the tributary and the outlet of a Martian paleolake located in the memnonia quadrangle. *J Geophys Res*, Planets 120:1597–1619. <https://doi.org/10.1002/2015JE004812>
- Basilevsky AT, Werner SC, Neukum G, Head JW, Gasselt SV, Gwinner K, Ivanov BA (2006) Geologically recent tectonic, volcanic and fluvial activity on the eastern flank of the Olympus Mons volcano, Mars. *Geophys Res Lett* 33. <https://ui.adsabs.harvard.edu/abs/2006GeoRL.3313201B/abstract>
- Basilevsky AT, Neukum G, Werner SC, Dumke A, van Gasselt S, Kneissl T, Zschneid W, Rommel D, Wendt L, Chapman M, Head JW, Greeley R (2009) Episodes of floods in Mangala Valles, Mars, from the analysis of HRSC, MOC and THEMIS images. *Planet Space Sci* 57:917–943. <https://doi.org/10.1016/j.pss.2008.07.023>
- Becerra P, Sori MM, Byrne S (2017) Signals of astronomical climate forcing in the exposure topography of the North Polar Layered Deposits of Mars. *Geophys Res Lett* 44(1):62–70. <https://doi.org/10.1002/2016GL071197>
- Becerra P, Sori MM, Thomas N, Pommerol A, Simioni E, Sutton SS, Tulyakov S, Cremonese G (2019) Timescales of the climate record in the south polar ice cap of Mars. *Geophys Res Lett* 46(13):7268–7277. <https://doi.org/10.1029/2019GL083588>
- Berman DC, Crown DA, Joseph ECS (2015) Formation and mantling ages of lobate debris aprons on Mars: insights from categorized crater counts. *Planet Space Sci* 111:83–99. <https://doi.org/10.1016/j.pss.2015.03.013>
- Berman DC, Chuang FC, Smith IB, Crown DA (2021) Ice-rich landforms of the southern mid-latitudes of Mars: a case study in Nereidum Montes. *Icarus* 355:114170. <https://doi.org/10.1016/j.icarus.2020.114170>
- Bernhardt H, Williams DA (2021) Geology and history of the Malea Planum region: a new view of Mars' oldest large volcanic province. *Icarus* 366:114518. <https://doi.org/10.1016/j.icarus.2021.114518>
- Bernhardt H, Hiesinger H, Ivanov MA, Ruesch O, Erkeling G, Reiss D (2016) Photogeologic mapping and the geologic history of the Hellas basin floor, Mars. *Icarus* 264:407–442. <https://doi.org/10.1016/j.icarus.2015.09.031>
- Bibring J-P, Soufflot A, Berthé M, Langevin Y, Gondet B, Drossart P, Bouyé M, Combes M, Puget P, Semery A, Bellucci G, Formisano V, Moro V, Kottsov V, The OMEGA Co-I team, Bonello G, Erard S, Forni O, Gendrin A, Manaud N, Poulet F, Poulleau G, Encrenaz T, Fouchet T, Melchiorri R, Altieri F, Ignatiev N, Titov D, Zasova L, Coradin A, Capaccioni F, Cerroni P, Fonti S, Mangol N, Pinet P, Schmitt B, Sotin C, Hauber E, Hoffmann R, Jaumann R, Keller U, Arvidson R, Mustard J, Forget F (2004) OMEGA: Observatoire pour la Minéralogie, l'Eau, les Glaces et l'Activité. In: ESA-SP-1240, pp 37–49
- Bibring JP, Langevin Y, Gendrin A, Gondet B, Poulet F, Berthé M, Omega Team (2005) Mars surface diversity as revealed by the OMEGA/Mars Express observations. *Science* 307(5715):1576–1581. <https://doi.org/10.1126/science.1108806>
- Bibring J-P, Langevin Y, Mustard JF, Poulet F, Arvidson RE, Gendrin A, Gondet B, Mangold N, Pinet P, Forget F et al (2006) Global mineralogical and aqueous Mars history derived from OMEGA/Mars Express data. *Science* 312:400–404. <https://doi.org/10.1126/science.1122659>

- Bishop JL et al (2008) Phyllosilicate diversity and past aqueous activity revealed at Mawrth Vallis, Mars. *Science* 321:830. <https://doi.org/10.1126/science.1159699>
- Bishop JL, Tirsch D, Tornabene LL, Jaumann R, McEwen AS, McGuire PC, Ody A, Poulet F, Clark RN, Parente M, McKeown NK, Mustard JF, Murchie SL, Voigt J, Aydin Z, Bamberg M, Petau A, Michael G, Seelos FP, Hash CD, Swayze GA, Neukum G (2013) Mineralogy and morphology of geologic units at Libya Montes, Mars: ancient aqueously derived outcrops, mafic flows, fluvial features, and impacts. *J Geophys Res, Planets* 118:487–513. <https://doi.org/10.1029/2012JE004151>
- Bishop JL, Fairén AG, Michalski JR, Gago-Duport L, Baker LL, Velbel MA, Gross C, Rampe EB (2018) Surface clay formation during short-term warmer and wetter conditions on a largely cold ancient Mars. *Nat Astron* 2(3):206–213. <https://doi.org/10.1038/s41550-017-0377-9>
- Boatwright BD, Head JW (2021) A Noachian proglacial paleolake on Mars: fluvial activity and lake formation within a closed-source drainage basin crater and implications for early Mars climate. *Planet Sci J* 2(2):52. <https://doi.org/10.3847/PSJ/abe773>
- Boatwright BD, Head JW (2022a) Constraining early Mars glacial conditions from paleodischarge estimates of intracrater inverted channels. *Geophys Res Lett* 49(21). <https://doi.org/10.1029/2022GL101227>
- Boatwright BD, Head JW (2022b) Noachian proglacial paleolakes on Mars: fluvial activity and lake formation within closed-source drainage basin craters. *Planet Sci J* 3(2):38. <https://doi.org/10.3847/PSJ/abe773>
- Bouley S, Ansan V, Mangold N, Masson P, Neukum G (2009) Fluvial morphology of Naktong Vallis, Mars: a late activity with multiple processes. *Planet Space Sci* 57(8–9):982–999. <https://doi.org/10.1016/j.pss.2009.01.015>
- Bouley S, Baratoux D, Matsuyama I, Forget F, Séjourné A, Turbet M, Costard F (2016) Late Tharsis formation and implications for early Mars. *Nature* 531(7594):344–347. <https://doi.org/10.1038/nature17171>
- Bouquety A, Sejourne A, Costard F, Mercier D, Bouley S (2019) Morphometric evidence of 3.6 Ga glacial valleys and glacial cirques in Martian highlands: south of Terra Sabaea. *Geomorphology* 334:91–111. <https://doi.org/10.1016/j.geomorph.2019.02.022>
- Bouquety A, Sejourne A, Costard F, Bouley S, Leyguarda E (2020) Glacial landscape and paleoglaciation in Terra Sabaea: evidence for a 3.6 Ga polythermal Plateau ice cap. *Geomorphology* 350:106858. <https://hal.science/hal-02407216/document>
- Bramble MS, Goudge TA, Milliken RE, Mustard JF (2019) Testing the deltaic origin of fan deposits at Bradbury Crater, Mars. *Icarus* 319:363–366. <https://doi.org/10.1016/j.icarus.2018.09.024>
- Bramson AM, Byrne S, Bapst J (2017) Preservation of midlatitude ice sheets on Mars. *J Geophys Res, Planets* 122:2250–2266. <https://doi.org/10.1002/2017JE005357>
- Breed CS, Grolrier MJ, McCauley JF (1979) Morphology and distribution of common ‘sand’ dunes on Mars – comparison with the Earth. *J Geophys Res* 84:8183–8204. <https://doi.org/10.1029/JB084iB14p08183>
- Brož P, Hauber E, Burgt I, Špillar V, Michael G (2019) Subsurface sediment mobilization in the southern chryse planitia on Mars. *J Geophys Res, Planets* 124:703–720. <https://doi.org/10.1029/2018JE005868>
- Buffo JJ, Ojha L, Meyer CR, Ferrier KL, Palucis MC (2022) Revisiting subglacial hydrology as an origin for Mars’ valley networks. *Earth Planet Sci Lett* 594:117699. <https://doi.org/10.1016/j.epsl.2022.117699>
- Buhler PB, Fassett CI, Head JW III, Lamb MP (2011) Evidence for paleolakes in Erythraea Fossa, Mars: implications for an ancient hydrological cycle. *Icarus* 213(1):104–115. <https://doi.org/10.1016/j.icarus.2011.03.004>
- Buhler PB, Fassett CI, Head III JW, Lamb MP (2014) Timescales of fluvial activity and intermittency in Milna Crater, Mars. *Icarus* 241:130–147. <https://doi.org/10.1016/j.icarus.2014.06.028>
- Burr DM, Zimbelman JR, Qualls FB, Chojnacki M, Murchie SL, Michaels TI (2011) The western medusae fossae formation, Mars: a possible source for dark aeolian sand. *Lunar Planet Inst Sci Conf Abstr* 42:1582
- Butcher FEG, Conway SJ, Arnold NS (2016) Are the Dorsa Argentea on Mars eskers? *Icarus* 275:65–84. <https://doi.org/10.1016/j.icarus.2016.03.028>
- Butcher FEG, Balme MR, Gallagher C, Arnold NS, Conway SJ, Hagermann A, Lewis SR (2017) Recent basal melting of a mid-latitude glacier on Mars. *J Geophys Res, Planets* 122:2445–2468. <https://doi.org/10.1002/2017JE005434>
- Butcher FEG, Balme MR, Conway SJ, Gallagher C, Arnold NS, Storrar RD, Lewis SR, Hagermann A, Davis JM (2021) Sinuous ridges in Chukhung crater, Tempe Terra, Mars: Implications for fluvial, glacial, and glaciofluvial activity. *Icarus* 357:114131
- Byrne S (2009) The polar deposits of Mars. *Annu Rev Earth Planet Sci* 37:535–560. <https://doi.org/10.1146/annurev.earth.031208.100101>
- Cabrol NA, Grin EA, Newsom HE, Landheim R, McKay CP (1999) Hydrogeologic evolution of Gale crater and its relevance to the exobiological exploration of Mars. *Icarus* 139(2):235–245. <https://doi.org/10.1006/icar.1999.6099>
- Cannon KM, Parman SW, Mustard JF (2017) Primordial clays on Mars formed beneath a steam or supercritical atmosphere. *Nature* 552(7683):88–91

- Carr MH (1996) *Water on Mars*. Oxford University Press, London. ISBN 9780195099386
- Carr MH (2012) The fluvial history of Mars. *Philos Trans R Soc A, Math Phys Eng Sci* 370(1966):2193–2215
- Carr MH, Clow GD (1981) Martian channels and valleys: their characteristics, distribution, and age. *Icarus* 48(1):91–117
- Carr MH, Head JW (2003) Oceans on Mars: an assessment of the observational evidence and possible fate. *J Geophys Res, Planets* 108:5042. <https://doi.org/10.1029/2002je001963>
- Carr MH, Head JW (2010) Geologic history of Mars. *Earth Planet Sci Lett* 294:185–203. <https://doi.org/10.1016/j.epsl.2009.06.042>
- Carr MH, Head JW (2015) Martian surface/near-surface water inventory: sources, sinks, and changes with time. *Geophys Res Lett* 42(3):726–732. <https://doi.org/10.1002/2014GL024644>
- Carr M, Head J, (2019) Mars: formation and fate of a frozen Hesperian ocean. *Icarus* 319:433–443. <https://doi.org/10.1016/j.icarus.2018.08.021>
- Carter J, Poulet F, Bibring J-P, Mangold N, Murchie S (2013) Hydrous minerals on Mars as seen by the CRISM and OMEGA imaging spectrometers: updated global view. *J Geophys Res, Planets* 118:831–858. <https://doi.org/10.1029/2012JE004145>
- Carter J, Loizeau D, Mangold N, Poulet F, Bibring J-P (2015) Widespread surface weathering on early Mars: a case for a warmer and wetter climate. *Icarus* 248:373–382. <https://doi.org/10.1016/j.icarus.2014.11.011>
- Carter J, Riu L, Poulet F, Bibring J-P, Langevin Y, Gondet B (2023) A Mars orbital catalog of aqueous alteration signatures (MOCAAS). *Icarus* 389:115164. <https://doi.org/10.1016/j.icarus.2022.115164>
- Carter J et al (2024) Twenty years of Mars mineralogy with Mars Express. *Space Sci Rev*
- Cassanelli JP, Head JW (2019) Glaciovolcanism in the Tharsis volcanic province of Mars: implications for regional geology and hydrology. *Planet Space Sci* 169:45–69. <https://doi.org/10.1016/j.pss.2019.02.006>
- Cassanelli JP, Head JW (2026) Lava heating and loading of ice sheets on early Mars: predictions for meltwater generation, groundwater recharge, and resulting landforms. *Icarus* 71:237–264. <https://doi.org/10.1016/j.icarus.2016.02.004>
- Cassanelli JP, Head JW, Fastook JL (2015) Sources of water for the outflow channels on Mars: implications of the late noachian “icy highlands” model for melting and groundwater recharge on the Tharsis rise. *Planet Space Sci* 108:54–65. <https://doi.org/10.1016/j.pss.2015.01.002>
- Chapman MG, Neukum G, Dumke A, Michael G, van Gasselt S, Kneissl T, Zuschneid W et al (2010b) Noachian–Hesperian geologic history of the Echus Chasma and Kasei Valles system on Mars: new data and interpretations. *Earth Planet Sci Lett* 294(3–4):256–271. <https://doi.org/10.1016/j.epsl.2009.11.032>
- Chapman MG, Neukum G, Dumke A, Michael G, van Gasselt S, Kneissl T, Zuschneid W, Hauber E, Mangold N (2010a) Amazonian geologic history of the Echus Chasma and Kasei Valles system on Mars: new data and interpretations. *Sci Lett* 294(3–4):238–255. <https://doi.org/10.1016/J.EPSL.2009.11.034>
- Chapman MG, Neukum G, Dumke A, Michael G, Kneissl T (2011) Dark material on valles marineris plateaus: a preliminary report. In: 42nd Lunar and Planetary Science Conference, p 2423. <https://www.lpi.usra.edu/meetings/lpsc2011/pdf/2423.pdf>
- Chojnacki M, Moersch JE, Burr DM (2010) Climbing and falling dunes in Valles Marineris, Mars. *Geophys Res Lett* 37. <https://doi.org/10.1029/2009GL042263>
- Chojnacki M, Burr DM, Moersch JE (2014a) Valles Marineris dune fields as compared with other Martian populations: diversity of dune compositions, morphologies, and thermophysical properties. *Icarus* 230:96–142. <https://doi.org/10.1016/j.icarus.2013.08.018>
- Chojnacki M, Burr DM, Moersch JE, Wray JJ (2014b) Valles Marineris dune sediment provenance and pathways. *Icarus* 232:187–219. <https://doi.org/10.1016/j.icarus.2014.01.011>
- Chojnacki M, Johnson JR, Moersch JE, Fenton LK, Michaels TI, Bell JF (2015) Persistent aeolian activity at Endeavour crater, Meridiani Planum, Mars; new observations from orbit and the surface. *Icarus* 251:275–290. <https://doi.org/10.1016/j.icarus.2014.04.044>
- Christensen PR (1983) Eolian intracrater deposits on Mars: physical properties and global distribution. *Icarus* 56:496–518. [https://doi.org/10.1016/0019-1035\(83\)90169-0](https://doi.org/10.1016/0019-1035(83)90169-0)
- Clifford SM, Parker TJ (1999) Hydraulic and Thermal Arguments Regarding the Existence and Fate of a Primordial Martian Ocean. In: 30th Lunar and Planetary Science Conference, p 1619. <https://www.lpi.usra.edu/meetings/LPSC99/pdf/1619.pdf>
- Clifford SM, Parker TJ (2001) The evolution of the Martian hydrosphere: implications for the fate of aprimordial ocean and the current state of the northern plains. *Icarus* 154:40–79. <https://doi.org/10.1006/icar.2001.6671>
- Costard F, Baker VR (2001) Thermokarst landforms and processes in Ares Vallis, Mars. *Geomorphology* 37:289–301. [https://doi.org/10.1016/S0169-555X\(00\)00088-X](https://doi.org/10.1016/S0169-555X(00)00088-X)
- Costard F, Séjourné A, Lagain A, Ormó J, Rodriguez JAP, Clifford S, Bouley S, Kelfoun K, Lavigne F (2019) The Lomonosov crater impact event: a possible mega-tsunami source on Mars. *J Geophys Res, Planets* 124:1840–1851. <https://doi.org/10.1029/2019JE006008>

- Craddock RA, Howard AD (2002) The case for rainfall on a warm, wet early Mars. *J Geophys Res, Planets* 107(E11):21–1–21–36. <https://doi.org/10.1029/2001JE001505>
- Dang Y, Zhang F, Zhao J, Wang J, Xu Y, Huang T, Xiao L (2020) Diverse Polygonal Patterned Grounds in the Northern Eridania Basin, Mars: Possible Origins and Implications. *J Geophys Res, Planets* 125. <https://doi.org/10.1029/2020JE006647>
- Dasgupta D, Kundu A, Dasgupta N (2022) An insight to the cryospheric level in Mars: case study from the Thaumasia minor. *Icarus* 372:114725. <https://doi.org/10.1016/j.icarus.2021.114725>
- Davila AF, Fairén AG, Stokes CR, Platz T, Rodriguez AP, Lacelle D, Dohm J, Pollard W (2013) Evidence for Hesperian glaciation along the Martian dichotomy boundary. *Geology* 41(7):755–758. <https://doi.org/10.1130/G34201.1>
- Davis JM, Gupta S, Balme M, Grindrod PM, Fawdon P, Dickeson ZI, Williams RME (2019) A diverse array of fluvial depositional systems in Arabia Terra: evidence for mid-Noachian to early Hesperian rivers on Mars. *J Geophys Res, Planets* 124:1913–1934. <https://doi.org/10.1029/2019JE005976>
- De Blasio FV (2014) Possible erosion marks of bottom oceanic currents in the northern lowlands of Mars. *Planet Space Sci* 93:10–21. <https://doi.org/10.1016/j.pss.2014.01.014>
- De Blasio FV (2018) The pristine shape of Olympus Mons on Mars and the subaqueous origin of its aureole deposits. *Icarus* 302:44–61. <https://doi.org/10.1016/j.icarus.2017.11.003>
- De Blasio FV (2020) Frontal aureole deposit on acheron fossae ridge as evidence for landslide-generated tsunamis on Mars. *Planet Space Sci* 187:104911. <https://doi.org/10.1016/j.pss.2020.104911>
- de Haas T, Conway SJ, Krautblatter M (2015) Recent (Late Amazonian) enhanced backweathering rates on Mars: paracratering evidence from gully alcoves. *J Geophys Res, Planets* 120:2169–2189. <https://doi.org/10.1002/2015JE004915>
- De Toffoli B, Plesa A-C, Hauber E, Breuer D (2021) Delta deposits on Mars: a global perspective. *Geophys Res Lett* 48:e94271. <https://doi.org/10.1029/2021GL094271>
- Dehouck E, Mangold N, Le Mouélic S, Ansan V, Poulet F (2010) Ismenius Cavus, Mars: a deep paleolake with phyllosilicate deposits. *Planet Space Sci* 58:941–946. <https://doi.org/10.1016/j.pss.2010.02.005>
- Deutsch A, Head III JW, Palumbo AMM (2020) Assessing the termination of valley networks at the proposed Noachian ocean shoreline on Mars. In: AGU Fall Meeting 2020, pp P065-0004. <https://ui.adsabs.harvard.edu/abs/2020AGUFMP065.0004D/abstract>
- Di Achille G, Hynke BM (2010) Ancient ocean on Mars supported by global distribution of deltas and valleys. *Nat Geosci* 3:459. <https://doi.org/10.1038/ngeo891>
- Di Achille G, Marinangeli L, Ori GG, Hauber E, Gwinner K, Reiss D, Neukum G (2006) Geological evolution of the Tyras Vallis paleolacustrine system, Mars. *J Geophys Res* 111:E04003. <https://doi.org/10.1029/2005JE002561>
- Di Achille G, Ori GG, Reiss D (2007) Evidence for late Hesperian lacustrine activity in Shalbatana Vallis, Mars. *J Geophys Res* 112:E07007. <https://doi.org/10.1029/2006JE002858>
- Di Achille G, Hynke BM, Searls ML (2009) Positive identification of lake strandlines in Shalbatana Vallis, Mars. *Geophys Res Lett* 36:L14201. <https://doi.org/10.1029/2009GL038854>
- Diamant S, Bahia R, Miguel Y, Sefton-Nash E (2022) Martian paleolake outlet canyons – evidence for controls on valley network formation and a waning water cycle. *EPSC Abstr* 16:EPSC2022-268. <https://doi.org/10.5194/epsc2022-268>
- Dickeson ZI, Davis JM (2020) Martian oceans. *Astron Geophys* 61:3.11–13.17. <https://doi.org/10.1093/astrogeo/ataa038>
- Dickson JL, Fassett CI, Head JW (2009) Amazonian-aged fluvial valley systems in a climatic microenvironment on Mars: melting of ice deposits on the interior of Lyot crater. *Geophys Res Lett* 36:L08201. <https://doi.org/10.1029/2009GL037472>
- Dickson JL, Palumbo AM, Head JW, Kerber L, Fassett CI, Kreslavsky MA (2023) Gullies on Mars could have formed by melting of water ice during periods of high obliquity. *Science* 80(6652):1363–1367. <https://doi.org/10.1126/science.abk2464>
- Dundas CM, Bramson AM, Ojha L, Wray JJ, Mellon MT, Byrne S et al (2018) Exposed subsurface ice sheets in the Martian mid-latitudes. *Science* 359(6372):199–201. <https://doi.org/10.1126/science.aa0161>
- Dundas CM, Mellon MT, Posiolova LV, Miljković K, Collins GS, Tornabene LL et al (2023) A large new crater exposes the limits of water ice on Mars. *Geophys Res Lett* 50:e2022GL100747. <https://doi.org/10.1029/2022GL100747>
- Duran S, Coulthard TJ (2020) The Kasei Valles, Mars: a unified record of episodic channel flows and ancient ocean levels. *Sci Rep* 10:18571. <https://doi.org/10.1038/s41598-020-75080-y>
- Duran S, Coulthard TJ, Baynes ERC (2019) Knickpoints in Martian channels indicate past ocean levels. *Sci Rep* 9:15153. <https://doi.org/10.1038/s41598-019-51574-2>
- Edgett KS, Lancaster N (1993) Volcaniclastic aeolian dunes: terrestrial examples and application to Martian sands. *J Arid Environ* 25:271–297. <https://doi.org/10.1006/jare.1993.1061>

- Ehlmann BL, Buz J (2015) Mineralogy and fluvial history of the watersheds of Gale, Knobel, and Sharp craters: a regional context for the Mars Science Laboratory Curiosity's exploration. *Geophys Res Lett* 42:264–273. <https://doi.org/10.1002/2014GL062553>
- Ehlmann BL, Edwards CS (2014) Mineralogy of the Martian surface. *Annu Rev Earth Planet Sci* 42:291–315. <https://doi.org/10.1146/annurev-earth-060313-055024>
- Ehlmann BL, Mustard JF, Murchie SL, Bibring JP, Meunier A, Fraeman AA, Langevin Y (2011) Subsurface water and clay mineral formation during the early history of Mars. *Nature* 479(7371):53–60. <https://doi.org/10.1038/nature10582>
- Ehlmann BL, Edgett KS, Sutter B, Achilles CN, Litvak ML, Lapotre MGA, Sullivan R, Fraeman AA, Arvidson RE, Blake DF, Bridges NT, Conrad PG, Cousin A, Downs RT, Gabriel TSJ, Gellert R, Hamilton VE, Hardgrove C, Johnson JR, Kuhn S, Mahaffy PR, Maurice S, McHenry M, Meslin PY, Ming DW, Minitti ME, Morookian JM, Morris RV, O'Connell-Cooper CD, Pinet PC, Rowland SK, Schröder S, Siebach KL, Stein NT, Thompson LM, Vaniman DT, Vasavada AR, Wellington DF, Wiens RC, Yen AS (2017) Chemistry, mineralogy, and grain properties at Namib and high dunes, Bagnold dune field, Gale crater, Mars: a synthesis of Curiosity rover observations. *J Geophys Res, Planets* 122:2510–2543. <https://doi.org/10.1002/2017JE005267>
- Erkeling G, Hiesinger H, Reiss D, Hielscher FJ, Ivanov MA (2011) The stratigraphy of the Amenthes region, Mars: time limits for the formation of fluvial, volcanic and tectonic landforms. *Icarus* 215(1):128–152. <https://doi.org/10.1016/j.icarus.2011.06.041>
- Erkeling G, Reiss D, Hiesinger H, Poulet F, Carter J, Ivanov MA, Hauber E, Jaumann R (2012) Valleys, paleolakes and possible shorelines at the Libya Montes/Isidis boundary: Implications for the hydrologic evolution of Mars. *Icarus* 219:393–413. <https://doi.org/10.1016/j.icarus.2012.03.012>
- Erkeling G, Reiss D, Hiesinger H, Ivanov MA, Hauber E, Bernhardt H (2014) Landscape formation at the Deuteronilus contact in southern Isidis Planitia, Mars: implications for an Isidis Sea? *Icarus* 242:329–351. <https://doi.org/10.1016/j.icarus.2014.08.015>
- Erkeling G, Ivanov MA, Tirsch D, Reiss D, Bishop JL, Tornabene LL, Hiesinger H, Jaumann R (2016) Bradbury crater, Mars: morphology, morphometry, mineralogy, and chronostratigraphy. In: 47th Lunar and Planetary Science Conference, p 1451. <https://core.ac.uk/download/pdf/77231194.pdf>
- Fairén AG, Haqq-Misra JD, McKay CP (2012) Reduced albedo on early Mars does not solve the climate paradox under a faint young Sun. *Astron Astrophys* 540:A13. <https://doi.org/10.1051/0004-6361/201118527>
- Fassett CI, Head JW III (2007) Valley formation on Martian volcanoes in the Hesperian: evidence for melting of summit snowpack, caldera lake formation, drainage and erosion on Ceraunius Tholus. *Icarus* 189(1):118–135. <https://doi.org/10.1016/j.icarus.2006.12.021>
- Fassett CI, Head JW (2006) Valleys on Hecates Tholus, Mars: origin by basal melting of summit snowpack. *Planet Space Sci* 54:370–378. <https://doi.org/10.1016/j.pss.2005.12.011>
- Fassett CI, Head JW (2008a) The timing of Martian valley network activity: constraints from buffered crater counting. *Icarus* 195:61–89. <https://doi.org/10.1016/j.icarus.2007.12.009>
- Fassett C, Head J (2008b) Valley network-fed, open-basin lakes on Mars: distribution and implications for Noachian surface and subsurface hydrology. *Icarus* 198:37–56. <https://doi.org/10.1016/j.icarus.2008.06.016>
- Fassett CI, Head JW (2011) Sequence and timing of conditions on early Mars. *Icarus* 211:1204–1214. <https://doi.org/10.1016/j.icarus.2010.11.014>
- Fassett CI, Dickson JL, Head JW, Levy JS, Marchant DR (2010) Supraglacial and proglacial valleys on Amazonian Mars. *Icarus* 208(1):86–100. <https://doi.org/10.1016/j.icarus.2010.02.021>
- Fassett CI, Levy JS, Dickson JL, Head JW III (2014) An extended period of episodic northern mid-latitude glaciation on Mars during the Middle to Late Amazonian: implications for long-term obliquity history. *Geology* 42:763–766. <https://doi.org/10.1130/G35798.1>
- Fastook JL, Head JW (2014) Amazonian mid- to high-latitude glaciation on Mars: supply-limited ice sources, ice accumulation patterns, and concentric crater fill glacial flow and ice sequestration. *Planet Space Sci* 91:60–76. <https://doi.org/10.1016/j.pss.2013.12.002>
- Fastook JL, Head JW, Marchant DR, Forget F (2008) Tropical mountain glaciers on Mars: altitude-dependence of ice accumulation, accumulation conditions, formation times, glacier dynamics, and implications for planetary spin-axis/orbital history. *Icarus* 198(2):305–317. <https://doi.org/10.1016/j.icarus.2008.08.008>
- Fastook JL, Head JW, Marchant DR, Forget F, Madeleine JB (2012) Early Mars climate near the Noachian–Hesperian boundary: independent evidence for cold conditions from basal melting of the south polar ice sheet (Dorsa Argentea Formation) and implications for valley network formation. *Icarus* 219(1):25–40. <https://doi.org/10.1016/j.icarus.2012.02.013>
- Favaro EA, Balme MR, Davis JM, Grindrod PM, Fawdon P, Barrett AM, Lewis SR (2021) The aeolian environment of the landing site for the ExoMars Rosalind Franklin Rover in Oxia Planum, Mars. *J Geophys Res, Planets* 126:e2020JE006723. <https://doi.org/10.1029/2020JE006723>

- Fenton LK (2020) Updating the global inventory of dune fields on Mars and identification of many small dune fields. *Icarus* 352:114018. <https://doi.org/10.1016/j.icarus.2020.114018>
- Ferguson RL, Hare TM, Laura J (2018) HRSC and MOLA blended digital elevation model at 200m v2. Astrogeology PDS Annex, U.S. Geological Survey. https://astrogeology.usgs.gov/search/map/mars_mgs_mola_mex_hrsc_blended_dem_global_200m
- Flahaut J, Quantin C, Allemand P, Thomas P (2010) Morphology and geology of the ILD in Capri/Eos Chasma (Mars) from visible and infrared data. *Icarus* 207. <https://doi.org/10.1016/j.icarus.2009.11.019>
- Flint JJ (1974) Stream gradient as a function of order, magnitude, and discharge. *Water Resour Res* 10:969–973. <https://doi.org/10.1029/WR010i005p00969>
- Forget F, Hourdin F, Fournier F, Hourdin C, Talagrand O, Collins M, Lewis SR, Read PL, Huot J-P (1999) Improved general circulation models of the Martian atmosphere from the surface to above 80 km. *J Geophys Res* 104(E10):24155–24175. <https://doi.org/10.1029/1999JE001025>
- Forget F, Haberle RM, Montmessin F, Levrard B, Head JW (2006) Formation of glaciers on Mars by atmospheric precipitation at high obliquity. *Science* 311:368–371. <https://doi.org/10.1126/science.1120335>
- Forget F, Millour E, González-Galindo F, Spiga A, Lewis SR, Montabone L, Read PL, López-Valverde MA, Gilli G, Desjean MC, Huot JP, The Mc/D/Gcm Development Team (2007) The new (version 4.2) Mars climate database. *LPI Contrib* 1353:3098
- Fuerten F, Stesky R, MacKinnon P, Hauber E, Zegers T, Gwinner K, Scholten F, Neukum G (2008) Stratigraphy and structure of interior layered deposits in West Candor Chasma, Mars, from High Resolution Stereo Camera (HRSC) stereo imagery and derived elevations. *J Geophys Res, Planets* 113:E10008. <https://doi.org/10.1029/2007JE003053>
- Fuller ER, Head JW, Planitia A (2002) The role of geologically recent volcanism and sedimentation in the formation of the smoothest plains on Mars. *J Geophys Res, Planets* 107:11-11–11-25. <https://doi.org/10.1029/2002je001842>
- García-Arnay Á, Gutiérrez F (2020) Reconstructing paleolakes in Nepenthes Mensae, Mars, using the distribution of putative deltas, coastal-like features, and terrestrial analogs. *Geomorphology* 359:107129. <https://doi.org/10.1016/j.geomorph.2020.107129>
- Gardin E, Allemand P, Quantin C, Silvestro S, Delacourt C (2012) Dune fields on Mars: recorders of a climate change? *Planet Space Sci* 60:314–321. <https://doi.org/10.1016/j.pss.2011.10.004>
- Gendrin A, Mangold N, Bibring J-P, Langevin Y, Gondet B, Poulet F, Bonello G, Quantin C, Mustard J, Arvidson R (2005) Mouélic, Sulfates in Martian layered terrains: the OMEGA/Mars Express view. *Science* 307:1587–1591. <https://doi.org/10.1126/science.1109087>
- Ghatan GJ, Head JW III (2002) Candidate subglacial volcanoes in the south polar region of Mars: Morphology, morphometry, and eruption conditions. *J Geophys Res* 107(E7). <https://doi.org/10.1029/2001JE001519>
- Ghatan GJ, Zimbelman JR (2006) Paucity of candidate coastal constructional landforms along proposed shorelines on Mars: implications for a northern lowlands-filling ocean. *Icarus* 185:171–196. <https://doi.org/10.1016/j.icarus.2006.06.007>
- Goddard K, Warner NH, Gupta S, Kim J-R (2014) Mechanisms and timescales of fluvial activity at Mojave and other young Martian craters. *J Geophys Res, Planets* 119:604–634. <https://doi.org/10.1002/2013JE004564>
- Goudge TA, Head JW, Mustard JF, Fassett CI (2012a) An analysis of open-basin lake deposits on Mars: evidence for the nature of associated lacustrine deposits and post-lacustrine modification processes. *Icarus* 219(1):211–229. <https://doi.org/10.1016/j.icarus.2012.02.027>
- Goudge TA, Mustard JF, Head JW, Fassett CI (2012b) Constraints on the history of open-basin lakes on Mars from the composition and timing of volcanic resurfacing. *J Geophys Res, Planets* 117. <https://doi.org/10.1029/2012JE004115>
- Goudge TA, Aureli KL, Head JW, Fassett CI, Mustard JF (2015) Classification and analysis of candidate impact crater-hosted closed-basin lakes on Mars. *Icarus* 260:346–367. <https://doi.org/10.1016/j.icarus.2015.07.026>
- Goudge TA, Fassett CI, Mohrig D (2019) Incision of paleolake outlet canyons on Mars from overflow flooding. *Geology* 47(1):7–10. <https://doi.org/10.1130/G45397.1>
- Goudge TA, Morgan AM, Stucky de Quay G, Fassett CI (2021) The importance of lake breach floods for valley incision on early Mars. *Nature* 597(7878):645–649. <https://doi.org/10.1038/s41586-021-03860-1>
- Grau Galofre AG, Bahia RS, Jellinek AM, Whipple KX, Gallo R (2020a) Did Martian valley networks substantially modify the landscape? *Earth Planet Sci Lett* 547:116482. <https://doi.org/10.1016/j.epsl.2020.116482>
- Grau Galofre A, Jellinek AM, Osinski GR (2020b) Valley formation on early Mars by subglacial and fluvial erosion. *Nat Geosci* 13(10):663–668. <https://doi.org/10.1038/s41561-020-0618-x>
- Grau Galofre A, Whipple KX, Christensen PR, Conway SJ (2022) Valley networks and the record of glaciation on ancient Mars. *Geophys Res Lett* 49(14). <https://doi.org/10.1029/2022GL097974>

- Greeley R, Spudis PD (1981) Volcanism on Mars. *Rev Geophys* 19:13–41. <https://doi.org/10.1029/RG019i001p00013>
- Greeley R, Skyepeck A, Pollack JB (1993) Martian aeolian features and deposits: comparisons with general circulation model results. *J Geophys Res* 98(E2):3183–3196. <https://doi.org/10.1029/92JE02580>
- Greeley R, Arvidson R, Bell JF III, Christensen P, Foley D, Haldemann A et al (2005) Martian variable features: new insight from the Mars Express Orbiter and the Mars Exploration Rover Spirit. *J Geophys Res, Planets* 110(E6). <https://doi.org/10.1029/2005JE002403>
- Greeley R, Whelley PL, Arvidson RE, Cabrol NA, Foley D, Franklin BJ et al (2006) Active dust devils in Gusev crater, Mars: observations from the Mars exploration rover spirit. *J Geophys Res, Planets* 111(E12). <https://doi.org/10.1029/2006JE002743>
- Grégoire M, Baratoux D, Mangold N, Arnalds O, Platvoet B, Bardinzeff J, Pinet P (2007) Which processes form the volcanic sands on Mars? AGU Fall Meeting abstracts, vol 31, p 0551
- Greve R, Grieger B, Stenzel OJ (2010) MAIC-2, a latitudinal model for the Martian surface temperature, atmospheric water transport and surface glaciation. *Planet Space Sci* 58(6):931–940. <https://doi.org/10.1016/j.pss.2010.03.002>
- Grotzinger JP, Gupta S, Malin MC, Rubin DM, Schieber J, Siebach K, Wilson SA (2015) Deposition, exhumation, and paleoclimate of an ancient lake deposit, Gale crater. *Mars Sci* 350(6257):aac7575. <https://doi.org/10.1126/science.aac7575>
- Guimpier A, Conway SJ, Mangeney A, Lucas A, Mangold N, Peruzzetto M, Pajola M, Lucchetti A, Munaretto G, Sæmundsson T, Johnsson A, Le Deit L, Grindrod P, Davis J, Thomas N, Cremonese G (2021) Dynamics of recent landslides (<20 My) on Mars: insights from high-resolution topography on Earth and Mars and numerical modelling. *Planet Space Sci* 206:105303. <https://doi.org/10.1016/j.pss.2021.105303>
- Gulick VC (2001) Origin of the valley networks on Mars: a hydrological perspective. *Geomorphology* 37(3–4):241–268. [https://doi.org/10.1016/S0169-555X\(00\)00086-6](https://doi.org/10.1016/S0169-555X(00)00086-6)
- Gulick V, Baker V (1989) Fluvial valleys and Martian palaeoclimates. *Nature* 341:514–516. <https://doi.org/10.1038/341514a0>
- Gulick VC, Tyler D, McKay CP, Haberle RM (1997) Episodic ocean-induced CO₂ greenhouse on Mars: implications for fluvial valley formation. *Icarus* 130:68–86. <https://doi.org/10.1006/icar.1997.5802>
- Gwinner K, Scholten F, Spiegel M, Schmidt R, Giese B, Oberst J, Heipke C, Jaumann R, Neukum G (2009) Deviation and validation of high-resolution digital terrain models from Mars Express HRSC data. *Photogramm Eng Remote Sens* 75:1127–1142. 0099-1112/09/7509-1127i
- Gwinner K, Scholten F, Preusker F, Elgner S, Roatsch T, Spiegel M, Schmidt R, Oberst J, Jaumann R, Heipke C (2010) Topography of Mars from global mapping by HRSC high-resolution digital terrain models and orthoimages: characteristics and performance. *Earth Planet Sci Lett* 294:506–519. <https://doi.org/10.1016/j.epsl.2009.11.007>
- Gwinner K, Jaumann R, Hauber HH, Heipke C, Oberst J, Neukum G, Ansan V, Bostelmann J, Dumke A, Elgner S, Erkeling G, Fueten F, Hoekzema NM, Kersten E, Loizeau D, Matz D-D, Mertens V, Michael G, Pasewaldt A, Pinet P, Preusker F, Reiss D, Roatsch T, Schmidt R, Scholten F, Spiegel M, Vestky R, Tirsch D, van Gasselt S, Wählisch M, Willner K (2016) The High Resolution Stereo Camera (HRSC) of Mars Express and its approach to science analysis and mapping for Mars and its satellites. *Planet Space Sci* 196:93–138. <https://doi.org/10.1016/j.pss.2016.02.014>
- Haack D, Adeli S, Hauber E (2021) Geological history of southeastern gorgonum chaos, Mars: a story of water and wind. *J Geophys Res, Planets* 126. <https://doi.org/10.1029/2021JE006903>
- Haberle RM, Murphy JR, Schaeffer J (2003) Orbital change experiments with a Mars general circulation model. *Icarus* 161(1):66–89. [https://doi.org/10.1016/S0019-1035\(02\)00017-9](https://doi.org/10.1016/S0019-1035(02)00017-9)
- Hack JT (1957) Studies of longitudinal stream profiles in Virginia and Maryland. Geological Survey Professional Paper, 294-B. <https://pubs.usgs.gov/pp/0294b/report.pdf>
- Harrison KP, Grimm RE (2005) Groundwater-controlled valley networks and the decline of surface runoff on early Mars. *J Geophys Res* 110:E12S16. <https://doi.org/10.1029/2005JE002455>
- Harrison TN, Malin MC, Edgett KS, Shean DE, Kennedy MR, Lipkaman LJ, Cantor BA, Posiolova LV (2010) Impact-induced overland fluid flow and channelized erosion at Lyot Crater, Mars. *Geophys Res Lett* 37(21). <https://doi.org/10.1029/2010GL045074>
- Harrison TN, Osinski GR, Tornabene LL, Jones E (2015) Global documentation of gullies with the Mars reconnaissance orbiter context camera and implications for their formation. *Icarus* 252:236–254. <https://doi.org/10.1016/j.icarus.2015.01.022>
- Hartmann WK, Neukum G (2001) Cratering chronology and the evolution of Mars. *Space Sci Rev* 96:165–194. https://doi.org/10.1007/978-94-017-1035-0_6
- Hauber E, van Gasselt S, Ivanov B, Werner S, Head JW, Neukum G, Jaumann R et al (2005) Discovery of a flank caldera and very young glacial activity at Hecates Tholus, Mars. *Nature* 434(7031):356–361. <https://doi.org/10.1038/nature03423>

- Hauber E, van Gasselt S, Chapman MG, Neukum G (2008) Geomorphic evidence for former lobate debris aprons at low latitudes on Mars: Indicators of the Martian paleoclimate. *J Geophys Res, Planets* 113. <https://doi.org/10.1029/2007JE002897>
- Hauber E, Gwinner K, Kleinhans M, Reiss D, di Achille G, Ori G-G, Scholten F, Marinangeli L, Jaumann R, Neukum G (2009) Sedimentary deposits in Xanthe Terra: implications for the ancient climate on Mars. *Planet Space Sci* 57:944–957. <https://doi.org/10.1016/j.pss.2008.06.009>
- Hauber E, Reiss D, Ulrich M, Preusker F, Trauthan F, Zanetti M, Hiesinger H, Jaumann R, Johansson L, Johansson A, Van Gasselt S (2011) Landscape evolution in Martian mid-latitude regions: insights from analogous periglacial landforms in Svalbard. *Geol Soc (Lond) Spec Publ* 356(1):111–131. <https://doi.org/10.1144/SP356.7>
- Hauber E, Platz T, Reiss D, Le Deit L, Kleinhans MG, Marra WA, de Haas T, Carbonneau P (2013) Asynchronous formation of Hesperian and Amazonian-aged deltas on Mars and implications for climate. *J Geophys Res, Planets* 118:1529–1544. <https://doi.org/10.1002/jgre.20107>
- Hayward RK (2011) Mars Global Digital Dune Database (MGD3): North polar region (MC-1) distribution, applications, and volume estimates. *Earth Surf Process Landf* 36:1967–1972. <https://doi.org/10.1002/esp.2219>
- Hayward RK, Mullins KF, Fenton LK, Hare TM, Titus TN, Bourke MC, Colaprete A, Christensen PR (2007) Mars global digital dune database and initial science results. *J Geophys Res* 112:E11007. <https://doi.org/10.1029/2007JE002943>
- Hayward RK, Fenton LK, Titus TN (2014) Mars Global Digital Dune Database (MGD3): global dune distribution and wind pattern observations. *Icarus* 230:38–46. <https://doi.org/10.1016/j.icarus.2013.04.011>
- Head III JW, Marchant DR, Ghatan GJ (2004) Glacial deposits on the rim of a Hesperian-Amazonian outflow channel source trough: Mangala Valles, Mars. *Geophys Res Lett* 31(10). <https://doi.org/10.1029/2004GL020294>
- Head JW (2011) Geologic evidence for latitude-dependent water-related deposits on Mars: implications for climate history and the hydrological cycle on Mars. In: *Mars atmosphere: modelling and observation*, pp 427–430. https://www-mars.lmd.jussieu.fr/paris2011/abstracts/head_paris2011.pdf
- Head JW, Marchant DR (2003) Cold-based mountain glaciers on Mars: western Arsia Mons. *Geology* 31(7):641–644. [https://doi.org/10.1130/0091-7613\(2003\)031<0641:CMGOMW>2.0.CO;2](https://doi.org/10.1130/0091-7613(2003)031<0641:CMGOMW>2.0.CO;2)
- Head JW, Marchant DR (2014) The climate history of early Mars: insights from the Antarctic McMurdo Dry Valleys hydrologic system. *Antarct Sci* 26(6):774–800. <https://doi.org/10.1017/S0954102014000686>
- Head JW, Pratt S (2001) Extensive Hesperian-aged south polar ice sheet on Mars: evidence for massive melting and retreat, and lateral flow and ponding of meltwater. *J Geophys Res, Planets* 106(E6):12275–12299. <https://doi.org/10.1029/2000JE001359>
- Head JW, Hiesinger H, Ivanov MA, Kreslavsky MA, Pratt S, Thomson BJ (1999) Possible ancient oceans on Mars: evidence from Mars Orbiter Laser Altimeter data. *Science* 286:2134–2137. <https://doi.org/10.1126/science.286.5447.2134>
- Head J, Mustard J, Kreslavsky M et al (2003) Recent ice ages on Mars. *Nature* 426:797–802. <https://doi.org/10.1038/nature02114>
- Head JW, Neukum G, Jaumann R, Hiesinger H, Hauber E, Carr M, Mangold N, Kreslavsky M, Milkovich S, The HRSC Co-Investigator Team (2005) Tropical to mid-latitude glaciation on Mars: evidence for snow and ice accumulation and flow in Mars Express HRSC data. *Nature* 434:346–351. <https://doi.org/10.1038/nature03359>
- Head JW, Marchant DR, Agnew MC, Fassett CI, Kreslavsky MA (2006) Extensive valley glacier deposits in the northern mid-latitudes of Mars: evidence for Late Amazonian obliquity-driven climate change. *Earth Planet Sci Lett* 241(3–4):663–671. <https://doi.org/10.1016/j.epsl.2005.11.016>
- Head JW, Marchant DR, Kreslavsky MA (2008) Formation of gullies on Mars: link to recent climate history and insolation microenvironments implicate surface water flow origin. *Proc Natl Acad Sci* 105(36):13258–13263. <https://doi.org/10.1073/pnas.0803760105>
- Head JW, Marchant DR, Dickson JL, Kress AM, Baker DM (2010) Northern mid-latitude glaciation in the Late Amazonian period of Mars: criteria for the recognition of debris-covered glacier and valley glacier landsystem deposits. *Earth Planet Sci Lett* 294(3–4):306–320. <https://doi.org/10.1016/j.epsl.2009.06.041>
- Head J, Forget F, Wordsworth R, Turbet M, Cassanelli J, Palumbo A (2018) Two oceans on Mars? History, problems and prospects. In: *The Ninth Moscow Solar System Symposium 9M-S3*, pp 15–18
- Hepburn AJ et al (2020b) Polyphase mid-latitude glaciation on Mars: chronology of the formation of superposed glacier-like forms from crater-count dating. *J Geophys Res, Planets* 125(2):e2019JE006102
- Hepburn AJ, Ng FSL, Holt TO, Hubbard B (2020a) Late Amazonian Ice Survival in Kasei Valles, Mars. *J Geophys Res, Planets* 125. <https://doi.org/10.1029/2020JE006531>
- Hobley DEJ, Howard AD, Moore JM (2014) Fresh shallow valleys in the Martian midlatitudes as features formed by meltwater flow beneath ice. *J Geophys Res, Planets* 119(1):128–153. <https://doi.org/10.1002/2013JE004396>

- Hodges CA, Moore HJ (1979) The subglacial birth of Olympus Mons and its aureoles. *J Geophys Res, Solid Earth* 84(B14):8061–8074. <https://doi.org/10.1029/JB084iB14p08061>
- Hoke MTR, Hynek BM (2009) Roaming zones of precipitation on ancient Mars as recorded in valley networks. *J Geophys Res* 114. <https://doi.org/10.1029/2008JE003247>
- Hoke MTR, Hynek BM, Tucker GE (2011) Formation timescales of large Martian valley networks. *Earth Planet Sci Lett* 312(1–2):1–12. <https://doi.org/10.1016/j.epsl.2011.09.053>
- Holt JW, Safaenili A, Plaut JJ, Head JW, Phillips RJ, Seu R et al (2008) Radar sounding evidence for buried glaciers in the southern mid-latitudes of Mars. *Science* 322(5905):1235–1238. <https://doi.org/10.1126/science.1164246>
- Howard AD, Moore JM, Irwin RP III (2005) An intense terminal epoch of widespread fluvial activity on early Mars: 1. Valley network incision and associated deposits. *J Geophys Res* 110:E12S14. <https://doi.org/10.1029/2005JE002459>
- Hubbard B, Souness C, Brough S (2014) Glacier-like forms on Mars. *Cryosphere* 8(6):2047–2061. <https://doi.org/10.5194/tc-8-2047-2014>
- Hynek BM, Phillips RJ (2001) Evidence for extensive denudation of the Martian highlands. *Geology* 29(5):407–410. [https://doi.org/10.1130/0091-7613\(2001\)029<0407:EFEDOT>2.0.CO;2](https://doi.org/10.1130/0091-7613(2001)029<0407:EFEDOT>2.0.CO;2)
- Hynek BM, Beach M, Hoke MR (2010) Updated global map of Martian valley networks and implications for climate and hydrologic processes. *J Geophys Res, Planets* 115(E9). <https://doi.org/10.1029/2009JE003548>
- Irwin III RP, Craddock RA, Howard AD (2005) Interior channels in Martian valley networks: discharge and runoff production. *Geology* 33(6):489–492. <https://doi.org/10.1130/G21333.1>
- Ivanov BA (2001) Mars/Moon cratering rate ratio estimates. *Space Sci Rev* 96:87–104. <https://doi.org/10.1023/A:1011941121102>
- Ivanov MA, Hiesinger H, Erkeling G, Hielscher FJ, Reiss D (2012) Major episodes of geologic history of Isidis Planitia on Mars. *Icarus* 218:24–46. <https://doi.org/10.1016/j.icarus.2011.11.029>
- Ivanov MA, Hiesinger H, Erkeling G, Reiss D (2014) Mud volcanism and morphology of impact craters in Utopia Planitia on Mars: evidence for the ancient ocean. *Icarus* 228:121–140. <https://doi.org/10.1016/j.icarus.2013.09.018>
- Jackson B, Lorenz R, Davis K (2018) A framework for relating the structures and recovery statistics in pressure time-series surveys for dust devils. *Icarus* 299:166–174. <https://doi.org/10.1016/j.icarus.2017.07.027>
- Jaumann R, Hauber E, Lanz J, Hoffmann H, Neukum G (2002) Geomorphological record of water-related erosion on Mars. In: Horneck G, Baumstark-Kahn C (eds) *Astrobiology*. Springer, Berlin, pp 89–109. https://doi.org/10.1007/978-3-642-59381-9_7
- Jaumann R, Reiss D, Frei S, Neukum G, Scholten F, Gwinner K, Roatsch T, Matz K-M, Hauber E, Köhler U, Head JW, Hiesinger H, Carr M (2005) Interior channels in Martian Valleys: constraints on fluvial erosion by measurements of the Mars Express high resolution stereo camera. *Geophys Res Lett* 32:L16203. <https://doi.org/10.1029/2005GL023415>
- Jaumann R, Neukum G, Behnke T, Duxbury TC, Eichtenopf K, van Gassel S, Giese B, Gwinner K, Hauber E, Hoffmann H, Hoffmeister A, Köhler U, Matz K-D, McCord TB, Mertens V, Oberst J, Pischel R, Reiß D, Ress E, Roatsch T, Saiger P, Scholten F, Schwarz G, Stephan K, Wählisch M, The HRSC Co-Investigator Team (2007) The High Resolution Stereo Camera (HRSC) experiment on Mars Express: instrument aspects and experiment conduct from interplanetary cruise through nominal mission. *Planet Space Sci* 55:928–952. <https://doi.org/10.1016/j.pss.2006.12.003>
- Jaumann R, Nass A, Tirsch D, Reiss D, Neukum G (2010) The Western Libya Montes Valley System on Mars: evidence for episodic and multi-genetic erosion events during the Martian history. *Earth Planet Sci Lett* 294:272–290. <https://doi.org/10.1016/j.epsl.2009.09.026>
- Jaumann R, Tirsch D, Hauber E, Erkeling G, Le Deit L, Sowe M, Adeli S, Petau A, Reiss D, Hiesinger H (2014) Water and Martian Habitability. *Planet Space Sci* 98:128–145. <https://doi.org/10.1016/j.pss.2014.02.013>
- Jaumann R, Tirsch D, Hauber E, Ansan V, Di Achille G, Erkeling G, Fueten F, Head J, Kleinhans MG, Mangold N, Michael GG, Pacifici A, Platz T, Ponderelli M, Raack J, Reiss D, Williams DA, Adeli S, Baratoux D, de Villiers G, Foing B, Gupta S, Gwinner K, Hiesinger H, Hoffmann H, Le Deit L, Marinangeli L, Matz K-D, Mertens V, Müller JP, Neukum G, Pasckert HJ, Roatsch T, Rossi AP, Scholten F, Sowe M, Voigt J, Warner N (2015) Quantifying geological processes on Mars – results of the High Resolution Stereo Camera (HRSC) on Mars Express. *Planet Space Sci* 112:53–97. <https://doi.org/10.1016/j.pss.2014.11.029>
- Jehl A, Pinet P, Baratoux D, Daydou Y, Chevrel S, Heuripeau F, Manaud N, Cord A, Rosemberg C, Neukum G, Gwinner K, Scholten F, Hoffman H, Roatsch T (2008) Gusev photometric variability as seen from orbit by HRSC/Mars-express. *Icarus* 197(2):403–428. <https://doi.org/10.1016/j.icarus.2008.05.022>

- Johnsson A, Reiss D, Hauber E, Hiesinger H, Zanetti M (2014) Evidence for very recent melt-water and debris flow activity in gullies in a young mid-latitude crater on Mars. *Icarus* 235:37–54. <https://doi.org/10.1016/j.icarus.2014.03.005>
- Jouannic G, Gargani J, Costard F, Ori GG, Marmo C, Schmidt F, Lucas A (2012) Morphological and mechanical characterization of gullies in a periglacial environment: the case of the Russell crater dune (Mars). *Planet Space Sci* 71:38–54. <https://doi.org/10.1016/j.pss.2012.07.005>
- Kadish SJ, Head JW, Barlow NG (2010) Pedestal crater heights on Mars: a proxy for the thicknesses of past, ice-rich, Amazonian deposits. *Icarus* 210(1):92–101. <https://doi.org/10.1016/j.icarus.2010.06.021>
- Kahn RA, Martin TZ, Zurek RW, Lee SW (1992) The Martian dust cycle. Kieffer HH, Jakosky BM, Snyder CW, Matthews MS (eds) Mars. Univ. of Arizona Press, Tuscon, pp 1017–1053. https://www.researchgate.net/publication/4664642_The_Martian_Dust_Cycle
- Kargel JS, Strom RG (1992) Ancient glaciation on Mars. *Geology* 20(1):3–7. [https://doi.org/10.1130/0091-7613\(1992\)020<0003:AGOM>2.3.CO;2](https://doi.org/10.1130/0091-7613(1992)020<0003:AGOM>2.3.CO;2)
- Kereszturi A (2010) Analysis of two sections of Shalbatana Vallis' tributary channels. *Planet Space Sci* 58:2008–2021. <https://doi.org/10.1016/j.pss.2010.10.001>
- Kereszturi Á (2014) Case study of climatic changes in Martian fluvial systems at Xanthe Terra. *Planet Space Sci* 96:35–50. <https://doi.org/10.1016/j.pss.2014.03.014>
- Keske AL, Hamilton CW, McEwen AS, Daubar IJ (2015) Episodes of fluvial and volcanic activity in Mangala Valles, Mars. *Icarus* 245:333–347. <https://doi.org/10.1016/j.icarus.2014.09.040>
- Kite ES (2019) Geologic constraints on early Mars climate. *Space Sci Rev* 215:1–47. <https://doi.org/10.1007/s11214-018-0575-5>
- Kleinbans MG, van de Kastele HE, Hauber E (2010) Palaeoflow reconstruction from fan delta morphology on Mars. *Earth Planet Sci Lett* 294:378–392. <https://doi.org/10.1016/j.epsl.2009.11.025>
- Kneissl T, Reiss D, van Gasselt S, Neukum G (2010) Distribution and orientation of northern-hemisphere gullies on Mars from the evaluation of HRSC and MOC-NA data. *Earth Planet Sci Lett* 294(3–4):357–367. <https://doi.org/10.1016/j.epsl.2009.05.018>
- Korteniemi J, Kreslavsky MA (2013) Patterned ground in Martian high northern latitudes: morphology and age constraints. *Icarus* 225(2):960–970. <https://doi.org/10.1016/j.icarus.2012.09.032>
- Kostama VP, Kreslavsky MA, Head JW (2006) Recent high-latitude icy mantle in the northern plains of Mars: characteristics and ages of emplacement. *Geophys Res Lett* 33:L11201. <https://doi.org/10.1029/2006GL025946>
- Kreslavsky MA, Head III J.W. (2002) Mars: nature and evolution of young latitude-dependent water-ice-rich mantle. *Geophys Res Lett* 29(15):14-1–14-4. <https://doi.org/10.1029/2002GL015392>
- Lapotre MGA, Rampe EB (2018) Curiosity's investigation of the bagnold dunes, Gale crater: overview of the two-phase scientific campaign and introduction to the special collection. *Geophys Res Lett* 45:10,200–10,210. <https://doi.org/10.1029/2018GL079032>
- Lapotre MGA, Ehlmann BL, Minson SE, Arvidson RE, Ayoub F, Fraeman AA, Ewing RC, Bridges NT (2017) Compositional variations in sands of the Bagnold Dunes, Gale crater, Mars, from visible-shortwave infrared spectroscopy and comparison with ground truth from the Curiosity rover. *J Geophys Res, Planets* 122:2489–2509. <https://doi.org/10.1002/2016JE005133>
- Laskar J, Correia ACM, Gastineau M, Joutel F, Levrard B, Robutel P (2004) Long term evolution and chaotic diffusion of the insolation quantities of Mars. *Icarus* 170:343–364. <https://doi.org/10.1016/j.icarus.2004.04.005>
- Le Deit L, Le Mouélic S, Bourgeois O, Combe J-P, Mège D, Sotin C, Gendrin A, Hauber E, Mangold N, Bibring J-P (2008) Ferric oxides in East Candor Chasma, Valles Marineris (Mars) inferred from analysis of OMEGA/Mars Express data: Identification and geological interpretation. *J Geophys Res, Planets* 113:E07001. <https://doi.org/10.1029/2007JE002950>
- Le Deit L, Flahaut J, Quantin C, Hauber E, Mège D, Bourgeois O, Gurgurewicz J, Massé M, Jaumann R (2012) Extensive surface pedogenic alteration of the Martian Noachian crust suggested by Plateau phyllosilicates around Valles Marineris. *J Geophys Res, Planets* 117:E00J05. <https://doi.org/10.1029/2011JE003983>
- Le Deit L, Hauber E, Fueten F, Pondrelli M, Rossi AP, Jaumann R (2013) Sequence of infilling events in Gale Crater, Mars: Results from morphology, stratigraphy, and mineralogy. *J Geophys Res, Planets* 118. <https://doi.org/10.1002/2012JE004322>
- Levrard B, Forget F, Montmessin F, Laskar J (2007) Recent formation and evolution of northern Martian polar layered deposits as inferred from a global climate model. *J Geophys Res* 112:E06012. <https://doi.org/10.1029/2006je002772>
- Levy JS, Head JW, Marchant DR (2009) Thermal contraction crack polygons on Mars: classification, distribution and climate implications from global HiRISE observations. *J Geophys Res* 114:E01007. <https://doi.org/10.1029/2008JE003273>

- Levy J, Head JW, Marchant DR (2010a) Concentric crater fill in the northern mid-latitudes of Mars: formation processes and relationships to similar landforms of glacial origin. *Icarus* 209:390–404. <https://doi.org/10.1016/j.icarus.2010.03.036>
- Levy JS, Marchant DR, Head JW (2010b) Thermal contraction crack polygons on Mars: a synthesis from HiRISE, Phoenix, and terrestrial analog studies. *Icarus* 206:229–252. <https://doi.org/10.1016/j.icarus.2009.09.005>
- Levy JS, Fassett CI, Head JW, Schwartz C, Watters JL (2014) Sequestered glacial ice contribution to the global Martian water budget: geometric constraints on the volume of remnant, midlatitude debris-covered glaciers. *J Geophys Res, Planets* 119:2188–2196. <https://doi.org/10.1002/2014JE004685>
- Levy JS, Fassett CI, Head JW (2016) Enhanced erosion rates on Mars during Amazonian glaciation. *Icarus* 264:213–219. <https://doi.org/10.1016/j.icarus.2015.09.037>
- Lewis SR, Collins M, Read PL, Forget F, Hourdin F, Fournier R, Hourdin C, Talagrand O, Huot J-P (1999) A climate database for Mars. *J Geophys Res* 104(E10):24177–24194. <https://doi.org/10.1029/1999JE001024>
- Liu J, Yue Z, Di K, Gou S, Niu S (2021) A study about the temporal constraints on the Martian Yardangs' development in medusae fossae formation. *Remote Sens* 13(7):1316. <https://doi.org/10.3390/rs13071316>
- Liu J et al (2023) Martian dunes indicative of wind regime shift in line with end of ice age. *Nature*. <https://doi.org/10.1038/s41586-023-06206-1/>
- Loizeau D, Mangold N, Poulet F, Bibring J-P, Gendrin A, Ansan V, Gomez C, Gondet B, Langevin Y, Masson P, Neukum G (2007) Phyllosilicates in the Mawrth Vallis region of Mars. *J Geophys Res, Planets* 112(E8):E08S08. <https://doi.org/10.1029/2006JE002877>
- Loizeau D, Mangold N, Poulet F, Ansan V, Hauber E, Bibring J-P, Gondet B, Langevin Y, Masson P, Neukum G (2010) Stratigraphy in the Mawrth Vallis region through OMEGA, HRSC color imagery and DTM. *Icarus* 205:396–418. <https://doi.org/10.1016/j.icarus.2009.04.018>
- Loizeau D, Werner SC, Mangold N, Bibring J-P, Vago JL (2012) Chronology of deposition and alteration in the Mawrth Vallis region, Mars. *Planet Space Sci* 72:31–43. <https://doi.org/10.1016/j.pss.2012.06.023>
- Loizeau D, Quantin-Nataf C, Carter J, Flahaut J, Thollot P, Lozac'h L, Millot C (2018) Quantifying widespread aqueous surface weathering on Mars: the plateaus south of Coprates Chasma. *Icarus* 302:451–469. <https://doi.org/10.1016/j.icarus.2017.11.002>
- Lopes RMC, Guest JE, Wilson CJ (1980) Origin of the Olympus Mons aureole and perimeter scarp. *Moon Planets* 22:221–234. <https://doi.org/10.1007/BF00898433>
- Lorenz RD (2020) Martian ripples making a splash. *J Geophys Res, Planets* 125(10):e2020JE006658. <https://doi.org/10.1029/2020JE006658>
- Lu Y, Edgett KS, Wu YZ (2021) Ripples, Transverse Aeolian Ridges, and Dark-Toned Sand Dunes on Mars: a Case Study in Terra Sabaea. *J Geophys Res, Planets* 126(10). <https://doi.org/10.1029/2021JE006953>
- Lu Y et al (2022) Aeolian disruption and reworking of TARs at the Zhurong rover field site, southern Utopia Planitia, Mars. *Earth Planet Sci Lett* 595:117785. <https://doi.org/10.1016/j.epsl.2022.117785>
- Lucchitta BK (2001) Antarctic ice streams and outflow channels on Mars. *Geophys Res Lett* 28(3):403–406. <https://doi.org/10.1029/2000GL011924>
- Lucchitta BK, McEwen AS, Clow GD et al (1992) The canyon systems on Mars. In: Kieffer HH, Jakosky BM, Snyder CW (eds) *Mars*. University of Arizona Press, Tucson, pp 453–492
- Luo W, Cang X, Howard A (2017) New Martian valley network volume estimate consistent with ancient ocean and warm and wet climate. *Nat Commun* 8:15766. <https://doi.org/10.1038/ncomms15766>
- Madeleine JB, Forget F, Head JW, Levrard B, Montmessin F, Millour E (2009) Amazonian northern mid-latitude glaciation on Mars: a proposed climate scenario. *Icarus* 203(3):90–405. <https://doi.org/10.1016/j.icarus.2009.04.037>
- Madeleine JB, Forget F, Millour E, Navarro T, Spiga A (2012) The influence of radiatively active water ice clouds on the Martian climate. *Geophys Res Lett* 39:L23202. <https://doi.org/10.1029/2012GL053564>
- Malin MC, Edgett KS (1999) Oceans or seas in the Martian northern lowlands: high resolution imaging tests of proposed coastlines. *Geophys Res Lett* 26:3049–3052. <https://doi.org/10.1029/1999g1002342>
- Malin MC, Edgett KS (2000) Sedimentary rocks of early Mars. *Science* 290:1927–1937. <https://doi.org/10.1126/science.290.5498.1927>
- Mandt K, Leone G (2015) Yardang. In: Hargitai H, Kereszturi Á (eds) *Encyclopedia of planetary landforms*. Springer, New York. https://doi.org/10.1007/978-1-4614-3134-3_575
- Mangold N (2003) Geomorphic analysis of lobate debris aprons on Mars at Mars Orbiter Camera scale: evidence for ice sublimation initiated by fractures. *J Geophys Res* 108(E4):8021. <https://doi.org/10.1029/2002JE001885>
- Mangold N (2005) High latitude patterned grounds on Mars: classification, distribution and climatic control. *Icarus* 174(2):336–359. <https://doi.org/10.1016/j.icarus.2004.07.030>
- Mangold N, Howard AD (2013) Outflow channels with deltaic deposits in Ismenius Lacus, Mars. *Icarus* 226:385–401. <https://doi.org/10.1016/j.icarus.2013.05.040>

- Mangold N et al (2007) Mineralogy of the Nili Fossae region with OMEGA/Mars Express data: 2. Aqueous alteration of the crust. *J Geophys Res* 112:E08S04. <https://doi.org/10.1029/2006JE002835>
- Mangold N, Gendrin A, Gondet B, Mouelic SL, Quantin C, Ansan V, Bibring J-P, Langevin Y, Masson P, Neukum G (2008) Spectral and geological study of the sulfate rich region of West Candor Chasma, Mars. *Icarus* 194:519–543. <https://doi.org/10.1016/j.icarus.2007.10.021>
- Mangold N, Adeli S, Conway S, Ansan V, Langlais B (2012a) A chronology of early Mars climatic evolution from impact crater degradation. *J Geophys Res, Planets* 117:E04003. <https://doi.org/10.1029/2011JE004005>
- Mangold N, Carter J, Poulet F, Dehouck E, Ansan V, Loizeau D (2012b) Late Hesperian aqueous alteration at Majuro crater, Mars. *Planet Space Sci* 72:18–30. <https://doi.org/10.1016/j.pss.2012.03.014>
- Marra WA, Hauber E, de Jong SM, Kleinhans MG (2015) Pressurized groundwater systems in Lunae and Ophir Plana (Mars): Insights from small-scale morphology and experiments. *Geo Res J* 8:1–13. <https://doi.org/10.1016/j.grj.2015.08.001>
- Martin P, Titov D, González-Galindo F, Jaumann R, Määttänen A, Spohn T, Wilson C, Kminek G, Sefton-Nash E (2024) Mars Express: Pioneering two decades of European exploration of Mars. *Space Sci Rev*
- Massé M, Le Mouélic S, Bourgeois O, Combe J-P, Le Deit L, Sotin C, Bibring J-P, Gondet B, Langevin Y (2008) Mineralogical composition, structure, morphology, and geological history of Aram Chaos crater fill on Mars derived from OMEGA Mars Express data. *J Geophys Res* 113:E12006. <https://doi.org/10.1029/2008JE003131>
- Masson P, Carr MH, Costard F, Greeley R, Hauber E, Jaumann R (2001) Geomorphologic evidence for liquid water. In: Kallenbach R, Geiss J, Hartmann WK (eds) *Chronology and evolution on Mars*. Space science series of ISSI, space science review, vol 96, pp 333–364. <https://doi.org/10.1023/A:1011913809715>
- Masursky H (1973) An overview of geological results from Mariner 9. *J Geophys Res* 78(20):4009–4030. <https://doi.org/10.1029/JB078i020p04009>
- McKee ED (1979) Introduction to a study of global sand seas. In: McKee ED (ed) *A study of global sand seas*. Geological Survey Professional Paper, 3. <https://doi.org/10.3133/pp1052>
- McKeown NK, Bishop JL, Dobreá EZN, Ehlmann BL, Parente M, Mustard JF, Murchie SL, Swayze GA, Bibring J-P, Silver EA (2009) Characterization of phyllosilicates observed in the central Mawrth Vallis region, Mars, their potential formational processes, and implications for past climate. *J Geophys Res, Planets* 114:E00D10. <https://doi.org/10.1029/2008JE003301>
- Melosh HJ (2011) *Planetary surface processes*. Cambridge University Press, Cambridge. <https://doi.org/10.1017/CBO9780511977848>
- Michael GG (2013) Planetary surface dating from crater size frequency distribution measurements: multiple resurfacing episodes and differential isochron fitting. *Icarus* 226:885–890. <https://doi.org/10.1016/j.icarus.2013.07.004>
- Michalski JR, Glotch TD, Rogers AD, Niles PB, Cuadros J, Ashley JW, Johnson SS (2019) The geology and astrobiology of McLaughlin crater, Mars: an ancient lacustrine basin containing turbidites, mudstones, and serpentinites. *J Geophys Res, Planets* 124:910–940. <https://doi.org/10.1029/2018JE005796>
- Milkovich SM, Head JW, Neukum G, HRSC Team (2008) Stratigraphic analysis of the northern polar layered deposits of Mars: implications for recent climate history. *Planet Space Sci* 56:266–288. <https://doi.org/10.1016/j.pss.2007.08.004>
- Milliken RE, Mustard JF, Goldsby DL (2003) Viscous flow features on the surface of Mars: observations from high-resolution Mars Orbiter Camera (MOC) images. *J Geophys Res* 108(E6):5057. <https://doi.org/10.1029/2002JE002005>
- Millour E, Forget F, González-Galindo F, Spiga A, Lebonnois S, Montabone L et al (2008) The latest (version 4.3) Mars climate database. In: *Mars atmosphere: modeling and observations*, pp 1–4. <http://www.lpi.usra.edu/meetings/modeling2008/>
- Milton DJ (1973) Water and processes of degradation in the Martian landscape. *J Geophys Res* 78(20):4037–4047. <https://doi.org/10.1029/JB078i020p04037>
- Mischna MA, Richardson MI, Wilson RJ, McCleese DJ (2003) On the orbital forcing of Martian water and CO₂ cycles: a general circulation model study with simplified volatile schemes. *J Geophys Res* 108(E6):5062. <https://doi.org/10.1029/2003JE002051>
- Morgan GA, Head JW III, Marchant DR (2009) Lineated valley fill (LVF) and lobate debris aprons (LDA) in the Deuteronilus Mensae northern dichotomy boundary region, Mars: constraints on the extent, age and episodicity of Amazonian glacial events. *Icarus* 202(1):22–38. <https://doi.org/10.1016/j.icarus.2009.02.017>
- Morgan GA, Putzig NE, Perry MR, Sizemore HG, Bramson AM, Petersen EI, Bain ZM et al (2021) Availability of subsurface water-ice resources in the northern mid-latitudes of Mars. *Nat Astron* 5(3):230–236. <https://doi.org/10.1038/s41550-020-01290-z>
- Mukherjee S, Singh D, Singh P, Roy N (2020) Morphological and morphometric analysis of a topographic depression near Huygens basin, Mars: identification of a putative endorheic playa. *Geomorphology* 351:106912. <https://doi.org/10.1016/j.geomorph.2019.106912>

- Murchie SL et al (2009) A synthesis of Martian aqueous mineralogy after 1 Mars year of observations from the Mars reconnaissance orbiter. *J Geophys Res, Planets* 114:E00D06. <https://doi.org/10.1029/2009JE003342>
- Murchie SL, Mustard JF, Ehlmann BL, Milliken RE, Bishop JL, McKeown NK, Bibring JP (2009) A synthesis of Martian aqueous mineralogy after 1 Mars year of observations from the Mars Reconnaissance Orbiter. *J Geophys Res, Planets* 114(E2). <https://doi.org/10.1029/2009JE003342>
- Murray JB, Muller J-P, Neukum G, Werner SC, van Gasselt S, Hauber E, Markiewicz WJ, Head JW, Foing BH, Page D, Mitchell KL, Portyankina G, Co-Investigator Team (2005) The evidence from the Mars Express high resolution stereo camera for a frozen sea close to Mars' equator. *Nature* 434:352–356. <http://www.nature.com/nature/index.html>
- Musiol S, Cailleau B, Platz T, Kneissl T, Dumke A, Neukum G (2011) Outflow activity near Hadriaca Patera, Mars: fluid-tectonic interaction investigated with high resolution stereo camera stereo data and finite element modeling. *J Geophys Res, Planets* 116:08001. <https://doi.org/10.1029/2010JE003791>
- Mustard J, Cooper C, Rifkin M (2001) Evidence for recent climate change on Mars from the identification of youthful near-surface ground ice. *Nature* 412:411–414. <https://doi.org/10.1038/35086515>
- Mustard JF et al (2008) Hydrated silicate minerals on Mars observed by the Mars reconnaissance orbiter CRISM instrument. *Nature* 454(7202):305–309. <https://doi.org/10.1038/nature07097>
- Nedell SS, Squyres SW, Andersen DW (1987) Origin and evolution of the layered deposits in the Valles Marineris, Mars. *Icarus* 70:409–441. [https://doi.org/10.1016/0019-1035\(87\)90086-8](https://doi.org/10.1016/0019-1035(87)90086-8)
- Neukum G, Ivanov B, Hartmann W (2001) Cratering records in the inner Solar System in relation to the lunar reference system. *Space Sci Rev* 96:55–86. <https://doi.org/10.1023/A:1011989004263>
- Neukum G, Jaumann R, Hoffmann H, Hauber E, Head JW, Basilevsky AT, Ivanov BA, Werner SC, van Gasselt S, Murray JB, McCord T, The HRSC Co-Investigator Team (2004) Mars: recent and episodic volcanic, hydrothermal, and glacial activity revealed by the Mars Express High Resolution Stereo Camera (HRSC) experiment. *Nature* 432:971–979. <https://doi.org/10.1038/nature03231>
- Neukum G, Basilevsky AT, Kneissl T, Chapman MG, van Gasselt S, Michael G, Jaumann R, Hoffmann H, Lanz JK (2010) The geologic evolution of Mars: episodicity of resurfacing events and ages from cratering analysis of image data and correlation with radiometric ages of Martian meteorites. *Earth Planet Sci Lett* 294:204–222. <https://doi.org/10.1016/j.epsl.2009.09.006>
- Niu S, Zhang F, Di K, Gou S, Yue Z (2022) Layered Ejecta Craters in the Candidate Landing Areas of China's First Mars Mission (Tianwen-1): Implications for Subsurface Volatile Concentrations. *J Geophys Res, Planets* 127. <https://doi.org/10.1029/2021JE007089>
- Orosei R et al (2024) Water ice in the subsurface and polar caps. *Space Sci Rev*
- Pacifici A (2008) Geomorphological map of Ares Vallis, ASI planetary map series – map no. 1. *Boll Soc Geol It (Ital J Geosci)* 127(1):75–92
- Pacifici A, Komatsu G, Pondrelli M (2009) Geological evolution of Ares Vallis on Mars: formation by multiple events of catastrophic flooding, glacial and periglacial processes. *Icarus* 202:60–77. <https://doi.org/10.1016/j.icarus.2009.02.029>
- Pajola M et al (2016a) The Simud-Tiu Valles hydrologic system: a multidisciplinary study of a possible site for future Mars on-site exploration. *Icarus* 268:355–381
- Pajola M et al (2016) Eridania Basin: an ancient paleolake floor as the next landing site for the Mars 2020 rover. *Icarus* 275:163–182
- Pajola M, Rossato S, Baratti E, Mangili C, Mancarella F, McBride K, Coradini M (2016a) The Simud–Tiu Valles hydrologic system: a multidisciplinary study of a possible site for future Mars on-site exploration. *Icarus* 268:355–381. <https://doi.org/10.1016/j.icarus.2015.12.049>
- Palucis MC, Dietrich WE, Williams RME, Hayes AG, Parker T, Sumner DY, Mangold N, Lewis K, Newsom H (2016) Sequence and relative timing of large lakes in Gale crater (Mars) after the formation of Mount Sharp. *J Geophys Res, Planets* 121:472–496. <https://doi.org/10.1002/2015JE004905>
- Palucis MC, Dietrich WE, Williams RME, Hayes AG, Parker T, Sumner DY, Mangold N, Lewis K, Newsom H (2016) Sequence and relative timing of large lakes in Gale crater (Mars) after the formation of Mount Sharp. *J Geophys Res, Planets* 121:472–496. <https://doi.org/10.1002/2015JE004905>
- Palumbo AM, Head JW (2017) Impact cratering as a cause of climate change, surface alteration, and resurfacing during the early history of Mars. *Meteorit Planet Sci* 53:687–725. <https://doi.org/10.1111/maps.13001>
- Palumbo A, Head J, Wordsworth R (2018) Late Noachian Icy Highlands climate model: exploring the possibility of transient melting and fluvial/lacustrine activity through peak annual and seasonal temperatures. *Icarus* 300:261–286. <https://doi.org/10.1016/j.icarus.2017.09.007>
- Pan C, Edwards CS, Bennett KA (2019) Composition and sources of dark aeolian sediments within Martian craters associated with central mounds. In: 50th Lunar and Planetary Science Conference, Houston. Abstract #2249. <https://www.hou.usra.edu/meetings/lpsc2019/pdf/2249.pdf>

- Parker TJ, Saunders RS, Schneeberger DM (1989) Transitional morphology in West Deuteronilus Mensae, Mars: implications for modification of the lowland/upland boundary. *Icarus* 82:111–145. [https://doi.org/10.1016/0019-1035\(89\)90027-4](https://doi.org/10.1016/0019-1035(89)90027-4)
- Parker TJ, Gorsline DS, Saunders RS, Pieri DC, Schneeberger DM (1993) Coastal geomorphology of the Martian northern plains. *J Geophys Res* 98:11061. <https://doi.org/10.1029/93JE00618>
- Parsons R, Holt J (2016) Constraints on the formation and properties of a Martian lobate debris apron: insights from high-resolution topography, SHARAD radar data, and a numerical ice flow model. *J Geophys Res, Planets* 121:432–453. <https://doi.org/10.1002/2015JE004927>
- Parsons RA, Moore JM, Howard AD (2013) Evidence for a short period of hydrologic activity in Newton crater, Mars, near the Hesperian-Amazonian transition. *J Geophys Res, Planets* 118(5):1082–1093. <https://doi.org/10.1002/jgre.20088>
- Parsons RA, Kanzaki T, Hemmi R, Miyamoto H (2021) Cold-based glaciation of pavonis mons, Mars: evidence for moraine deposition during glacial advance. *Prog Earth Planet Sci* 7:1–21. <https://doi.org/10.1186/s40645-020-0323-9>
- Peel SE, Fassett CI (2013) Valleys in pit craters on Mars: characteristics, distribution, and formation mechanisms. *Icarus* 225(1):272–282. <https://doi.org/10.1016/j.icarus.2013.03.031>
- Penido JC, Fassett CI, Som SM (2013) Scaling relationships and concavity of small valley networks on Mars. *Planet Space Sci* 75:105–116. <https://doi.org/10.1016/j.pss.2012.09.009>
- Peterson CM (1981) Hebes Chasma – Martian pyroclastic sink. Lunar and Planetary Science Conference XII, abstract 828-829. <https://adsabs.harvard.edu/full/1981LPI....12.828P>
- Plaut JJ, Safaeinili A, Holt JW, Phillips RJ, Head JW III, Seu R, Putzig NE, Frigeri A (2009) Radar evidence for ice in lobate debris aprons in the mid-northern latitudes of Mars. *Geophys Res Lett* 36:L02203. <https://doi.org/10.1029/2008GL036379>
- Pondrelli M, Rossi AP, Ori GG, Gasselt S, Praeg D, Ceramicola S (2011a) Mud volcanoes in the geologic record of Mars: the case of firsoff crater. *Earth Planet Sci Lett* 304:511–519. <https://doi.org/10.1016/j.epsl.2011.02.027>
- Pondrelli M, Rossi AP, Platz T, Ivanov A, Marinangeli L, Baliva A (2011b) Geological, geomorphological, facies and allostratigraphic maps of the Eberswalde fan delta. *Planet Space Sci* 59:1166–1178. <https://doi.org/10.1016/j.pss.2010.10.009>
- Pondrelli M, Rossi AP, Le Deit L, Gasselt S, Fueten F, Glamoclija M (2015) Equatorial layered deposits in the Firsoff crater area: process variability and habitability potential. *Geol Soc Am Bull* 127:1064–1089. <https://doi.org/10.1130/B31225.1>
- Pondrelli M, Rossi AP, Le Deit L, Schmidt G, Pozzobon R, Hauber E, Salese F (2019) Groundwater control and process variability on the Equatorial Layered Deposits of Kotido crater, Mars. *J Geophys Res, Planets* 124:779–800. <https://doi.org/10.1029/2018JE005656>
- Poulet F et al (2007) Martian surface mineralogy from observatoire Pour La Minéralogie, l'Eau, Les Glaces et l'Activité on Board the Mars Express Spacecraft (OMEGA/MEX): global mineral maps. *J Geophys Res, Planets* 112(E8). <https://doi.org/10.1029/2006JE002840>
- Poulet F et al (2008) Abundance of minerals in the phyllosilicate-rich units on Mars. *Astron Astrophys* 487(2):L41–L44. <https://doi.org/10.1051/0004-6361/200810150>
- Poulet F, Carter J, Bishop JL, Loizeau D, Murchie SM (2014) Mineral abundances at the final four Curiosity study sites and implications for their formation. *Icarus* 231:65–76. <https://doi.org/10.1016/j.icarus.2013.11.023>
- Poulet F, Gross C, Horgan B, Loizeau D, Bishop JL, Carter J, Orgel C (2020) Mawrth Vallis, Mars: a fascinating place for future in situ exploration. *Astrobiology* 20(2). <https://doi.org/10.1089/ast.2019.2074>
- Quantin C, Allemand P, Mangold N, Dromart G, Delacourt C (2005) Fluvial and lacustrine activity on layered deposits in Melas Chasma, Valles Marineris, Mars. *J Geophys Res, Planets* 110(E12). <https://doi.org/10.1029/2005JE002440>
- Quantin-Nataf C, Carter J, Mandon L, Thollot P, Balme M, Volat M, Pan L, Loizeau D, Millot C, Breton S, Dehouck E, Fawdon P, Gupta S, Davis J, Grindrod PM, Pacifici A, Bultel B, Allemand P, Ody A, Lozach L, Broyer J (2021) Oxia planum: the landing site for the ExoMars “Rosalind Franklin” rover mission: geological context and prelanding interpretation. *Astrobiology* 21(3):345–366. <https://doi.org/10.1089/ast.2019.2191>
- Raack J, Reiss D, Hiesinger H (2012) Gullies and their relationships to the dust–ice mantle in the northwestern Argire Basin, Mars. *Icarus* 219(1):129–141. <https://doi.org/10.1016/j.icarus.2012.02.025>
- Ramsdale JD, Balme MR, Conway SJ, Gallagher C (2015) Ponding, draining and tilting of the cerberus plains: a cryolacustrine origin for the sinuous ridge and channel networks in Rahway Vallis, Mars. *Icarus* 253:256–270. <https://doi.org/10.1016/j.icarus.2015.03.005>
- Reiss D, Jaumann R (2003) Recent debris flows on Mars: Seasonal observations of the Russell Crater dune field. *Geophys Res Lett* 30(6). <https://doi.org/10.1029/2002GL016704>

- Reiss R, Zanetti M, Neukum G (2011) Multitemporal observations of identical active dust devils on Mars with the High Resolution Stereo Camera (HRSC) and Mars Orbiter Camera (MOC). *Icarus* 215(1):358–369. <https://doi.org/10.1016/j.icarus.2011.06.011>
- Richardson M, Wilson R (2002) A topographically forced asymmetry in the Martian circulation and climate. *Nature* 416:298–301. <https://doi.org/10.1038/416298a>
- Ringrose TJ, Townner MC, Zarnecki JC (2003) Convective vortices on Mars: a reanalysis of Viking Lander 2 meteorological data, sols 1–60. *Icarus* 163:78–87. [https://doi.org/10.1016/S0019-1035\(03\)00073-3](https://doi.org/10.1016/S0019-1035(03)00073-3)
- Rivera-Hernández F, Palucis MC (2019) Do deltas along the crustal dichotomy boundary of Mars in the Gale crater region record a northern ocean? *Geophys Res Lett* 46:8689. <https://doi.org/10.1029/2019GL083046>
- Rodriguez JP, Tanaka KL, Yamamoto A, Berman DC, Zimbleman JR, Kargel JS, Sasaki S, Jinguo Y, Miyamoto H (2010) The sedimentology and dynamics of crater-affiliated wind streaks in western Arabia Terra, Mars and Patagonia, Argentina. *Geomorphology* 121(1–2):30–54. <https://doi.org/10.1016/j.geomorph.2009.07.020>
- Rodriguez JAP, Leonard GJ, Platz T, Tanaka KL, Kargel JS, Fairén AG, Gulick V, Baker VR, Glines N, Miyamoto H, Jianguo Y, Oguma M (2015) New insights into the Late Amazonian zonal shrinkage of the Martian south polar Plateau. *Icarus* 248:407–411. <https://doi.org/10.1016/j.icarus.2015.01.009>
- Rodriguez JPA, Robertson DK, Kargel JS, Baker VR, Berman DC, Cohen J, Costard F, Komatsu G, Lopez A, Miyamoto H, Zarroca M (2022) Evidence of an oceanic impact and megatsunami sedimentation in Chryse Planitia, Mars. *Sci Rep* 12:19589. <https://doi.org/10.1038/s41598-022-18082-2>
- Rossi AP, Neukum G, Pondrelli M, Gasselt S, Zegers T, Hauber E, Chicarro FB (2008) Large-scale spring deposits on Mars? *J Geophys Res, Planets* 113. <https://doi.org/10.1029/2007JE003062>
- Russell PS, Head JW III (2002) The Martian hydrosphere/cryosphere system: implications of the absence of hydrologic activity at Lyot crater. *Geophys Res Lett* 29(17):8-1–8-4. <https://doi.org/10.1029/2002GL015178>
- Salese F, Di Achille G, Neesemann A et al (2016) Hydrological and sedimentary analyses of well-preserved paleofluvial-paleolacustrine systems at Moa Valles, Mars. *J Geophys Res, Planets* 121:194–232. <https://doi.org/10.1002/2015JE004891>
- Sautter V, Toplis MJ, Wiens RC, Cousin A, Fabre C, Gasnault O, Maurice S, Forni O, Lasue J, Ollila A, Bridges JC, Mangold N, Le Mouélic S, Fisk M, Meslin PY, Beck P, Pinet P, Le Deit L, Rapin W, Stolper EM, Newsom H, Dyar D, Lanza N, Vaniman D, Clegg S, Wray JJ (2015) In situ evidence for continental crust on early Mars. *Nat Geosci* 8:605. <https://doi.org/10.1038/ngeo2474>. <https://www.nature.com/articles/ngeo2474#supplementary-information>
- Scanlon KE, Head JW, Fastook JL, Wordsworth RD (2018) The dorsa argentea formation and the noachian-hesperian climate transition. *Icarus* 299:339–363. <https://doi.org/10.1016/j.icarus.2017.07.031>
- Schmidt G, Pondrelli M, Salese F, Rossi AP, Le Deit L, Fueten F, Salvini F (2021) Depositional controls of the layered deposits of Arabia Terra, Mars: hints from basin geometries and stratigraphic trends. *J Geophys Res, Planets* 126:e2021JE006974. <https://doi.org/10.1029/2021JE006974>
- Scholten F, Gwinner K, Roatsch T, Matz K-D, Wählisch M, Giese B, Oberst J, Jaumann R, Neukum G, The HRSC Co-Investigator Team (2005) Mars Express HRSC data processing – methods and operational aspects. *Photogramm Eng Remote Sens* 71:1143–1152. <https://doi.org/10.14358/PERS.71.10.1143>
- Schultz PH, Lutz AB (1988) Polar wandering of Mars. *Icarus* 73:91–141. [https://doi.org/10.1016/0019-1035\(88\)90087-5](https://doi.org/10.1016/0019-1035(88)90087-5)
- Seybold HJ, Kite E, Kirchner JW (2018) Branching geometry of valley networks on Mars and Earth and its implications for early Martian climate. *Sci Adv* 4(6):eaar6692. <https://doi.org/10.1126/sciadv.aar6692>
- Shi Y, Zhao J, Xiao L, Yang Y, Wang J (2022) An arid-semiarid climate during the Noachian-Hesperian transition in the Huygens region, Mars: evidence from morphological studies of valley networks. *Icarus* 373:114789. <https://doi.org/10.1016/j.icarus.2021.114789>
- Sholes SF, Rivera-Hernández F (2022) Constraints on the uncertainty, timing, and magnitude of potential Mars oceans from topographic deformation models. *Icarus* 378:114934. <https://doi.org/10.1016/j.icarus.2022.114934>
- Sholes SF, Montgomery DR, Catling DC (2019) Quantitative high-resolution reexamination of a hypothesized ocean shoreline in Cydonia Mensae on Mars. *J Geophys Res, Planets* 124:316–336. <https://doi.org/10.1029/2018JE005837>
- Sholes SF, Dickeson ZI, Montgomery DR, Catling DC (2021) Where are Mars' hypothesized ocean shorelines? Large lateral and topographic offsets between different versions of paleoshoreline maps. *J Geophys Res, Planets* 126:e06486. <https://doi.org/10.1029/2020je006486>
- Silvestro S, Fenton LK, Ori GG (2008) Complex dunes in the southern hemisphere of Mars: age and wind regimes. In: Lunar and Planetary Science Conference, vol 39, p 1893. <https://www.lpi.usra.edu/meetings/lpsc2008/pdf/1893.pdf>


- Silvestro S, Di Achille G, Ori GG (2010) Dune morphology, sand transport pathways and possible source areas in East Thaumasia Region (Mars). *Geomorphology* 121:84–97. <https://doi.org/10.1016/j.geomorph.2009.07.019>
- Sinha RK, Ray D (2021) Extensive glaciation in the Erebus Montes region of Mars. *Icarus* 367:114557. <https://doi.org/10.1016/j.icarus.2021.114557>
- Smith DE, Zuber MT, Solomon SC, Phillips RJ, Head JW, Garvin JB, Banerdt WB, Muhleman DO, Pettengill GH, Neumann GA, Lemoine FG, Abshire JB, Aharonson O, Brown CD, Hauck SA, Ivanov AB, McGovern PJ, Zwally HJ, Duxbury TC (1999) The global topography of Mars and implications for surface evolution. *Science* 285:1495–1503. <https://doi.org/10.1126/science.284.5419.1495>
- Smith IB, Putzig NE, Holt JW, Phillips RJ (2016) An ice age recorded in the polar deposits of Mars. *Science* 352(6289):1075–1078. <https://doi.org/10.1126/science.aad6968>
- Smith IB, Hayne PO, Byrne S, Becerra P, Kahre M, Calvin W, Hvidberg C et al (2020) The holy grail: a road map for unlocking the climate record stored within Mars' polar layered deposits. *Planet Space Sci* 184:104841. <https://doi.org/10.1016/j.pss.2020.104841>
- Soare JR, Williams J-P, Hepburn AJ, Butcher FEG (2022) A billion or more years of possible periglacial/glacial cycling in Protonilus Mensae, Mars. *Icarus* 385:115115. <https://doi.org/10.1016/j.icarus.2022.115111>
- Sowe M (2009) Interior layered deposits in chaotic terrains on Mars. PhD thesis, FU, Berlin. <https://refubium.fu-berlin.de/handle/188/2695?locale-attribute=en>
- Sowe M, Wendt L, McGuire PC, Neukum G (2012) Hydrated minerals in the deposits of Aureum Chaos. *Icarus* 218:406–419. <https://doi.org/10.1016/j.icarus.2011.12.009>
- Squyres SW, Carr MH (1986) Geomorphic evidence for the distribution of ground ice on Mars. *Science* 231(4735):249–252. <https://doi.org/10.1126/science.231.4735.249>
- Squyres SW, Clifford SM, Kuz'min RO, Zimbelman JR, Costard FM (1992) Ice in the Martian regolith. In: Kieffer HH et al (eds) *Mars*. University of Arizona Press, Tucson, pp 523–554. <https://repository.si.edu/bitstream/handle/10088/8625/199220.pdf?sequence=1&isAllowed=y>
- Stanzel C, Pätzold M, Greeley R, Hauber E, Neukum G (2006) Dust devils on Mars observed by the high resolution stereo camera. *Geophys Res Lett* 33:L11202. <https://doi.org/10.1029/2006GL025816>
- Stanzel C, Pätzold M, Williams DA, Whelley PL, Greeley R, Neukum G, The HRSC Co-Investigator Team (2008) Dust devil speeds, directions of motion and general characteristics observed by the Mars Express high resolution stereo camera. *Icarus* 197:39–51. <https://doi.org/10.1016/j.icarus.2008.04.017>
- Stillman DE, Michaels TI, Grimm RE, Hanley J (2016) Observations and modeling of northern mid-latitude recurring slope lineae (RSL) suggest recharge by a present-day Martian briny aquifer. *Icarus* 265:125–138. <https://doi.org/10.1016/j.icarus.2015.10.007>
- Stucky de Quay G, Goudge TA, Fassett CI (2020) Precipitation and aridity constraints from paleolakes on early Mars. *Geology* 48(12):1189–1193. <https://doi.org/10.1130/G47886.1>
- Sturman CM, Osinski GR, Holt JW, Levy JS, Brothers TC, Kerrigan M, Campbell BA (2016) SHARAD detection and characterization of subsurface water ice deposits in Utopia Planitia, Mars. *Geophys Res Lett* 43:9484–9491. <https://doi.org/10.1002/2016GL070138>
- Tanaka KL (1985) Ice-lubricated gravity spreading of the Olympus Mons aureole deposits. *Icarus* 62(2):191–206. [https://doi.org/10.1016/0019-1035\(85\)90117-4](https://doi.org/10.1016/0019-1035(85)90117-4)
- Tanaka K (2000) Dust and ice deposition in the Martian geologic record. *Icarus* 144(2):254–266. <https://doi.org/10.1006/icar.1999.6297>
- Tanaka KL, Kolb EJ (2001) Geologic history of the polar regions of Mars based on Mars Global Surveyor data: I. Noachian and Hesperian Periods. *Icarus* 154(1):3–21. <https://doi.org/10.1006/icar.2001.6676>
- Tanaka KL, Scott DH (1987) Geology map of the polar regions of Mars. USGS Miscellaneous Investigations Series Map I-1802-C, 1:15,000,000. <https://doi.org/10.3133/I1802C>
- Tanaka KL, Skinner JA, Hare TM (2005) Geologic map of the northern plains of Mars. U.S. geological survey sci. inv. map, vol 28888. <http://purl.access.gpo.gov/GPO/LPS92955>
- Tanaka KL, Skinner JA Jr, Dohm JM, Irwin RP III, Kolb EJ, Fortezzo CM, Platz T, Michael GG, Hare TM (2014) Geologic map of Mars: U.S. Geological Survey Scientific Investigations Map 3292, scale 1:20,000,000, pamphlet 43 p. <https://doi.org/10.3133/sim3292>
- Thomas P (1984) Martian intracrater spots: occurrence, morphology, and colors. *Icarus* 57:205–227. [https://doi.org/10.1016/0019-1035\(84\)90066-6](https://doi.org/10.1016/0019-1035(84)90066-6)
- Thomas P, Veverka J, Lee S, Bloom A (1981) Classification of wind streaks on Mars. *Icarus* 45(1):124–153. [https://doi.org/10.1016/0019-1035\(81\)90010-5](https://doi.org/10.1016/0019-1035(81)90010-5)
- Thomas P, Squyres S, Herkenhoff K, Howard A, Murray B (1992) Polar deposits of Mars. In: Kieffer HH et al (eds) *Mars*. University of Arizona Press, Tucson, pp 767–795
- Thomas N et al (2024) Seasonal and short timescale changes on the Martian surface: Multi-spacecraft perspectives. *Space Sci Rev* 220

- Tirsch D (2009) Dark Dunes on Mars – Analyses on origin, morphology, and mineralogical composition of the dark material in Martian craters. PhD thesis, Freie Universität Berlin. <https://doi.org/10.17169/refubium-13574>
- Tirsch D, Jaumann R, Helbert J, Reiss D, Forget F, Poulet F, Neukum G (2006) Recent and fossil deposits of dark material in Martian Craters. *Eur Planet Sci Congr* 2006:406. https://elib.dlr.de/48047/1/Europlanet_poster_2006.pdf
- Tirsch D, Jaumann R, Pacifici A, Poulet F (2011) Dark aeolian sediments in Martian craters: Composition and sources. *J Geophys Res, Planets* 116. <https://doi.org/10.1029/2009JE003562>
- Tirsch D, Erkeling G, Bishop JL, Tornabene LL, Hiesinger H, Jaumann R (2016) Lacustrine mineral deposits and their geologic context at bradbury crater on Mars. In: 7th Lunar and Planetary Science Conference. <https://www.hou.usra.edu/meetings/lpsc2016/pdf/1444.pdf>
- Tirsch D, Bishop JL, Voigt JRC, Tornabene LL, Erkeling G, Jaumann R (2018) Geology of central Libya Montes, Mars: aqueous alteration history from mineralogical and morphological mapping. *Icarus* 314:12–34. <https://doi.org/10.1016/j.icarus.2018.05.006>
- Tornabene LL, Osinski GR, McEwen AS, Wray JJ, Craig MA, Sapers HM, Christensen PR (2013) An impact origin for hydrated silicates on Mars: a synthesis. *J Geophys Res, Planets* 118(5):994–1012. <https://doi.org/10.1002/jgre.20082>
- Tuhi S, Harish AA, Kimi KB, Vigneshwaran K, Sharini KS, Priya RKS, Vijayan S (2022) Ma'adim Vallis, Mars: insights into episodic and late-stage water activity from an impact crater. *Icarus* 387:115214. <https://doi.org/10.1016/j.icarus.2022.115214>
- van Berk W, Fu Y, Ilger J-M (2012) Reproducing early Martian atmospheric carbon dioxide partial pressure by modeling the formation of Mg-Fe-Ca carbonate identified in the Comanche rock outcrops on Mars. *J Geophys Res* 117:E10008. <https://doi.org/10.1029/2012JE004173>
- van Gasselt S, Hauber E, Neukum G (2010) Lineated valley fill at the Martian dichotomy boundary: nature and history of degradation. *J Geophys Res* 115:E08003. <https://doi.org/10.1029/2009JE003336>
- van Kan Parker M, Zegers T, Kneissl T, Ivanov B, Foing B, Neukum G (2010) 3D structure of the Gusev crater region. *Earth Planet Sci Lett* 294(3–4):411–423. <https://doi.org/10.1016/j.epsl.2010.01.013>
- Viola D, McEwen AS (2018) Geomorphological evidence for shallow ice in the southern hemisphere of Mars. *J Geophys Res, Planets* 123:262–277. <https://doi.org/10.1002/2017JE005366>
- Volat M, Quantin-Nataf C, Dehecq A (2022) Digital elevation model workflow improvements for the MarsSI platform and resulting orthorectified mosaic of Oxia Planum, the landing site of the ExoMars 2022 rover. *Planet Space Sci* 222:105552. <https://doi.org/10.1016/j.pss.2022.105552>
- von Paris P, Petau A, Grenfell JL, Hauber E, Breuer D, Jaumann R, Rauer H, Tirsch D (2014) Estimating precipitation on early Mars using a radiative-convective model of the atmosphere and comparison with inferred runoff from geomorphology. *Planet Space Sci* 105:133–147. <https://doi.org/10.1016/j.pss.2014.11.018>
- Walter SHG, Muller JP, Sidiropoulos P, Tao Y, Gwinner K, Putri ARD, Kim JR, R van Gasselt S S, Michael GG, Watson G, Schreiner BP (2018) The Web-Based Interactive Mars Analysis and Research System for HRSC and the iMars Project. *Earth Space Sci* 5:308–323. <https://doi.org/10.1029/2018EA000389>
- Wang J, Xiao L, Reiss D, Hiesinger H, Huang J, Xu Y et al (2018) Geological features and evolution of Yardangs in the Qaidam Basin, Tibetan Plateau (NW China): a terrestrial analogue for Mars. *J Geophys Res, Planets* 123:2336–2364. <https://doi.org/10.1029/2018JE005719>
- Ward AW (1979) Yardangs on Mars: evidence of recent wind erosion. *J Geophys Res* 84(B14):8147–8166. <https://doi.org/10.1029/JB084iB14p08147>
- Ward AW, Doyle KB, Helm PJ, Weisman MK, Witbeck NE (1985) Global map of eolian features on Mars. *J Geophys Res, Solid Earth* 90(B2):2038–2056. <https://doi.org/10.1029/JB090iB02p02038>
- Warner N, Gupta S, Muller J-P, Kim J-R, Lin S-Y (2009) A refined chronology of catastrophic outflow events in Ares Vallis, Mars. *Earth Planet Sci Lett* 288:58–69. <https://doi.org/10.1016/j.epsl.2009.09.008>
- Warner N, Gupta S, Kim JR, Lin SY, Muller JP (2010b) Hesperian equatorial thermokarst lakes in Ares Vallis as evidence for transient warm conditions on Mars. *Geology* 38(1):71–74. <https://doi.org/10.1130/G30579.1>
- Warner N, Gupta S, Lin SY, Kim JR, Muller JP, Morley J (2010a) Late Noachian to Hesperian climate change on Mars: Evidence of episodic warming from transient crater lakes near Ares Vallis. *J Geophys Res, Planets* 115(E6). <https://doi.org/10.1029/2009JE003522>
- Warner NH, Gupta S, Kim J-R, Muller J-P, Le Corre L, Morley J, Lin S-Y, McGonigle C (2011) Constraints on the origin and evolution of Iani Chaos, Mars. *J Geophys Res, Planets* 116:E06003. <https://doi.org/10.1029/2010JE003787>
- Warner NH, Sowe M, Gupta S, Dumke A, Goddard K (2013) Fill and spill of giant lakes in the eastern Valles Marineris region of Mars. *Geology* G34172. <https://doi.org/10.1130/G34172.1>
- Weiss DK, Head JW, Palumbo AM, Cassanelli JP (2017) Extensive Amazonian-aged fluvial channels on Mars: evaluating the role of Lyot crater in their formation. *Geophys Res Lett* 44(11):5336–5344. <https://doi.org/10.1002/2017GL073821>

- Weitz CM, Bishop JL, Grant JA (2013) Gypsum, opal, and fluvial channels within a trough of noctis labyrinthus, Mars: implications for aqueous activity during the Late Hesperian to Amazonian. *Planet Space Sci* 87:130–145. <https://doi.org/10.1016/j.pss.2013.08.007>
- Weitz CM, Bishop JL, Baker LL, Berman DC (2014) Fresh exposures of hydrous Fe-bearing amorphous silicates on Mars. *Geophys Res Lett* 41:8744–8751. <https://doi.org/10.1002/2014GL062065>
- Wendt L, Gross C, Kneissl T, Sowe M, Combe J-P, Le Deit L, McGuire PC, Neukum G (2011) Sulfates and iron oxides in Ophir Chasma, Mars, based on OMEGA and CRISM observations. *Icarus* 213:86–103. <https://doi.org/10.1016/j.icarus.2011.02.013>
- Werner SC (2009) The global Martian volcanic evolutionary history. *Icarus* 201(1):44–68. <https://doi.org/10.1016/j.icarus.2008.12.019>
- Wezel FC, Baioni D (2010) Evidence for subaqueously resedimented sulphate evaporites on Mars. *Planet Space Sci* 58:1500–1505. <https://doi.org/10.1016/j.pss.2010.07.003>
- Williams DA, Greeley R, Zuschneid W, Werner SC, Neukum G, Crown DA, Gregg TKP, Gwinner K, Raitala J, Patera H (2007) Insights into its volcanic history from Mars Express high resolution stereo camera. *J Geophys Res, Planets* 112:E10004. <https://doi.org/10.1029/2007JE002924>
- Williams JP, Dohm JM, Soare RJ, Flahaut J, Lopes RMC, Pathare AV, Fairén AG, Schulze-Makuch D, Buczkowski DL (2017) Long-lived volcanism within Argyre basin, Mars. *Icarus* 293:8–26. <https://doi.org/10.1016/j.icarus.2017.04.001>
- Wilson IG (1972) Aeolian bedforms – their development and origins. *Sedimentology* 19:173–210. <https://doi.org/10.1111/j.1365-3091.1972.tb00020.x>
- Wilson L, Ghatan GJ, Head JW III, Mitchell KL (2004) Mars outflow channels: a reappraisal of the estimation of water flow velocities from water depths, regional slopes, and channel floor properties. *J Geophys Res, Planets* 109(E9). <https://doi.org/10.1029/2004JE002281>
- Wilson SA, Howard AD, Moore JM, Grant JA (2016) A cold-wet middle-latitude environment on Mars during the Hesperian–Amazonian transition: Evidence from northern Arabia valleys and paleolakes. *J Geophys Res, Planets* 121. <https://doi.org/10.1002/2016JE005052>
- Woodley SZ, Butcher FEG, Fawdon P, Clark CD, Ng FSL, Davis JM, Gallagher C (2022) Multiple sites of recent wet-based glaciation identified from eskers in western Tempe Terra, Mars. *Icarus* 386:115147. <https://doi.org/10.1016/j.icarus.2022.115147>
- Woodyer KD, Brookfield E (1966) The land system and its stream net. Technical Memorandum 66/5, CISRO Canberra
- Wordsworth RD (2016) The climate of early Mars. *Annu Rev Earth Planet Sci* 44:381–408. <https://doi.org/10.1146/annurev-earth-060115-012355>
- Wordsworth R, Forget F, Millour E, Head JW, Madeleine J-B, Charnay B (2013) Global modelling of the early Martian climate under a denser CO₂ atmosphere: water cycle and ice evolution. *Icarus* 222:1–19. <https://doi.org/10.1016/j.icarus.2012.09.036>
- Wordsworth RD, Kerber L, Pierrehumbert RT, Forget F, Head JW (2015) Comparison of “warm and wet” and “cold and icy” scenarios for early Mars in a 3-D climate model. *J Geophys Res, Planets* 120(6):1201–1219. <https://doi.org/10.1002/2015JE004787>
- Wray JJ, Milliken RE, Dundas CM, Swayze GA, Andrews-Hanna JC, Baldrige AM, Squyres SW (2011) Columbus crater and other possible groundwater-fed paleolakes of Terra Sirenum, Mars. *J Geophys Res, Planets* 116(E1). <https://doi.org/10.1029/2010JE003694>
- Xiao L, Huang J, Kusky T, Head JW, Zhao J, Wang J, Wang L, Yu W, Shi Y, Wu B, Qian Y (2023) Evidence for marine sedimentary rocks in Utopia Planitia: Zhurong rover observations. *Nat Sci Rev* 10:nwad137. <https://doi.org/10.1093/nsr/nwad137>

Publisher's Note Springer Nature remains neutral with regard to jurisdictional claims in published maps and institutional affiliations.

Authors and Affiliations

R. Jaumann¹  · D. Tirsch² · S. Adeli² · R. Bahia³ · G. Michael^{1,4} · L. Le Deit⁵ · A. Grau Galofre⁵ · J. Head⁶ · E. Bohacek³ · C. Gross¹ · S.G.H. Walter¹ · H. Hiesinger⁷

✉ R. Jaumann
ralf.jaumann@fu-berlin.de

- ¹ Freie Universität Berlin, Institute of Geological Sciences, Planetary Sciences and Remote Sensing, Berlin, Germany
- ² Institute of Planetary Research, Deutsches Zentrum für Luft- und Raumfahrt (DLR), Berlin, Germany
- ³ European Space Agency, Noordwijk, The Netherlands
- ⁴ Center for Lunar and Planetary Sciences, CAS Institute of Geochemistry, Guiyang, China
- ⁵ Nantes Université, Univ Angers, Le Mans Université, CNRS, Laboratoire de Planétologie et Géosciences, LPG UMR 6112, 44000, Nantes, France
- ⁶ Department of Earth, Environmental and Planetary Sciences, Brown Univ. Providence, RI02912, USA
- ⁷ Institut für Planetologie, Universität Münster, Münster, Germany